Respiratory Mechanics in the Mechanically Ventilated Patient

11

11.1 Introduction

Mark Heulitt and Katherine C. Clement

Educational Aims

- To review the physiologic aspects of respiratory mechanics on positive pressure ventilation
- To understand the aspects of passive aspects of the respiratory system and its implications on monitoring of respiratory mechanics
- To understand the technical aspects of the measurement of respiratory mechanics and potential limitations and applications

Infants and young children have a number of anatomical reasons and physiological reasons for making accurate measurement of respiratory mechanics in the intensive care unit. Despite advances in the measurement of respiratory mechanics in non-intubated infants, these advances have been slow to be adapted to intubated patients due to technical limitations. Thus, the major role of lung function testing in the ICU has been limited to the research arena. However, despite these limitations it is essential the person caring for the intubated pediatric patient have an in-depth understanding of the respiratory mechanics involved with the use of a positive pressure ventilator.

The same model describing the normal interactions between the airways and the lungs can be applied to the interaction of the mechanical ventilator with the respiratory system. In simple terms, the lung-ventilator unit can be considered as a tube with a balloon network at the end, with the tube representing the ventilator tubing, endotracheal tube and airways, and the balloon network of the alveoli. The movement of gas is determined by forces, displacements, and the rate of change of displacements of the components that are distensible.

In physiology, force is measured as pressure (pressure = force/area), displacement is measured as volume (volume = area × displacement), and the relevant rate of change is measured as

P.C. Rimensberger (ed.), *Pediatric and Neonatal Mechanical Ventilation*,
DOI 10.1007/978-3-642-01219-8_11, © Springer-Verlag Berlin Heidelberg 2015

flow (e.g., average flow = (Δvolume/Δtime); instantaneous flow = d*v*/d*t*; the derivative of volume with respect to time). The pressure necessary to cause gas flow into the airways and to increase the volume of gas into the airways and to increase the volume of gas in the lungs is the key component in positive pressure mechanical ventilation. The volume of gas (ΔV) to any lung unit (or balloon in simplified example) and the gas flow $\left(\dot{V}\right)$ are related to the applied pressure ΔP by

$$\Delta P = \frac{\Delta V}{C} + \dot{V} \times R + k$$

where R is the airway resistance and C is the lung compliance. This equation is known as the equation of motion for the respiratory system. The sum of the muscle pressures and the ventilator pressures is the applied pressure to the respiratory system. Muscle pressure represents the pressure generated by the patients to expand the thoracic cage and lungs. In contrast, ventilator pressure is the transrespiratory pressure generated by the ventilator during inspiration. Combinations of these pressures are generated when a patient is breathing on a positive pressure ventilator. For example, when the respiratory muscles are at complete rest, the muscle pressure is 0; therefore, the ventilator must generate all the pressure necessary to deliver the tidal volume and inspiratory flow. The reverse is also true, and there are degrees of support depending upon the amount of force generated by the patient's respiratory muscles. Therefore, the total pressure applied to the respiratory system (P_{RS}) of a ventilated patient is the sum of the pressures generated by the ventilator (measured at the airway) P_{AO} and the pressure developed by the respiratory muscles (P_{MUS}). Therefore,

$$P_{RS} = P_{AO} + P_{MUS} = \frac{V}{C} + \dot{V} \times R + k$$

where P_{RS} is the respiratory system pressure, P_{AO} is the airway pressure, and P_{MUS} is the pressure developed by the respiratory muscle.

11.2 Terminology and Conventions

Main Symbols:

C	Compliance
E	Elastance
f	Frequency
G	Conductance
I	Inertance
PEEP	Positive end-expiratory pressure
P	Pressure
R	Resistance
τ	Time constant (tau)
V	Volume
V_T	Tidal volume
Z	Impedance
$\dot{X}$	Dot above any symbol indicates first time derivative, e.g., $\dot{V}$ is flow of gas

Modifiers:

A	Alveolar
ao	Airway opening
dyn	Dynamic
E	Expiratory
El	Elastic
es	Esophageal
I	Inspiratory
L	Lung
η	Is the viscosity of the gas
p_{aw}	Airway pressure
p_l	Pleural
rs	Respiratory system
st	Static

Examples of Combinations

C_{CW}	Chest wall compliance
C_{dyn}	Dynamic compliance
C_L	Lung compliance
$C_{st,L}$	Static lung compliance
$E_{dyn,rs}$	Dynamic elastance of the respiratory system
P_A	Alveolar pressure
P_{AO}	Pressure at airway opening
P_{bs}	Pressure at the body surface (atmospheric pressure)

$PEEP_i$	Intrinsic PEEP
P_{ES}	Esophageal pressure
P_{plat}	Plateau pressure
P_{pL}	Pleural pressure
P_{RS}	Pressure respiratory system
R_{aw}	Airway resistance
R_{dyn}	Dynamic resistance
R_{ti}	Lung tissue resistance
$\dot{V}_{max}$	Flow max

11.3 Mechanical Model of the Passive Respiratory System

A model of the respiratory system is considered passive because the lungs respond to forces external to the lungs. The respiratory muscles generate these forces in a patient breathing spontaneously. In contrast, during positive pressure mechanical ventilation, the movement of gases is in response to a pressure gradient that is developed between the airway and the environment. However, in both cases it is the physical impedance of the respiratory system that determines the pattern of response of the lung. Generally the major causes of the impedance can be categorized into either the forces related to the (1) elastic resistance of tissue and alveolar gas/liquid interface and (2) frictional resistance to gas flow. Under static conditions when no gas is flowing, it is the elastic resistance to gas flow that governs the relationship between pressure and lung volume. Minor causes of impedance include the inertia of gas and tissue and the friction of tissue deformation.

It has been recognized that the elastic recoil of the lung is not isolated to the stretching fibers of the lung parenchyma but to the combination of these fibers plus the surface tension acting throughout the vast air/water interface lining the alveoli.

Elastic resistance is only one component of the total impedance to gas flow; a much greater part of the residual forms of impedance are provided by what can be categorized as "nonelastic resistance" provided by resistance to airflow and tissue deformation. These can be categorized as pulmonary resistance and are related to gas flow rate.

In a passive system, the extent of lung inflation reflects a balance between the elastic recoils of the lungs and chest wall, gravitational force, and tension in the respiratory muscles. In this system, when movement occurs, the equilibrium is disturbed and the rate of movement is influenced by the strength of the applied force and by the elasticity, resistance to movement, and the inertia of the thoracic cage, lung tissue, and gas contained in the lung.

Thus, the force applied to a body is met by an opposing force of equal magnitude and is related to the elasticity, resistance, and inertia of the system.

The elasticity of the system can be expressed as elastance which is the reciprocal of compliance (C) and is related to the volume (V), resistance (R), velocity of gas flow, and the inertia (I) to acceleration. All these variables influence the pressure difference across the lung. These can be expressed in Newton's third law of motion:

$$P = \left(\frac{1}{C}\right)V + \left(R\frac{\mathrm{d}V}{\mathrm{d}t} + I\frac{\mathrm{d}^2V}{\mathrm{d}t^2}\right)$$

This equation states that a force applied to a body is met by an opposing force of equal magnitude and that this latter force has components related to elasticity, resistance, and inertia.

The necessary force generated to overcome the resistance to movement of the lungs and thorax represents a large energy expenditure and consumption of oxygen. Thus, it is usually the frictional resistance of the lungs and chest wall that limit exercise and the maximal rate that air can move in and out of the lungs. The resistance can be further subdivided into thoracic resistance, pulmonary resistance, lung tissue resistance, and airway resistance.

Inertia according to the laws of physics, force (F) equals mass (M) times acceleration ($G = \mathrm{d}u/\mathrm{d}t$, where u is the velocity of the gas molecules). Pressure is F/A, where A is the area the force is acting on. The mass of a column of gas is $L \times A \times \rho$ where L is the length of the column, A its

cross-sectional area, and ρ the gas density. From this it follows that

$$P = \frac{F}{A} = \left(L \times A \times \rho\right) \times G = L \times \rho \times \frac{\mathrm{d}u}{\mathrm{d}t}$$

However, $u = V/A$, and $\mathrm{d}u/\mathrm{d}t = (1/A) \times \mathrm{d}V/\mathrm{d}t$ where V is the volumetric gas flow. $\mathrm{d}V/\mathrm{d}t$ is the volume acceleration, which is the same as $\mathrm{d}^2V/\mathrm{d}t^2$, where V is volume. From this it follows that

$$P = \left(\frac{L \times \rho}{A}\right) \times \frac{\mathrm{d}^2V}{\mathrm{d}t^2}$$

The inertance I therefore equals $L \times \rho/A$. The pressure drop due to inertance is greatest when the flow increases rapidly, as occurs if the frequency of breathing rises. The work performed to achieve the acceleration is stored in the lung as kinetic energy.

Inertial forces are of negligible magnitude except when a high-frequency oscillation is applied for purposes of assisting ventilation or for investigating the mechanical characteristics of the lung.

The forces necessary to overcome the resistance to movement of the lungs and thorax are relatively large and when ventilation is increased requires large energy expenditure and oxygen consumption. Thus, the maximal rate at which air can move into and out of the lungs can be limited. Resistance can be subdivided according to tissue involved including total thoracic resistance, total pulmonary resistance, lung tissue resistance, and airway resistance.

Total thoracic resistance is the sum of the components attributable to the rib cage, the diaphragm, the abdominal wall and contents, the lung tissue, and the gas in the lung and airways. These effects are additive; thus,

$$P_{\mathrm{total}} = P_{\mathrm{th}} + P_{\mathrm{ti}} + P_{\mathrm{aw}}$$

where P is the force required to overcome the frictional resistance and th, ti, aw refer, respectively, to the thoracic rib cage and diaphragm, the lung tissue, and the lung airways. For the thoracic cage the force is a simple function of the velocity of linear movement. The velocity cannot be measured directly but can be described approximately in terms of the rate of airflow. Then, as a first approximation

$$P_{\mathrm{th}} = R_{\mathrm{th}} \times \dot{v}^{nl}$$

where R_{th} is the resistance of the thoracic cage, in kPa (or cm H_2O) $l^{-1}s$, and $\dot{v}$ is the airflow (ls^{-1}). In most instances the value of the exponent $n1$ lies between 1.0 and 1.1; hence, the relationship is linear.

Total pulmonary resistance is the sum of lung tissue resistance (R_{ti}) and airway resistance (R_{aw}):

$$R_{\mathrm{l}} = R_{\mathrm{ti}} + R_{\mathrm{aw}}$$

where R_1 is the pulmonary flow resistance in kPa (or cm H_2O) $l^{-1}s$; it is therefore the pressure difference that must be applied between the pleural surface of the lungs and the lip in order to secure a velocity of flow of 1 $l^{-1}s$. This quantity can be derived from the slope of the initial part of the isovolume flow–pressure curve.

Lung tissue resistance (R_{ti}) normally represents 10 % of the total pulmonary resistance. However, due to changes in airway resistance, its contribution is greater at large as compared to small lung volumes. Tissue resistance can be affected by pathology of the tissue such as in pulmonary fibrosis. It cannot be measured directly; thus, it is estimated by subtracting airway resistance from total pulmonary resistance. This estimation can be inaccurate.

Airway resistance (R_{ti}) is the sum of the resistances attributable to all airways individually. Each airway's resistance is determined by its diameter that varies with lung volume. Poiseuille's equation can provide a theoretical basis for understanding resistance of the airway. It states

$$R = \frac{8\ \eta L}{\pi r^4}$$

where r is the radius of the tube, L it the length of the tube, and η is viscosity in poise.

This states that for a simple tube, the resistance is related inversely to the fourth power of the radius (Poiseuille 1840). Because in all airways the radius varies with lung size, the airway resistance varies throughout the respiratory cycle. Thus, resistance is lower at large lung volumes when the airways are expanded; it rises during expiration as the airways diminish in size and becomes infinite at residual volume when some airways close. The reciprocal of airway resistance is conductance (G_{aw}) and increases almost linearly with volume. Specific conductance (sG_{aw}) is G_{aw}/TGV where TGV is thoracic gas volume. It varies less with lung volume than G_{aw}.

In order to overcome the impedance of the respiratory system and to allow gas flow to occur, work must be performed. During breathing, the work overcomes the resistance to movement of the lungs and the chest cage. This work can be categorized by whether the energy is retained or lost from the system. The work performed to overcome the frictional resistance is dissipated as heat and subsequently lost from the system. In contrast, the work performed in overcoming elastic resistance is stored as potential energy and elastic deformation during inspiration and is usually the source of energy for expiration during both spontaneous and artificial breathing. A further discussion of resistance and gas flow will occur in the next section.

11.4 Signals for Respiratory Mechanics Measurements

11.4.1 Measurement Devices (Principles and Technical Requirements)

Our knowledge of physiology is based upon what we are able to measure. In respiratory mechanics for the most part, that is pressure and flow of gas. Modern transducer technology and the availability of computers mean that the pressure and flow can be described and modeled in detail. This is what has led to the preeminent place of mathematical models in respiratory mechanics. However, the success of such models is only as good as the measurements upon which they are based.

The general process by which a biological signal is captured and recorded for analysis is illustrated in Fig. 11.1. A mean feature of this system is the use of a transducer. A transducer is a device that transforms some signal of interest into a signal (usually electrical) that can be recorded.

11.4.1.1 Static Properties

The static properties of a transducer describe its behavior with signals that do not vary with time. In practice one deals with quasistatic signals (almost non-varying with time). However, if the signals were truly static, they would never change and it would be impossible to apply different signals to the transducer. Ideally, one would like to have a transducer that is as linear, stable, and efficient as possible, with the least amount of hysteresis and the greatest signal-to-noise ratio, resolution, and dynamic range.

The signal-to-noise ratio of a transducer is a measure that quantifies how much a signal is corrupted by noise. It is important since a transducer never produces a perfectly accurate representation of a signal. Instead, there is always a bit of unwanted contamination accompanying the measurement.

The resolution of a transducer is the smallest change it can discern in the signal it is measuring. Its dynamic range is the difference between the largest and smallest change in the input that can be accurately measured. The accuracy of a transducer is dependent on its degree of hysteresis and its stability, signal-to-noise ratio, and resolution.

The efficiency of a passive transducer relates to the ratio of the output power over the input power, while powered transducer efficiency depends upon its external power source.

11.4.1.2 Dynamic Properties

The dynamic properties of a transducer describes how its output $y(t)$ is related to its

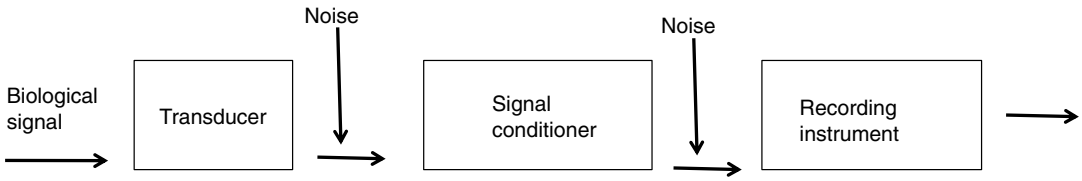

Fig. 11.1 The general process by which a biological signal is captured and recorded

input $x(t)$, when $x(t)$ varies with time (t). If the transducer is nonlinear, then its dynamic response is complex. However, with a stable linear transducer, the properties can be described in terms of its effects on input sinusoids of various frequencies.

Another important property of linear transducers is that they obey the principle of superposition, which means that the output sum of two different waveforms at the input is equal to the sum of the outputs produced by each input individually. Since any input waveform can be expressed as a sum of sinusoids (via the Fourier transform), and each of these sinusoids is altered in an amplitude and phase by an amount that depends only on frequency, the output of a linear transducer can be calculated by figuring out how each component sinusoid of the input is altered and then adding up the results.

11.4.1.3 Frequency Response

The frequency response of a transducer is a description of the way in which it alters sinusoids of different frequencies and consists of two functions $A(f)$ and $\varphi(f)$. $A(f)$ is the equivalent of the ratio A_1/A_2 above and is called the amplitude response because it is the factor by which a sinusoid of frequency f is altered in amplitude. $\varphi(f)$ is the equivalent of $\varphi_1 - \varphi_2$ above and is the corresponding alteration in its phase. Transducers can be overdamped or underdamped. The overdamped transducer has an amplitude response $A(f)$ that decreases monotonically with frequency f. When such a transducer is subjected to a sudden steplike change in the input, it responds sluggishly.

An overdamped transducer has an amplitude response $A(f)$ that increases above 1.0 on the step response before eventually falling off with increasing frequency f. When such a transducer is subjected to a sudden steplike change in input, it responds with an overshoot and subsequent "ringing."

11.4.1.4 Input Impedance

A transducer can never take the role of being a "passive observer." Whenever a signal is measured by a transducer, the signal itself is always altered to some degree by the transducer itself because energy from the signal is required to produce a change within the transducer. The change in the input signal resulting from the presence of the transducer is inversely related to the transducers input impedance, which obviously should be as high as possible. In particular, the input impedance should be high enough that the change in the measured signal resulting from the presence of the transducer is negligible compared to the resolution of the transducer.

11.4.1.5 Analog-to-Digital Conversion

Data acquisition by a computer requires an analog-to-digital (AD) converter. This is a device that samples the incoming analog voltage signal and converts each voltage reading into a number that can be stored in the computer's memory. AD converters have resolution depending upon its ability to convert a signal into 4,096–65,536 parts (12 bit to 16 bit converters).

The analog range of an AD converter is the voltage range over which it will accept and digitize a signal. It is desirable to have the voltage signal being sampled fill as much of the analog range of the AD converter as possible, so that the resolution of the digitized signal is maximized. If the voltage signal occupies a small fraction of the analog range, it may suffer discretization error when digitized. A digitized signal that has significant discretization error can be seen to jump about between discrete levels.

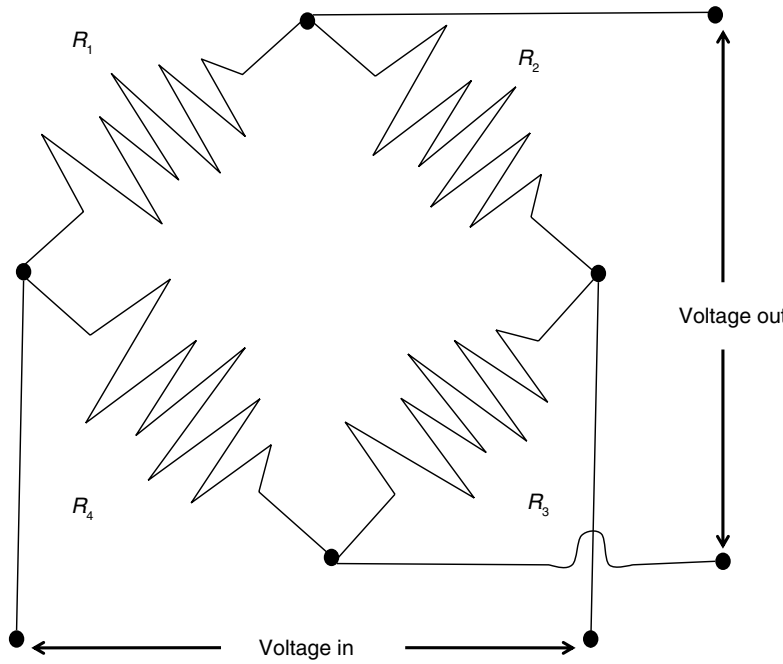

Fig. 11.2 A Wheatstone bridge circuit measuring the change in resistance of a piezoresistive strain gauge

11.4.1.6 Transducers for Measuring Pressure and Flow

Today most transducers are solid state. However, traditionally all force transducers consisted of some kind of elastic material whose deformation under the applied force is measured. A piezoresistive force transducer (often called a strain gauge) is one whose resistivity changes as a result of an applied force. An example is a wire whose resistance increases when pulled end to end as it stretches in length and narrows in cross section. The change in resistance of a piezoresistive strain gauge is measured by making the gauge one arm of a Wheatstone bridge (Fig. 11.2). When the bridge is balanced, the output voltage is zero, which occurs when $R_1/R_2 = R_3/R_4$. As the resistance of R_1 changes, the output voltage V changes from zero. The Wheatstone bridge needs a power supply (a constant DC voltage) and the output voltage usually needs some amplification before being recorded.

The conventional device used by respiratory physiologists for measuring flow at the tracheal or airway opening is the pneumotachograph which consists of a known resistance (R) across

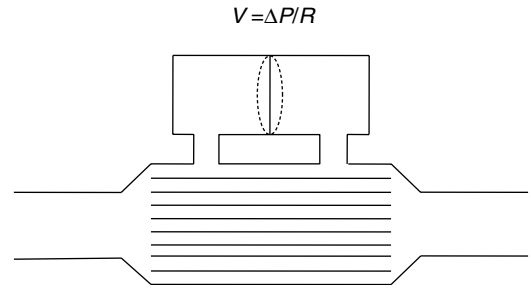

Fig. 11.3 A pneumotachograph, consisting of a differential pressure transducer to measure the drop across a known resistance. R is a known resistance across which a pressure difference is measured. Flow is then calculated by the formula in the diagram

which a pressure difference (ΔP) is measured (Fig. 11.3). The flow $\dot{V}$ through the device is then calculated as

$$\dot{V} = \Delta P / R$$

To satisfy the equation above, the known resistance inside the pneumotachograph must be designed so that the flow through it is laminar up to a certain limit. The nature of the flow

profile inside the pneumotachograph is affected by the shape of the conduit leading into it, so it is advisable to have straight lengths of tubing leading into the pneumotachograph in both directions. This conditions the flow before it reaches the point where ΔP is measured. Some pneumotachographs also contain heating elements or shells so that moisture will not condense in the resistor and change its characteristics during use.

A problem with the pneumotachograph is the frequency response of a pneumotachograph can be rather limited. If a rapidly responding pressure transducer is used with the shortest possible connection between the transducer ports and those of the pneumotachograph, the frequency response of a typical pneumotachograph may be relatively flat up to 20 Hz or so. Eventually the device achieves a resonance. It is important to keep the tubing on the pneumotachograph as short as possible.

Another aspect of the pneumotachograph that can cause problems is its input impedance. If the flow of gas required to travel between the pneumotachograph and the differential pressure transducer (in order to pressurize the latter) is significant compared to the flow through the pneumotachograph itself, then there can be significant differences between the flow through the device and the differential pressure recorded. This problem becomes worse as the diameter of the pneumotachograph decreases with the tubing and pressure transducer remaining the same. It also becomes worse as the frequency of the flow through the device increases because it may take some time for the differential pressure transducer to become pressurized via the lateral ports, resulting in phase differences between the recorded differential pressure and the flow. However, some of these limitations due to size can be overcome by utilizing a technique such as force oscillation (Schuessler and Bates 1995).

11.4.2 Airway Gas Flow

The resistance to airflow in a tube depends on the type of flow, the dimensions of the tube, and the viscosity and density of the gas. Airflows through tubes can either be laminar or turbulent.

11.4.2.1 Laminar Flow

Laminar flow can be described as organized, and the streamlines are everywhere parallel to the sides of the tube and are capable of sliding over one another. The streamlines at the center of the tube move faster than those close to the walls, producing a flow profile that is parabolic. With laminar flow, the relation between pressure and flow is given by Poiseuille's equation:

$$P = \frac{8\eta l \dot{V}}{\pi r^4} = K_1 \dot{V}$$

or

$$\dot{V} = \left(\frac{P \pi r^4}{8\ \eta l} \right)$$

where $\dot{V}$ is the flow rate; P is the driving pressure (pressure drop between the beginning and the end of the tube); r and l are the radius and the length of the tube, respectively; and η is the viscosity of the gas. Because flow resistance (R) is the driving pressure divided by the flow, the resistance with laminar flow is independent of the flow rate:

Laminar flow $P = K_1 \dot{V}$

$$R = \frac{8\ \eta l}{\pi r^4} = K_1$$

Note the critical importance of the tube radius. If the radius of the tube is halved, the airway resistance increases 16-fold. Note also that laminar flow is dependent on the viscosity of gas but is independent of its density.

11.4.2.2 Turbulent Flow

Turbulent flow occurs at high flow rates and is characterized by a complete disorganization of the streamlines so that molecules of gas move laterally, collide with one another, and change velocities. Owing to this disorganization, the pressure drop across the tube is not proportionate to the flow rate as with laminar flow but rather is proportional to the square of the flow rate:

$$P = K_2 \dot{V}^2$$

Thus, the resistance to airflow is proportional to the flow rate:

$$R = K\dot{V}$$

in contrast with laminar flow. In addition, with turbulent flow, there is an increase in the pressure drop for a given flow, but the viscosity of the gas becomes unimportant.

11.4.2.3 Reynolds Number

Whether the airflow is laminar or turbulent depends to a large extent on a dimensionless quantity called the Reynolds number, *R*e, which is given by

$$Re = \frac{2\ rvdl}{\eta}$$

where r is the radius of the tube, v is the average velocity, d is the density of the gas, and η is the viscosity of the gas. In a straight, smooth, rigid tube, turbulence occurs when *Re* exceeds 2,000.

In the lung, laminar flow occurs only in small peripheral airways, where, owing to the large overall cross-sectional area, flow through any given airway is extremely slow. Turbulent flow occurs in the trachea. In the remainder of the lung, owing in large part to the multiple branching of the tracheobronchial tree, flow is neither laminar nor turbulent but rather mixed or transitional. With transitional flow pattern, flow is dependent on both the viscosity and the density of the gas:

$$P = K_1 \dot{V} + K_2 \dot{V}^2$$

11.4.2.3.1 Threshold Resistors

A threshold resistor is a resistor that allows no gas to pass until a threshold pressure is reached. Once that pressure is reached, gas passes freely with little further rise in pressure as the flow rate increases. The Starling valve (Fig. 11.4) is the classic prototype of the threshold resistor. In this model gas will only flow when the upstream pressure exceeds the pressure in the chamber surrounding the collapsing tubing. Another example of a threshold resistor is a spring-loaded valve that was commonly used in ventilators to maintain end-expiratory pressure.

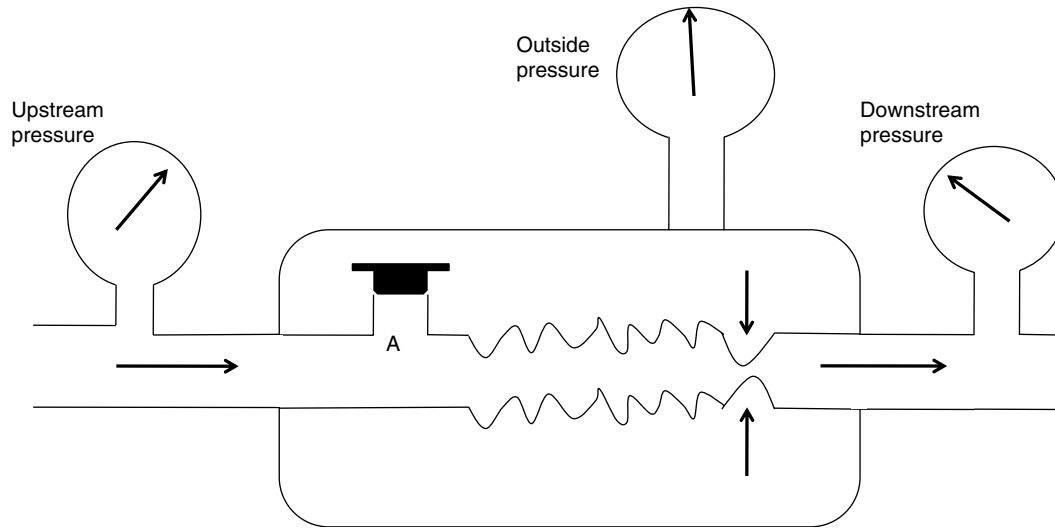

Fig. 11.4 The Starling resistor consists of a length of a flaccid collapsible tubing passing through a rigid box. When the outside pressure surrounding the tube exceeds the upstream pressure, the tubing collapses as illustrated by the *arrows*. Thus, no gas can flow no matter the level of downstream pressure. If orifice *A* is opened, the outside pressure rises with the upstream pressure and so limits flow rate to a level which is independent of the magnitude of the upstream pressure

Another property of the threshold resistor is that once gas begins to flow, an increase in downstream pressure will distend the tubing thus decreasing the resistance of the device. However, a decreased downstream pressure cannot initiate flow. This model can also be used to explain the behavior of a collapsing airway during expiration.

11.4.3 Airway Pressure

The airway pressure is the force that the mechanical ventilator and patient apply on the respiratory system. The measurement requires of a pressure transducer. Pressure transducers used in clinical practice are essentially of two types: (1) variable reluctance transducer, where an element is deformed by the pressure changing the magnetic flux linkage between two coils receiving electrical current, and (2) piezoresistive transducers where there is an element that when deformed changes the resistance to electrical current.

The airway pressure (P_{aw}) may be measured at different points of the mechanical ventilator–patient circuit. A pressure sensor or transducer may be placed at the airway opening, P_{AO} (the Y-piece just before connecting to the endotracheal tube); at the inspiratory or expiratory ventilator outlets; or at the trachea (using a catheter). The place of measurement of airway pressure may yield different results, as the effects of the interface (circuit, humidifier, and endotracheal tube) may interfere with the measurements. Almost all current mechanical ventilators have sensors for airway pressure; if absent, P_{aw} can be measured with stand-alone devices.

The effect of flow in the accuracy of airway pressure measurements must be accounted. During dynamic conditions, there is flow as a result of a driving pressure. The effect of flow and the position of the pressure transducer are described by the Bernoulli effect. If a catheter or an opening in the system, where the pressure is going to be measured, is perpendicular to the direction of flow, the value measured is the lateral pressure (P_{lat}) rather than the driving pressure. The following equation demonstrates the factors that affect the P_{lat}. The P_{lat} is lower than the driving pressure, unless there is no flow (P_{stat}), or if the cross-sectional area where the pressure being measured is large.

$$P_{lat} = P_{stat} - \frac{\beta \rho \dot{V}^2}{2A^2}$$

where P_{stat} is the static pressure, A is cross-sectional area, $\dot{V}^2$ is flow, ρ is density of the gas, and β is the flow velocity profile (1 = linear, 2 = parabolic).

The Bernoulli effect can be eliminated by the use of an opening or catheter for measurement that faces the flow; this is called a pitot tube. By facing the flow, the opening of the tube makes a small amount of gas to stop, and hence, the effect of flow is eliminated and we can measure P_{stat}.

The P_{aw} is the transrespiratory system pressure and is a manifestation of the respiratory system characteristics (elastic P_{EL} and resistive P_R):

$$P_{aw} = P_{EL} + P_R$$

This can be written as

$$P_{aw} = \left(\frac{V}{C} + P_{EX} \right) + \dot{V}R$$

where V indicates volume relative to the end-expiratory position, C is compliance, P_{ex} is end-expiratory alveolar pressure, $\dot{V}$ is flow, and R is resistance.

During static conditions, the airway pressure is a manifestation of the respiratory system compliance:

$$P_{aw} = P_{El},$$

or

$$P_{aw} = \left(\frac{V}{C} + P_{EX} \right) = P_{plat}$$

During mechanical ventilation, the airway pressure signal (Fig. 11.5) may be used to obtain direct measurements (peak inspiratory pressure, plateau pressure) or calculated parameters (mean airway pressure).

The peak inspiratory pressure (PIP) is the maximum pressure during assisted ventilation. According to the mode of ventilation, the value may represent different respiratory system characteristics. In a volume- or flow-controlled mode,

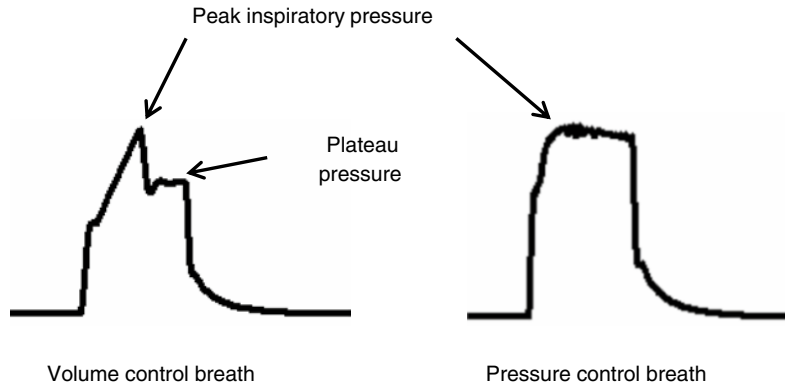

Fig. 11.5 Airway pressure signal according to mode of ventilation

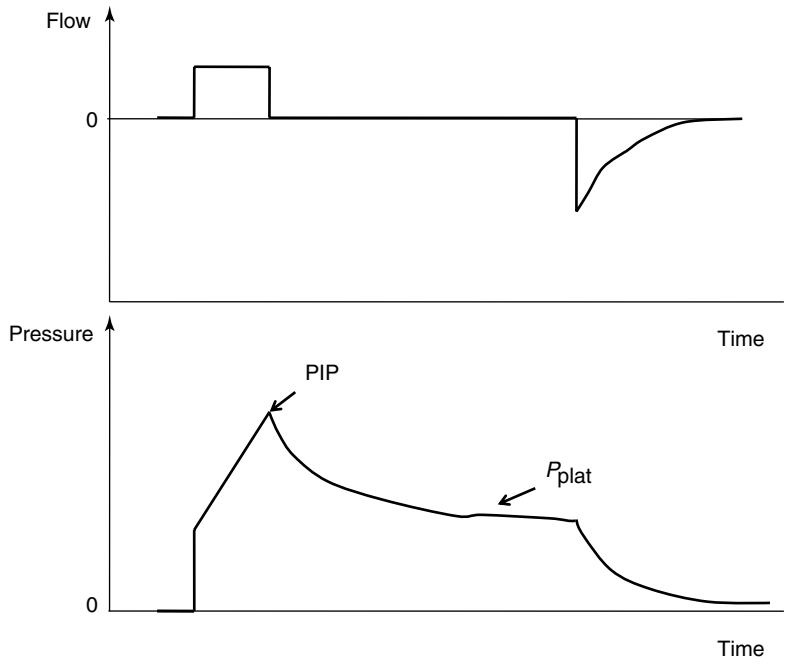

Fig. 11.6 The figure shows flow–time and pressure–time waveforms from a constant flow mode of ventilation and illustrates various landmarks for the waveform

the PIP is the manifestation of the respiratory system compliance, resistance, and patient effort (Fig. 11.6). In a pressure-controlled mode, the PIP is a manifestation of the operator set inspiratory pressure.

The plateau pressure, P_{plat}, is the airway pressure during an inspiratory hold while a patient is on mechanical ventilation. By creating an inspiratory hold, the effects of lung resistance and impedance are annulled, leaving a measure of the respiratory system compliance. As described before, the respiratory system compliance is a manifestation of the lung, chest wall, and abdomen.

The mean airway pressure, $\bar{P}_{aw}$, is the average pressure of the airway over a given time interval. In a static model, where all the breaths are identical, the mean airway pressure is the area under the curve of a pressure–time curve for one breath divided by the total cycle time (inspiration + exhalation). In an active model, the mean airway pressure can be calculated as an average over several breaths. Several mechanical ventilators will display a $\bar{P}_{aw}$ value; it depends on the brand of mechanical ventilator and the technique it uses to measure it. Some use a number of breaths, while others do it breath to breath. To obtain the measurement, the

ventilator or measuring instrument must average a large number of pressure measurements.

The formula to calculate P_{aw} is

$$\bar{P}_{aw} = \left(\frac{1}{TT}\right)\int_{t=0}^{t=TT} \bar{P}_{aw}\,dt$$

where TT is the total cycle time in seconds.

The $\bar{P}_{aw}$ will be affected by the PIP, PEEP, type of pressure waveform, frequency, and inspiratory and expiratory time. The larger the PIP, PEEP, frequency, and inspiratory time, the higher the $\bar{P}_{aw}$. The larger the PEEP, the lower the $\bar{P}_{aw}$. The closer the waveform is to a perfect square, the higher the $\bar{P}_{aw}$. At a single-compartment level with linear equal inspiratory and expiratory resistance, $\bar{P}_{aw}$ is equal to the mean alveolar pressure. If the inspiratory resistance is higher than the expiratory resistance, the $\bar{P}_{aw}$ will be higher than the mean alveolar pressure. If the expiratory resistance is higher than the inspiratory resistance, the $\bar{P}_{aw}$ will be lower than the alveolar pressure.

11.4.4 Transesophageal Pressure (Meaning and Measurement)

The esophagus lays in the posterior mediastinum inside the thorax and is surrounded by a scant amount of soft tissue and the pleura. Its location allows to use transducers to obtain pressure measurements (Fig. 11.7). The changes in esophageal pressure, ΔP_{es}, correlates and is used as a surrogate for the changes in intrapleural pressure, ΔP_{pl}. The position of the patient (supine versus prone or standing), type of catheter used, and underlying condition may affect pleural pressures (Washko et al. 2006). Nonetheless, P_{ES} as a surrogate of P_{pl} allows the practitioner to obtain and calculate and separate the lung and chest wall compliances from the respiratory system compliance. As follows,

$$C_{RS} = \frac{\Delta V}{\Delta\left(P_{AO} - P_{BS}\right)}$$

where ΔV is change in volume, P_{AO} is the pressure at the airway opening, and P_{BS} is pressure at the body surface. During mechanical ventilation, this value is $\Delta V = V_t$, and $\Delta(P_{aw} - P_{BS})$ is

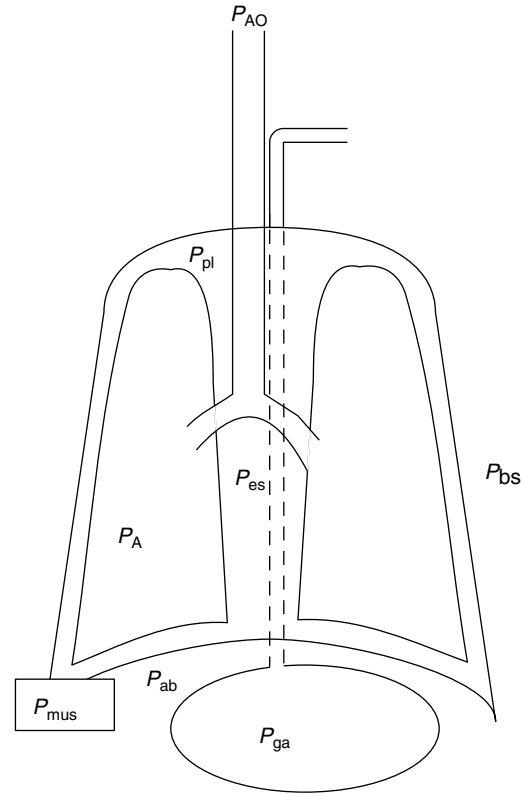

Fig. 11.7 Diagram of the respiratory system: P_{AO} pressure at the airway opening, P_{pl} pleural pressure, P_{es} esophageal pressure, P_{bs} body surface pressure, P_A alveolar pressure, P_{mus} muscle pressure, P_{ab} abdominal pressure, P_{ga} gastric pressure

$(P_{plat} - PEEP_{TOT})$ (in the setting of mechanical ventilation, P_{BS} can be substituted by total PEEP). If we take into consideration the P_{ES} as a marker of P_{pl}, then we can divide the respiratory system compliance into lung and chest wall:

$$C_L = \frac{\Delta V}{\Delta\left(P_{AO} - P_{es}\right)}$$

$$C_{CW} = \frac{\Delta V}{\Delta\left(P_{es} - P_{BS}\right)}$$

The measurement of the esophageal pressure can be done with a balloon-tipped catheter, a liquid-filled catheter, or a transducer at the tip of a catheter. The most common method is the balloon-tipped catheter.

The placement of an esophageal balloon is essential to obtain consistent measurements. The

catheter is inserted under topical lubrication and in some cases topical anesthesia through the nose. The catheter is advanced to the gastric chamber, where, if the patient is actively breathing, the balloon will demonstrate positive deflections (the abdominal pressure increases during inspiration). The esophageal catheter is then retrieved until negative deflections are seen; from that point one must retract the esophageal balloon the amount of distance to maintain the whole balloon in the thoracic esophagus. It is essential to use low volumes to inflate the balloon (<1 cc air) as this will cause false elevation in the measurements.

To ensure that the balloon catheter is appropriately placed, the patient or clinician must generate transpulmonary pressure swings so that the ΔP_{es} and ΔP_{AO} can be compared. In a patient who can cooperate, the maneuver consists of measuring the P_{AO} and P_{ES} simultaneously while the patient performs forceful breathing efforts. The most common test used to assess accuracy is the dynamic "occlusion test." It is performed by occluding (blocking) the airway while 3–5 respiratory efforts happen. The ΔP_{es} and ΔP_{AO} are then compared. A ratio of difference between $\Delta P_{es}/\Delta P_{AO}$ should approach 1 to ensure measurement agreement.

11.4.4.1 Alveolar Pressure

Direct measurement of alveolar pressure in patients is not feasible but has been performed in animal studies. Subpleural alveolar pressure (P_A) is measured using an alveolar capsule technique. A small plastic capsule is attached to the exposed pleural surface and a small area is punctured with a needle and isolated so changes can be measured utilizing a small piezoresistive pressure transducer. Multiple sites can be measured simultaneously.

11.5 Measurement of Passive Respiratory Mechanics

11.5.1 Mechanics of the Passive Respiratory System

The two most common methods of measuring passive mechanics are the single and multiple occlusion techniques. For the occlusion technique, the Hering–Breuer reflex must be invoked to elicit relaxation of the respiratory system, thus allowing accurate assessment of respiratory mechanics measurements. To perform these techniques, airflow, pressure, and volume changes at the mouth must be recorded and analyzed.

As stated previously a model of the respiratory system is considered passive because the lungs respond to forces external to the lungs. The single-compartment linear model is linear because its independent variables $\left(V \text{ and } \dot{V}\right)$ are linearly related to the dependent variable P.

$$P = EV + R\dot{V} + P_0$$

The single-compartment linear model can be made more realistic by adding extra features in two ways: (1) by making it nonlinear and (2) by adding more mechanical degrees of freedom.

The resistive pressure drop can be made nonlinear as follows, which includes two resistive parameters and flow squared:

$$\Delta P = K_1\dot{V} + K_2\dot{V}^2$$

This equation is used to describe a conduit with both laminar and turbulent fluid flow known as the Rohrer's equation.

Further, the elastic pressure nonlinear can be converted as follows:

$$E = L_1V + L_2V^2$$

11.5.2 Resistance, Compliance, Inertance, Tissue Damping, and Elastance

11.5.2.1 Resistance

Resistance during mechanical ventilation describes the airflow conditions during both inspiration and expiration. Resistance represents the flow-resistive elements of the respiratory system. It is expressed as a pressure variation over gas flow using the following general equation:

$$\text{Resistance} = \frac{\Delta\text{Pressure}}{\text{Flow}}$$

By substituting standard units, it becomes

$$\text{Resistance} = \frac{\text{cm}\,H_2O}{\text{ml} \bullet \text{s}^{-1}}$$

Flow, tidal volume, and the dimensions of the ventilator and airway components affect airway resistance. The size of the endotracheal tube is an important element in gas flow through the breathing circuit and thus affects the measured resistance. When delivering a set tidal volume, the volume at a set flow is affected by a smaller and longer tube that will produce larger resistance to gas flow.

11.5.2.1.1 Compliance and Elastance

Compliance is how much a compartment will expand if the pressure in that compartment is changed. A balloon has a high compliance because a small pressure increase inside the balloon will greatly expand the balloon. A rigid tube has a low compliance because a small pressure increase inside the rigid tube will not result in a significant increase in the volume of the rigid tube. Two major forces contribute to lung compliance: tissue elastic forces and surface tension forces. The compliance (C) is determined by the change in elastic recoil pressure (ΔP) produced by a change in volume (ΔV):

$$C = \frac{\Delta V}{\Delta P}$$

The compliance of the lungs (C_L), chest wall (C_{CW}), and respiratory system (C_{RS}) can be determined by measuring the change in distending pressure and the associated change in volume. The distending pressure represents the pressure change across the structure. Where P_{ao}, P_{pl}, and P_{bs} represent the pressure measured at the airway opening, pleural pressure, and pressure at the body surface (atmospheric pressure), respectively.

$$C_L = \frac{\Delta V}{\Delta\left(P_{ao} - P_{pl}\right)}$$

$$C_{CW} = \frac{\Delta V}{\Delta\left(P_{pl} - P_{bs}\right)}$$

$$C_{RS} = \frac{\Delta V}{\Delta\left(P_{ao} - P_{bs}\right)}$$

Lung volume and volume–pressure relationships (e.g., compliance) reflect parenchymal (air space) development, whereas airflow and pressure–flow relationships (resistance and conductance) predominantly reflect airway development. The lungs become stiffer (compliance decreases) at higher lung volumes.

Total respiratory compliance (C_{rs}) is related to lung compliance and chest wall compliance by the following equation:

$$\frac{1}{C_{rs}} = \frac{1}{C_{pulm}} + \frac{1}{C_{CW}}$$

Total static compliance (during no flow activity at the end of inspiration and expiration) and total dynamic characteristics (during active inspiration) are usually monitored via a volume–pressure relationship during mechanical ventilation.

11.5.2.2 Chest Wall Compliance

Chest wall compliance (C_{CW}) describes the changes in tidal volume (V_T) relative to the pleural pressure, reflected by the esophageal pressure (P_{eso}), and is expressed by the following equation:

$$C_{CW} = \frac{V_T}{P_{eso}}$$

To calculate chest wall compliance, the patient should be completely passive. In patients this is usually accomplished by the use of a neuromuscular blocking agent or inducing apnea by hyperventilation, thus removing respiratory drive. Chest wall compliance is an essential component in the calculation of total work of breathing.

11.5.2.3 Lung Compliance

Lung compliance (C_{pulm}) describes the changes in tidal volume relative to transpulmonary pressure $P_{plat} - P_{eso}$ where P_{plat} is the plateau pressure, also referred to as the alveolar pressure, and P_{eso}

is the esophageal pressure under quasistatic conditions.

Lung compliance is expressed by the following equation:

$$C_{\text{pulm}} = \frac{V_{\text{T}}}{P_{\text{plat}} - P_{\text{eso}}}$$

Lung compliance can be obtained on passively or spontaneously breathing patients.

11.5.2.4 Elastance

Elastance is defined as the change in distending pressure divided by the associated change in volume:

$$E = \frac{\Delta P}{\Delta V}$$

Elastance is therefore the reciprocal of compliance; thus, stiff lungs have a high elastance. The end-inspiratory airway occlusion method is clinically used to measure the static compliance of the respiratory system or its reciprocal, elastance of the respiratory system ($E_{\text{st, rs}}$), according to the following equation (Rossi et al. 1998):

$$E_{\text{st,rs}} = \frac{\left(P_{\text{plat}} - \text{PEEP}_{\text{i}}\right)}{V_{\text{T}}}$$

where P_{plat} is plateau pressure obtained after occlusion of the airway, PEEP_{i} is intrinsic positive end-expiratory pressure (PEEP), and V_{T} is tidal volume.

11.5.2.5 Inertance

Inertance of the respiratory system is the analog of inertia and is a measure of the tendency of the respiratory system to resist changes in flow. Forces due to inertance increase with increasing frequency, and since they are opposite in direction to those forces produced by elastance, resistance is thus reduced. At normal respiratory frequencies, inertance is usually insignificant. The inertance I therefore equals $L \times \rho / A$. The pressure drop due to inertance is greatest when the flow increases rapidly, as occurs if the frequency of breathing rises.

11.5.2.6 Tissue Damping

Tissue damping is closely related to tissue resistance and reflects the energy dissipation in the lung tissues. Tissue damping is independent of frequency. In a constant phase model, the calculation of input impedance is

$$z(f) = R_{\text{aw}} + i2\pi f I_{\text{aw}} + \frac{G_{\text{t}} - iH_{\text{t}}}{(2\pi f)^{\alpha}}$$

where

$$\alpha = \left(\frac{2}{\pi}\right) \arctan\left(\frac{H_{\text{t}}}{G_{\text{t}}}\right)$$

R_{aw} represents the resistance of the pulmonary airways to gas flow, I_{aw} is the inertance of the gas in the airways, G_{t} (tissue damping) characterizes viscous dissipation of energy within the lung tissues during inflation and deflation, and H_{t} (tissue elastance) characterizes energy storage in the tissues. G_{t} is thus related to tissue resistance, while H_{t} is related to tissue elastance.

11.5.3 Dynamic Hyperinflation

When breathing on the ventilator with increased time constants secondary to increased inspiratory resistance, hyperinflation develops secondary to incomplete emptying of the lung during expiration. For the patient to generate inspiratory airflow in the next breath, the patient must generate a negative pressure equal in magnitude to the opposing elastic recoil pressures. Secondary to these increased elastic load related to the patient, there is a shift in their compliance curve to the upper less compliant part of the curve. This coupled with a decrease in the efficiency of force generation by their respiratory muscles increases their work of breathing. In a patient breathing on the ventilator, this elevated static recoil pressure leads to intrinsic PEEP or static PEEP_{i}. PEEP_{i} poses a significant inspiratory threshold that has to be fully counterbalanced by increasing inspiratory muscle effort in order to generate a negative pressure in the central airways in order to trigger the ventilator.

11.5.4 Principals and Practice of Classical Measurement of Respiratory System

Most techniques for measuring the mechanics of the respiratory system are based on the assumption that a single balloon on a pipe can model the lung. When breathing is simulated in this model, the balloon is inflated and deflated and the dynamics of the system may be described by the general equation of motion for a linear single-compartment model (SCM):

$$P = EV + R\dot{V} + I\ddot{V}$$

That is, the driving pressure of the system (P) is the sum of its elastic (EV = elastance × volume), resistance $\left(R\dot{V} = resistance \times flow\right)$, and inertive $\left(I\ddot{V} = inertance \times acceleration\right)$ components. For the most practical applications, the contribution of inertance in this equation is negligible and can be ignored. Thus, the equation can be written as follows:

$$P = EV + R\dot{V}$$

If we apply this equation to the respiratory system during mechanical ventilation, dynamic elastance (E_{RS}) (or compliance (C_{RS})) and dynamic resistance (R_{RS}) may be estimated by relating pressure measured at the airway opening (P_{ao}) to simultaneous measurements of flow $\left(\dot{V}\right)$ and volume (V).

The equation of motion for an SCM of the respiratory system is as follows:

$$P_{ao} = E_{RS}V + R_{RS}\dot{V} \qquad (11.11)$$

or

$$P_{ao} = \frac{1}{C_{RS}}V + R_{RS}\dot{V}$$

Similarly, dynamic lung elastance (E_l) and lung resistance (R_l) may be calculated by relating transpulmonary pressure (P_{tp}) to flow and volume. The P_{tp} may be calculated by subtracting pleural pressure estimate form and esophageal catheter (P_{es}) from airway opening pressure measurements ($P_{tp} = P_{ao} - P_{es}$). The equation of motion for an SCM of the lung is

$$P_{tp} = E_l V + R_l \dot{V}$$

11.5.5 Simplified Methods to the Measurement of Total Respiratory Mechanics

There are a number of published articles describing different techniques to measure dynamic respiratory mechanics in children. Below is a summary of some of those techniques.

11.5.5.1 Mead–Whittenberger Technique

Traditionally this technique has been used to measure dynamic compliance (C_{dyn}) and resistance (R_{dyn}) in spontaneously breathing subjects (Mead and Whittenberger 1953). This technique assumes that resistance and compliance are constant throughout inspiration and expiration. Changes in transpulmonary pressure (P_{tp}) are related to changes in flow and volume over the tidal volume range. Compliance is calculated by examining the points of zero flow at end-inspiration and end-expiration. The pressure change and corresponding volume change between these points can be used to determine dynamic compliance, $C_{dyn} = \Delta V / \Delta \dot{V}$, and is measured during expiration. Similarly, dynamic resistance is measured as a change in flow between points of equal volume in the mid-volume range $R_{dyn} = \Delta P / \Delta \dot{V}$. Under these conditions elastic forces are assumed to be equal and opposite.

A limitation of this technique is that the assumption of equality of resistance and compliance throughout both inspiration and expiration may not be true for measurements with evidence of hyperinflation. This may be difficult to apply to ventilated subjects as the points when flow = 0 at mid-tidal and end-tidal volume occur with rapidly changing pressure patterns. Some of these limitations may be overcome utilizing the technique of handbagging the patient during the measurement.

11.5.5.2 Mortola–Saetta Method

This is a method which is a variation of the least-squares regression technique described below. This technique involves occluding the airways of spontaneously breathing subject at end-expiration with a resultant inspiratory effort against the occlusion. This effort results in a pressure change, which is thought to reflect the driving pressure of the respiratory system. When pressure is measured at known intervals from the beginning of inspiration, it can be by the measurement of volume from the corresponding time points during the previous unoccluded breaths and plotted against the flow/volume relationship. In this model, the slope of this relationship is a measure of lung resistance and the intercept is a measure of lung elastance (Mortola and Saetta 1987).

11.5.5.3 Volume Corrected Resistance

As can be inferred by the name, this technique corrects the measurement of resistance from the pressure–flow relationship for changes over the tidal volume range. By plotting pressure divided by flow (R_{dyn}) against volume, resistance can be examined over the tidal volume range (Beardsmore et al. 1986).

11.5.5.4 Forced Oscillation Technique

Forced oscillation technique is a general term for methods that apply broadband flow signals to the airway opening, with a measure of the resulting pressure also at the airway opening or at the body surface (Solymar et al. 1989). This technique allows the calculation of respiratory impedance that includes both the resistive and elastic properties of the system. This technique requires a signal-producing device that is usually either done with a loud speaker or a piston oscillator.

The key measurement considerations when implementing the forced oscillation techniques relate to characteristics of the flow transducer, filtering, error reduction, and sampling. For this technique pressure and flow transducers must be linear over the range of interest. The frequency response of pressure and flow transducers must be adequate over the frequency range investigated. Most importantly, they must be matched. The dynamic common mode rejection ratio of the flow transducer must be high over the frequency range of interest (i.e., input impedance must be high). Appropriate filtering for anti-aliasing must be done, so as to satisfy the sampling theorem. In order to minimize discretization error, the pressure and flow signals must be suitably amplified to occupy a significant fraction of the A/D converter range. Data must be sampled at greater than twice the highest frequency of interest.

The best implementation of the forced oscillation technique requires careful construction of the perturbation signal. This is the flow to be applied to the lungs, and the preferred approach for its constructing is to use composite signals consisting of sums of sine waves; thus,

$$\dot{V}(t) = \sum_{i=1}^{n} A_i \sin\left(2\pi f_i t + \phi_i\right)$$

The frequencies (f_i) of the sine waves are distributed across frequency range of interest. The amplitudes (A_i) of the sine waves are chosen to give good signal to noise at each frequency of interest (e.g., constant). The phases (φ_i) of the sine waves may be chosen randomly. For example, the sine waves can be selected to try to minimize the peak–peak excursions in the final flow signal.

11.5.5.5 Passive Flow–Volume Technique

The passive flow–volume technique involves invoking the Hering–Breuer inflation reflex to relax the respiratory muscles at the end-inspiration after occlusion of the airway (LeSouef et al. 1984). Pressure is measured during this occlusion and the resultant flow–volume relationship during passive expiration is examined. The slope of the flow–volume relationship during passive expiration is examined. The slope of the flow–volume profile during expiration is the expiratory time constant (τ_{exp}), and the extrapolation of this slope to zero flow allows the estimation of the FRC. Compliance is calculated from the ratio of the volume above FRC, at which the occlusion was made, to the end-inspiratory recoil pressure at this volume. Resistance is then calculated by relating (τ_{exp}) to the measured compliance ($\tau_{exp} = RC$; $R = \tau_{exp}/C$). This assumes

a linear relationship over the volume range measured and the inactivity of respiratory muscles during expiration. This assumption is obviously fulfilled when performed in paralyzed subjects; however, the resistive properties of the endotracheal tube may affect the shape of the flow–volume curve especially when a small endotracheal tube is used in infants (Brown et al. 1989).

11.5.5.6 Interrupter Technique

In order to partition respiratory resistance into components representing the conducting airways (R_{aw}) and a peripheral phenomena representing the tissue viscoelastic components P_{dif}, an interrupter technique with occlusion of the airway during expiration can be utilized (Sly and Bates 1988). When the airway is occluded during expiration, there is an initial rapid jump in pressure after occlusion (P_{int}). A slower, secondary rise in pressure to a plateau occurs after occlusion (P_{dif}). This component represents stress recovery within the tissues and the chest wall as well as any redistribution of gas (pendelluft) occurring between different lung units. Thus, this technique allows measurement of R_{aw} (airway resistance including endotracheal tube and chest wall resistance), static elastance, and the viscoelastic properties of the lung from each occlusion. It is important to note that respiratory muscle activity may affect the accuracy of these measurements.

11.5.6 Respiratory Mechanics by Least-Squares Fitting

The single-compartment model of the respiratory system captures the essential mechanical feature of the respiratory system; it can be inflated and deflated to mimic breathing. This model has a single mechanical freedom because its state is completely defined by its compartmental volume. Figure 11.8 illustrates a single-compartment linear model. In this model by choosing the dimensions of the conduit appropriately, we can give it a resistance similar to any particular set of pulmonary airways. By choosing the stiffness of the spring appropriately, we can give the compartment an elastance similar to that of a real lung.

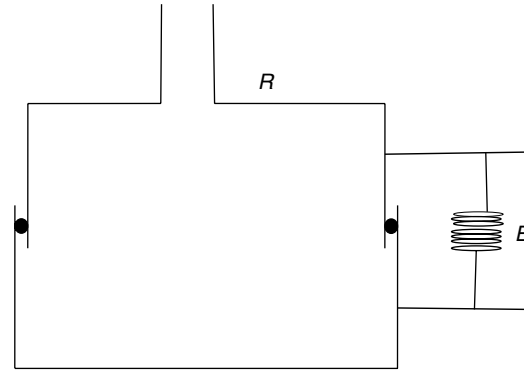

Fig. 11.8 Single-compartment linear model. *R* is the resistance of conduit and *E* is elastance illustrated as a spring. The stiffness of the spring offers an elastance similar to the lung. In this model *R* is resistance and is controlled by choosing the dimensions of the conduit. *E* is elastance and is determined by the stiffness of the spring

Utilizing fitting models to data by least squares, we can make the single-compartment linear model behave like a real respiratory system. If the model were to be driven by the same flow signal as the real system, it would require a pressure signal that is similar to that applied to the real system. This is achieved by choosing appropriate values for the model parameters resistance (R), elastic (E), resting pressure (P_0). The values chosen are required that the behavior of the model matches that of the real system in the "least-squares sense." Fortunately, for the single-compartment linear model, this can be done by multiple linear regressions.

The least-squares regression method of measuring resistance involves relating the driving pressure of the system (P_{dr}) to the corresponding flow (Mortola et al. 1982). Driving pressure is corrected by subtracting the contribution of the elastic and viscoelastic pressure components from transpulmonary pressure (P_{tp}). Then P_{dr} is plotted against flow, and linear regression is used to determine the slope that is the resistance of the system. This technique also assumes a linear relationship of the data. Most physical systems will exhibit approximately linear behavior provided they operate within a sufficiently modest amplitude range. When a system is forced to operate over a large amplitude range, its behavior often becomes highly nonlinear.

Least mean squares analysis minimizes the mean squared error between the measured pressure and the calculated pressure for each sampled point using a particular equation. Multiple linear regressions allow multiple independent variables to be simultaneously included in the regression calculation.

11.5.7 Practical Application and Result Interpretation

Measurement of respiratory mechanics in a relaxed ventilated patient can be obtained using the technique of rapid airway occlusion during constant flow inflation (Rossi et al. 1985a). Rapid airway occlusion at the end of a passive inflation produces an immediate drop in both airway pressure (P_{aw}) and transpulmonary pressure (P_l) from a peak value (P_{peak}) to a lower initial value (P_{init}) followed by a gradual decrease until a plateau (P_{plat}) is achieved after 3–5 s (Rossi et al. 1985b) (Fig. 11.9). P_{init} is measured by back extrapolation of the slope of the latter part of the pressure tracing to the time of the airway occlusion. P_{plat} on the P_{aw}, P_l, and pleural pressure (P_{es}) tracings represent the static end-inspiratory recoil pressure of the total respiratory system, lung, and chest wall, respectively.

11.5.7.1 Elastance/Static Compliance

Total static compliance of the respiratory system ($C_{st,tot}$) is frequently measured and monitored during mechanical ventilation. Total static compliance is the pressure to overcome the elastic forces of the respiratory system for a given tidal volume and under a zero flow (static) condition. The end-inspiratory airway occlusion method is clinically used to measure static compliance of the respiratory system or its reciprocal, elastance of the respirator system ($E_{st,rs}$), according to the following equation (Foti et al. 1997):

$$E_{st,rs} = \frac{\left(P_{plat} - PEEP_i\right)}{V_T}$$

where P_{plat} is plateau pressure obtained after occluding the airway. $PEEP_i$ is intrinsic PEEP and

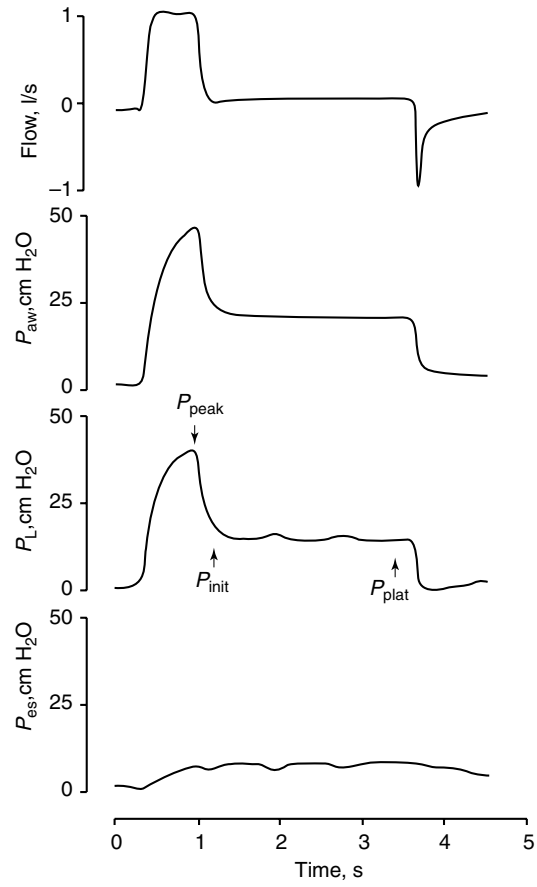

Fig. 11.9 Flow (inspiration upward), P_{aw}, P_l, and P_{es} tracings in a representative patient during passive ventilation. An end-inspiratory occlusion produced a rapid decline in both P_{aw} and P_l from P_{peak} to a lower P_{init}, followed by gradual decrease to P_{plat} (From Jubran and Tobin (1997))

V_T is tidal volume. Using an esophageal balloon catheter, $E_{st,rs}$ can be partitioned into its lung and chest wall components by dividing (P_{plat}–$PEEP_i$) by V_T on the P_l and P_{es} tracings, respectively.

Specific measuring conditions must be met for a valid static compliance value including passive tidal volume (inspiration and expiration) and compressible volume correction for tubing; the plateau must have an end-inspiratory pause of at least 1 s with a stable pressure within 0.5 cm H_2O over 2 readings at least 10 ms apart.

Changes in static compliance are associated with changes in lung elasticity; lung pathology that increases lung recoil or decreases lung volume will decrease the static compliance.

11.5.7.2 Dynamic Compliance

Formerly known as the effective dynamic compliance, the dynamic characteristics (DynChar) can be derived by dividing the ventilator delivered V_T by (peak P_{aw} – PEEP). Since the relationship of volume versus pressure during a dynamic event is subject to resistive forces inside the system, it is not considered a measure of dynamic compliance.

Total dynamic characteristics describe the components of total lung or parenchymal compliance plus the pressure required to overcome the airway resistance in the delivery of a tidal volume. Dynamic characteristics thus reflect resistive and elastic properties of the respiratory system. It is the tidal volume relative to the peak airway pressure under a dynamic condition and is expressed by the following relation:

$$\text{DynChar} = \frac{V_T}{\text{PIP} - \text{PEEP}}$$

Trended values are thus clinically helpful reflecting resistive and elastic properties of the respiratory system.

Figure 11.10 is a volume–pressure loop from a constant flow mode of ventilation. The slope of AC reflects the total dynamic characteristics of the respiratory system.

The difference between static compliance and dynamic characteristics can be used as an indirect index of flow-resistive properties of the respiratory system.

Alternatively, dynamic elastance of the respiratory system ($E_{dyn,rs}$) can be obtained by dividing the difference in P_{aw} at points of zero flow by delivered V_T (Nicolai et al. 1993). Accordingly, $E_{dyn,rs}$ can be computed according to the formula:

$$E_{dyn,rs} = \frac{P_{init} - \text{PEEP}_i}{V_T}$$

$E_{dyn,rs}$ can be partitioned into its lung ($E_{dyn,L}$) and chest wall components by dividing ($P_{init} - \text{PEEP}_i$) pm P_l and P_{es} tracings.

11.5.7.3 Pressure–Volume Curves

A pressure–volume curve of the respiratory system can be constructed in a paralyzed patient by measuring the airway pressure as the lungs are progressively inflated with a 1.5–2 l syringe. A lower inflection point and an upper inflection point may be seen on the pressure–volume curve (Fig. 11.11) (Mergoni et al. 2001). A lower inflection point is thought to reflect the point at which small airways and alveoli reopen, corresponding to closing volume. It has been recommended that the PEEP level should be set slightly above this closing volume (Mergoni et al. 2001).

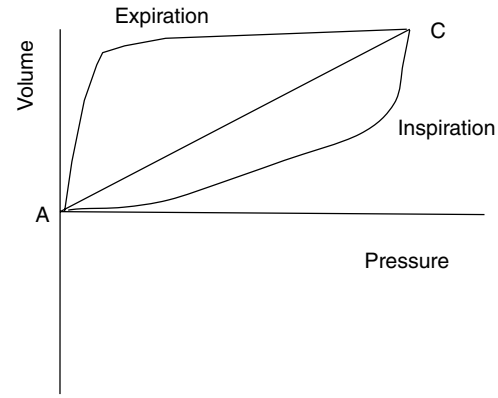

Fig. 11.10 Volume–pressure loop from a constant flow mode of ventilation. The slope of AC reflects the total dynamic characteristics of the respiratory system. Pressure–volume loop of patient's lung with acute respiratory distress syndrome

11.5.7.4 Resistance

Airway resistance can be measured in ventilator patients by using the technique of rapid airway occlusion during constant flow inflation (Polese et al. 1991). This technique implies that flow is interrupted at the end of inspiration while pressure is kept constant during a period of time (pause time). The interrupter technique is only valid when the ventilator operates in a constant flow mode that means that flow is constant throughout inspiration. Resistance in mechanical ventilation describes the airflow condition during both inspiration and expiration. Resistance represents the flow-resistive elements of the respiratory system. It is expressed as a pressure variation over gas flow using the following general equation:

$$\text{Resistance} = \frac{\Delta\text{Pressure}}{\text{Flow}}$$

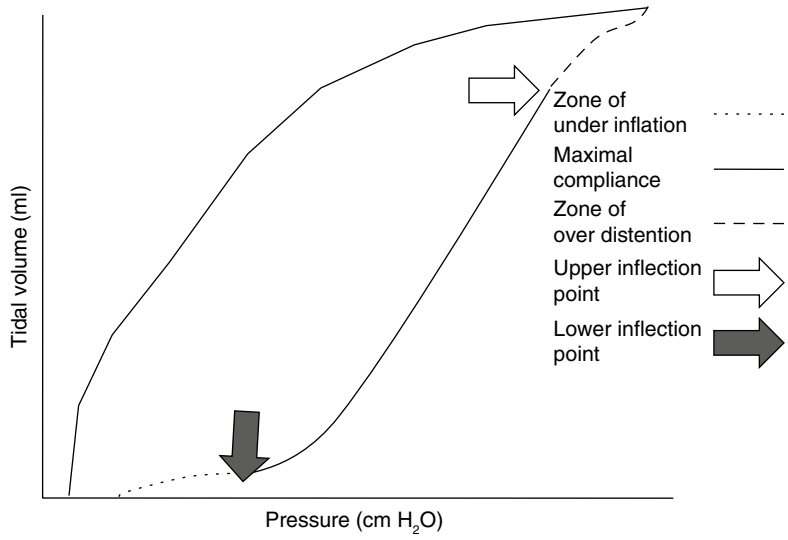

Fig. 11.11 In this loop airway pressure continues to increase beyond the zone of maximal compliance, and the inspiratory limb flattens into the zone of overdistension (*dashed line*). This portion of the *curve* represents alveolar overdistension and decreased compliance. The point at which this occurs is called the upper inflection point (*UIP*). The airway pressure at the upper inflection point identifies the pressure beyond which alveolar overdistension occurs

By substituting standard units, it becomes

$$\text{Resistance} = \frac{\text{cm}\,H_2O}{\text{ml} \bullet \text{s}^{-1}}$$

Airway resistance is affected by flow, tidal volume, and the network dimensions. The size of the endotracheal tube is an important element in gas flow through the breathing circuit and thus affects resistance. When delivering a set tidal volume at a set flow, smaller and longer tubes will produce larger resistance to gas flow.

When a ventilator operates in a constant flow mode, the resistive elements of the respiratory system/breathing circuit can be visualized and calculated with the pressure–time waveform (Fig. 11.12). The pressure–time waveform begins with an exponential rise to peak inspiratory pressure.

The first step is a function of flow and resistance during the initial portion of inspiration. The higher the step, the larger the resistance. The second portion of the waveform is a linear increase to peak inspiratory pressure and is a function of flow being constant throughout inspiration. This second portion represents the elastic properties of the respiratory system.

As peak inspiratory pressure is reached, a pause time or plateau is maintained, while pressure inside the airways and the breathing circuit equilibrates at plateau pressure (P_{plat}). Flow then stops while pressure equilibrates.

Figure 11.12 is a pressure–time waveform from a constant flow mode of ventilation and illustrates various elements related to resistive and elastic properties of the respiratory system.

Inspiratory resistance is the difference between PIP and P_{plat} over flow value at PIP, as expressed by the following equation:

$$R_I = \frac{\text{PIP} - P_{plat}}{\text{PIF}}$$

Expiratory resistance is the difference between P_{plat} and total PEEP over flow value at the onset of exhalation, as expressed by the following equation:

$$R_E = \frac{\text{PIP} - \text{PEEP}_{TOT}}{\text{Flow at onset of exhalation}}$$

11.5.7.4.1 Limitations

Specific measuring conditions must be met for a valid inspiratory and expiratory resistance value which includes a passive tidal volume (inspiration and expiration) and constant flow over a fixed inspiratory time for inspiratory resistance only; the P_{plat} must have an end-inspiratory pause of at least 1 s with a stable pressure within 0.5 cmH_2O over 2 readings at least 10 ms apart.

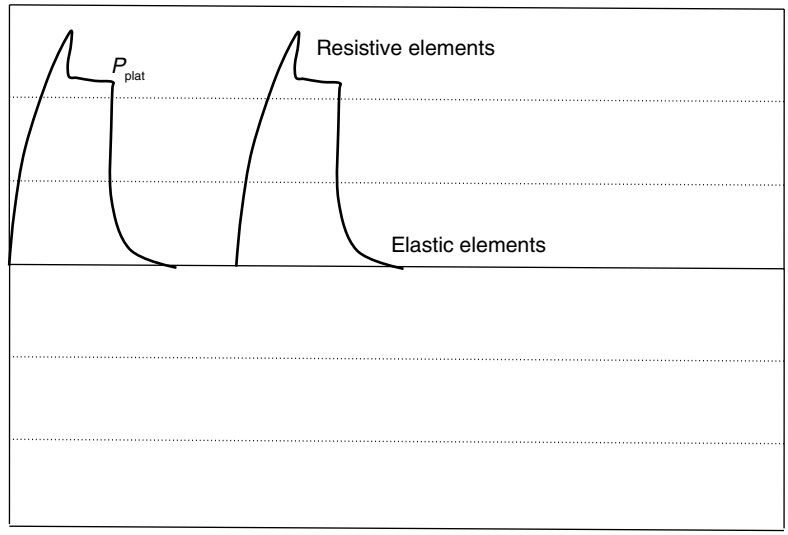

Fig. 11.12 When a ventilator operates in a constant flow mode, the resistive elements of the respiratory system/breathing circuit can be visualized and calculated with the pressure–time waveform

11.6 Respiratory Time Constants

11.6.1 Time Constants: Basic Meaning and Concepts of Intrapulmonary Pressure Equilibration

The time constant of the lung (TC) is a concept borrowed from electrical engineering that describes the phenomenon whereby a given percentage of a passively exhaled breath of air will require a constant amount of time to be exhaled regardless of the starting volume given constant lung mechanics. Exponential functions are often described with time constants, designated by the Greek letter τ (tau). The time constant characterizes the rate of variation of the function over a period of time. Short time constants imply a fast rate of change and, vice versa, long time constant implies a slow rate of change.

During quiet breathing, equilibration between alveolar and mouth pressures occur at both the end of expiration and the end of inspiration such that time constants of the respiratory units are relatively small (0.01 s). Therefore, during quiet breathing the change in volume divided by the change in pleural pressure is dynamic compliance of the respiratory system and is the same as the static compliance. In the normal lung, since the time constants are small and equilibration between alveolar and mouth pressure still occurs, increases in breathing frequency to rates of 80/min do not affect the measured compliance. In contrast, in patients with peripheral airway disease, with more rapid breathing, the time constants of at least some of the respiratory units are increased so that equilibration between the alveolar and mouth pressure does not occur at either end-inspiration or end-expiration. Accordingly, the volume change with a given pleural pressure change falls with increasing respiratory rate, and the compliance is said to be frequency dependent (Woodcock et al. 1969).

Changes in dynamic compliance with increasing respiratory rate in patients with relatively normal expiratory flow rates may be marked. Woodcock et al. (1969) found that the dynamic compliance was reduced to less than 50 % of static compliance in mild asthmatics breathing at a respiratory frequency of 80/min. A large proportion of the decrease in dynamic compliance owes to the pendelluft effect where at times of zero flow at the mouth, air flows from one region to another. This mechanism is illustrated in Fig. 11.13. During inspiration, alveolus 1 fills more rapidly than alveolus 2 because of the increased airway resistance of the airways leading to alveolus 2 and hence its larger time constant. If the inspiratory time is short, alveolus 2 never becomes completely filled. Then on expiration, the pressure in alveolus 1 is higher than the pressure in alveolus 2 because of its larger volume; therefore, flow goes not only from

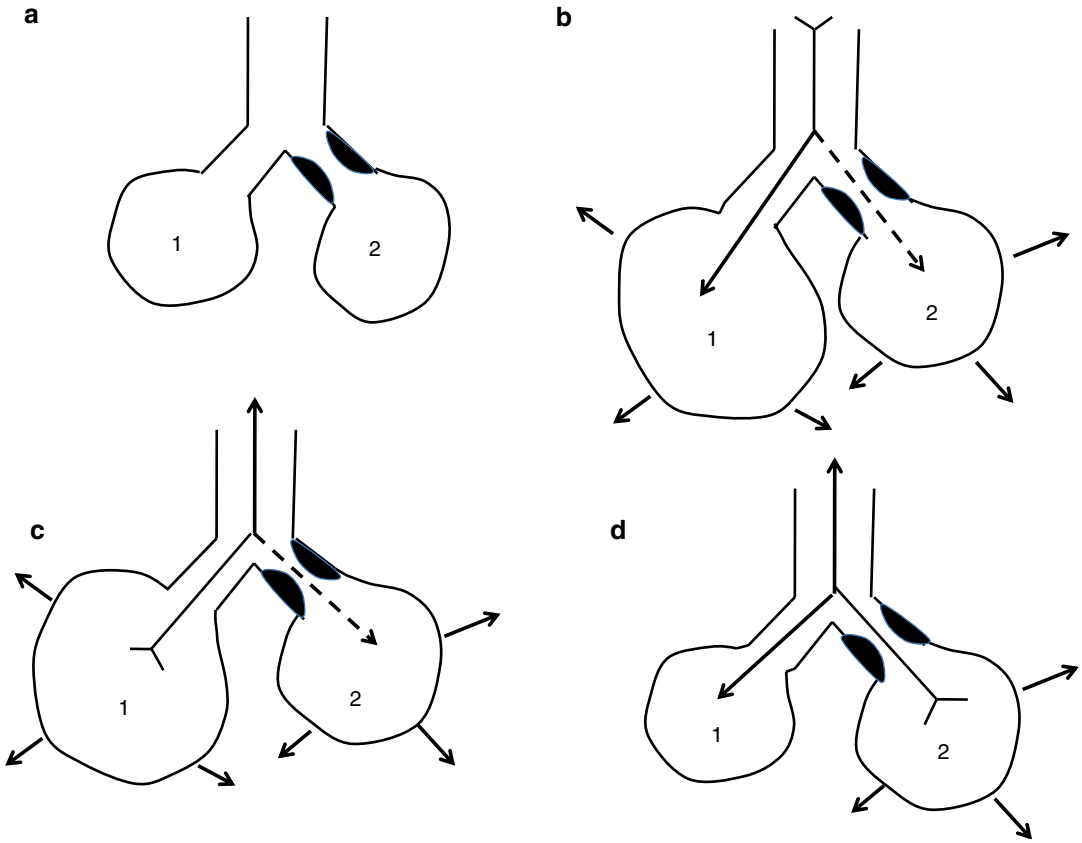

Fig. 11.13 Effects of uneven time constants on ventilation. The airway leading to unit 2 is partially obstructed and therefore unit 2 has a longer time constant. After a slow expiration (**a**), the units have the same size. With a rapid inspiration (**b**), unit 1 fills more than unit 2 because it has a faster time constant. Shortly after the start of a rapid expiration (**c**), air moves not only from unit 1 to the airway opening but also from unit 1 to unit 2 because the pressure in unit 2 is less than pressure in unit 1. During the later phases of expiration (**d**), flow moves from unit 2 to unit 1. As the respiratory rate is progressively increased, the tidal volume of the abnormal region becomes smaller and smaller

alveolus 1 to the mouth but also from alveolus 1 to alveolus 2. The higher the frequency, the lower the tidal volume to the abnormal region.

Tests of dynamic compliance are sensitive indicators of peripheral airway disease. The time constants of the lung units distal to airway 2 mm in diameter are on the order of 0.01 s. Fourfold increase in some time constants is necessary to cause dynamic compliance to become frequency dependent.

Time constants of the respiratory units markedly influence the distribution of ventilation. A second factor that is influential is the regional differences in pleural pressures. Owing to the regional differences in pleural pressure, dependent parts of the lung are ventilated better. Other factors that influence the distribution of ventilation are the interdependence that exists between adjacent lung units and the presence of collateral pathways for ventilation.

11.6.1.1 Concepts of Intrapulmonary Pressure Equilibration

A model can be constructed in which the alveoli are represented by an elastic sac and the intrathoracic airways by a compressible tube, both of which are enclosed within a pleural space. The concept of an equal pressure point (EPP) described by Mead is when sufficient expiratory effort is generated then the pleural pressure becomes positive, and in this situation the intrabronchial pressure at some point

along the airways is equal to the pleural pressure extrabronchial pressure. The EPP divides the airways into two components arranged in series with an upstream segment from the alveoli to the equal pressure point, where the distending pressure of the bronchi is positive, and a downstream segment from the EPP to the airway opening, where the distending pressure of the bronchi intrathoracic is negative. In these downstream segments collapse will occur during forced expiration.

There is no EPP when the pleural pressure is subatmospheric. However, when the pleural pressure becomes atmospheric, the EPP is at the airway opening. The EPP moves upstream as the pleural pressure becomes more positive. The alveolar pressure minus the pleural pressure represents the pressure drop from the alveolus to the EPP. This pressure represents the elastic recoil pressure of the lung. The resistance of the upstream segment is designated Rus. Therefore, flow is

$$\dot{V} = P_{st(L)} / R_{us}$$

$P_{st(L)}$ is constant at a constant lung volume. Thus, $\dot{V}$ can only increase if R_{us} decreases, which can be accomplished by moving the EPP upstream. The movement of the EPP upstream is caused by more and more effort until the pleural pressure reaches a level at which further increases in it do not lead to further increase in $\dot{V}$. This lack of change in flow is called $\dot{V}_{max}$ and corresponds to point on pressure–flow curve where the waveform is flat.

$\dot{V}_{max}$ is dependent on two factors:

$$\dot{V}_{max} = P_{st(L)} / R_{us}$$

R_{us} is the resistance of the upstream segment and $P_{st(L)}$ being the recoil pressure of the lung. Thus, in reducing $\dot{V}_{max}$ a decrease in elastic recoil of the lung is just as important as is increased airway resistance.

Figure 11.14 represents a model described by Pride (Pride et al. 1967) where the airways are divided into two rigid tubes connected in series by a short segment of a collapsible tube. The airways are divided into an upstream segment between the alveoli and airways into an upstream segment between the alveoli and the distal end of the collapsible segment to the airway opening. They defined the critical closing pressure of the collapsible segment (P'_{tm}) as the transmural pressure (P_{tm}), at which the segment collapsed. Thus, the transmural pressure, in this distensible object, is the pressure inside the wall minus the pressure outside the wall. The value of P'_{tm} represents the necessary distending pressure to maintain the collapsible segment patent. So this segment would be fully open when the distending pressure exceeds P'_{tm} and fully collapsed when P_{tm} fell below P'_{tm}. Calculation of the transmural pressure in the collapsible segment is

$$P_{tm} = P_A - \left(\dot{V} \times R_s\right) - P_{pl}$$

where R_s is the resistance of the segment upstream from the collapsible segment. Since

$$P_A = P_{st(L)} + P_{pl}$$

then

$$P_{tm} = P_{st(L)} - \left(\dot{V} \times R_s\right)$$

Therefore, as $\dot{V}$ increases, P_{tm} decreases. When $\dot{V}$ increases to a critical level ($\dot{V}_{max}$), P_{tm} drops to P'_{tm}. This is demonstrated in Fig. 11.14 where $P_{tm} = 6 - 6 = 0$ and it is assumed $P'_{tm} = 0$. If flow rates increase more, as seen in Fig. 11.14, the P_{tm} would fall below P'_{tm} and there would be no flow due to the collapse of the segment (Fig. 11.14d). However, in this situation the intrabronchial pressure becomes the same as the alveolar pressure, due to the absence of flow, and P_{tm} would exceed P'_{tm} and flow would resume. If the collapsible segment opens all the way, $\dot{V}$ again exceeds $\dot{V}_{max}$, P_{tm} falls below P'_{tm} and airflow ceases. Thus, the best way to explain this interrelationship is to consider the collapsible segment as a variable resistor illustrated in Fig. 11.14e, f. Partial collapse of the segment occurs when pleural pressure is reached to level necessary to cause collapse with P_{tm} equal to P'_{tm}. While pleural pressure increases further, there is a corresponding pressure drop across the collapsible segment. So as can be seen in Fig. 11.14b, e, f, once flow limitation is met, flow and intrabronchial pressure downstream do not change. If we examine this from our mathematical model, we recognize that flow limitation

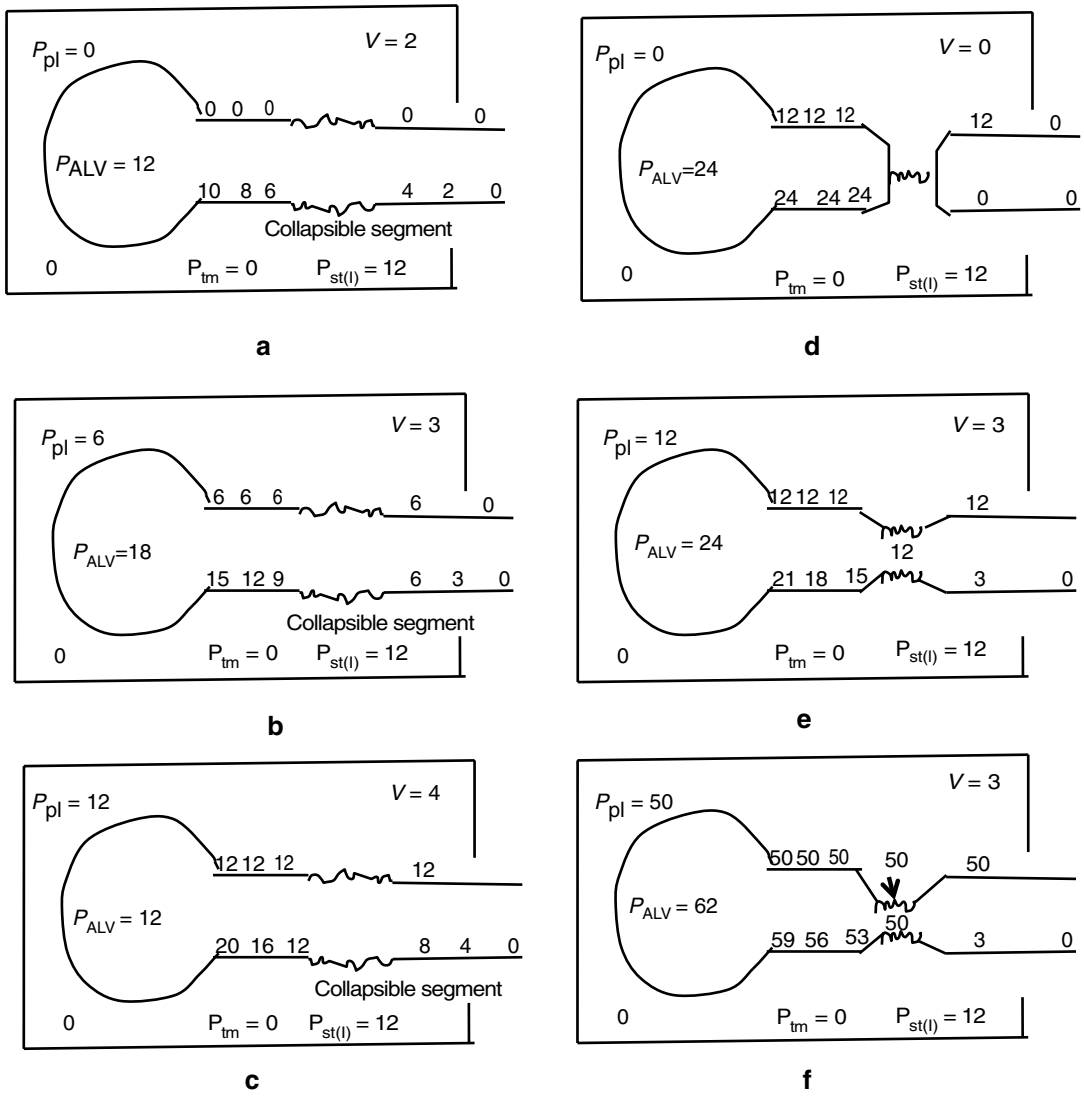

Fig. 11.14 A schematic representation of the collapsible-segment concept. In these diagrams the lung volume is that giving a $P_{st(I)}$ of 12 and it is assumed that P'_{tm} is zero. (**a**) Pressure along the airways when P_{tm} still exceeds P'_{tm}. There is no collapse. (**b**) Pressure along the airways when P_{tm} approaches P'_{tm}. Note that the flow rate increases from (a). (**c**) Pressures along the airways when pleural pressures are increased more. Note that P_{tm} at the collapsed segment is now $8-12=-4$ which is below $P'_{tm}=0$, so this higher flow is impossible since the collapsible segment must collapse. (**d**) Pressures along the airways when there is no flow. Now P_{tm} is $24-12=12$, so the airway must open. (**e**) Pressure along the airways when the collapsible segment is partially collapsed such tat $P_{tm}=P'_{tm}$. (**f**) Pressures along the airways when the collapsible segment is partially collapsed such that $P_{tm}=P'_{tm}$. (**f**) Pressures along the airways when the alveolar pressure is raised much higher. Note that the collapsible segment is more collapsed than in (e) and that the flows in (b, e, and f) are also identical. The airway pressures downstream from the collapsible segment in (b, e, and f) are also identical

occurs when $P_{tm}=P'_{tm}$. If we substitute P_{tm}'s for P_{tm} in our previous equation, then

$$P'_{tm} = P_{st(L)} - \dot{V}_{max} \times R_s$$

or can be rewritten to calculate maximum flow as

$$\dot{V}_{max} = \left(P_{st(L)} - p'_{tm}\right) / R_s$$

Thus, $\dot{V}$ max depend upon three different factors: (1) the resistance of the upstream segment (R_s), (2) the elastic recoil of the lung ($R_{st(L)}$), and (3) the tendency of the airways to collapse (P'_{tm}). Clinical examples of this relationship with reduced flow rate during expiration can be seen in asthma with constriction of the bronchial smooth muscles increasing the tendency of the airways to collapse (P'_{tm}) and thereby reduce flow rates, and the lungs cannot empty to a lung volume below which P'_{tm} exceeds $P_{st(L)}$.

11.6.2 Measurement of the Time Constant

The pressure applied by the ventilator and the respiratory muscles is necessary to overcome the extrinsic and intrinsic forces on the lungs and chest wall during ventilation in intubated patients.

Theoretically, inspiratory volume production is active and can be forced by external pressure application; but since exhalation is passive, it cannot. Thus, time is required to empty the lungs and that time depends on the expiratory time constant.

Expiratory time constant is defined as the product of the total respiratory system compliance and the total expiratory resistance. While the former is determined by factors internal to the subject, the latter is the sum of airway resistance, any viscous tissues resistance, and externally applied resistance, such as valves and hoses in intubated patients. The calculation of the expiratory time constant requires knowledge about all of these elements and thus the measurement of flow and pressure at the airway opening.

The actual expiratory time constant can be calculated as (Brunner et al. 1995)

$$\left(R_{rs} + R_{ext}\right) \bullet C_{rs}$$

R_{rs} is the resistance of the respiratory system, R_{ext} the resistance of the expiratory valve and circuit, and C_{rs} the compliance of the total respiratory system. The expiratory resistance of the ventilator, R_{ext}, can be measured separately by dividing the pressure drop with a flow rate directed through the expiratory valve and hoses: (R_{ext} = AP/AV prime).

11.6.3 Simplified Approach (Analysis of the Flow–Time Curve and the Flow–Volume Loop)

11.6.3.1 Flow–Time Curve

In mechanical ventilation, for practical purposes, an event is considered complete after three time constants. For the adult respiratory system, the normal time constant is 0.79 s.

The actual value of one time constant is obtained through the product of compliance × resistance:

$$\tau = C \times R$$

$$\tau = \frac{\text{ml}}{\text{cm}\,H_2O} \times \frac{\text{cm}\,H_2O}{\text{ml} \bullet \text{s}^{-1}}$$

As an example, a system with a total lung/thorax static compliance of 60 ml/cm H_2O, an expiratory resistance of 0.13 cm H_2O/ml, and no auto-PEEP has a time constant τ of

$$\tau = C \times R$$

$$\tau = \frac{60\text{ml}}{\text{cm}\,H_2O} \times 0.13\text{cm}\,H_2O / ml / s$$

$$\tau = 0.78s$$

Figure 11.15 illustrates a flow–time waveform during a constant pressure mode of ventilation with a short and long time constant. In a decaying exponential function, a time constant of 0.78 s means that after one time constant (0.78 s) the value of the variable on the *y*-axis decreases to 37 % of its final value; after two time constants (1.56 s), it decreases to 13.5 % of its final value; and after three time constants (2.34 s), the value of the variable on the *y*-axis decreases to 5 % of its final value.

In this example of a flow–time waveform from a constant flow mode of ventilation (Fig. 11.16),

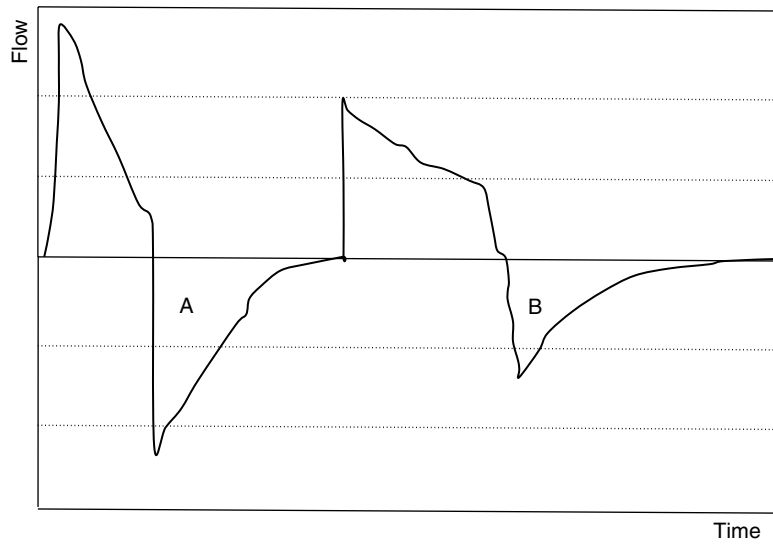

Fig. 11.15 Flow–time waveform from a constant pressure mode of ventilation. *A* represents an exponential function with a short time constant. *B* represents exponential function with a long time constant

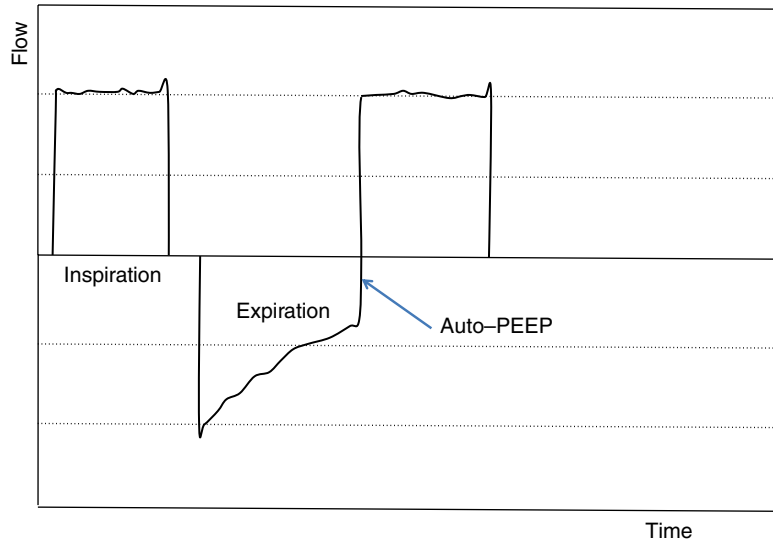

Fig. 11.16 Flow–time waveform from a constant flow mode of ventilation. Tracing reveals increased resistance with evidence seen with the linear decay during expiration with a slow decay to baseline with nonzero flow conditions at the end of expiration with evidence of auto-PEEP

if the expiratory time is shorter than 2.34 s (3×0.78), air trapping will be present, causing auto-PEEP.

To prevent auto-PEEP and air trapping, the expiratory time should always be longer than three time constants.

11.6.3.2 Flow–Volume Loop

The flow–volume loop (Fig. 11.17) has an inspiratory and expiratory phase. During the inspiratory phase, there is a rapid rise to peak inspiratory flow throughout inspiration with a rapid decay from peak inspiratory flow to baseline. In expiration there again is a rapid decay to peak expiratory flow, and then the flow progressively returns to baseline. During a constant flow mode of ventilation, resistive changes are not reflected in the inspiratory profile. An airflow limitation that is reflective of resistive changes is associated with a convex (to the volume axis) shape of the second phase of the expiratory profile of the loop. These changes are reflective of dynamic changes and no static characteristics of the respiratory system can described with a flow–volume loop.

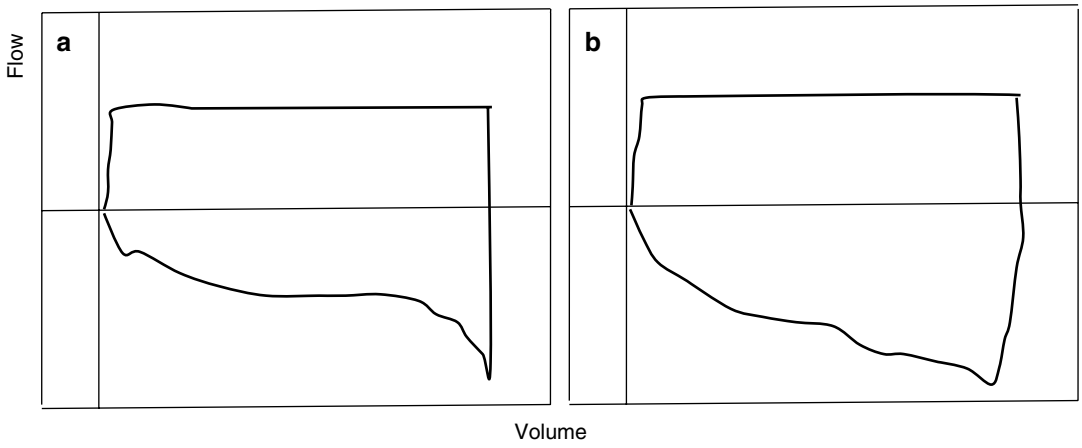

Fig. 11.17 Flow–volume loop from a constant flow mode of ventilation. Tracing (**a**) illustrates increased resistance and (**b**) normal resistance. In tracing (**a**) increased resistance can be seen with linear return to baseline

11.7 Lung Volume Measurements in the Ventilated Patient

11.7.1 Techniques and Methods

In order to use measurement of respiratory mechanics in clinical decision making for mechanically ventilated patients, some measurement of volume is required. Volume in mechanically ventilated patients can consist of the volume delivered by the ventilator or some measurement of the patient's actual lung volume. The discussion below will first discuss measurement of volume by the ventilator and on methods of measuring the patient's actual lung volumes.

11.7.1.1 Measurement of the Delivered Volume by the Mechanical Ventilator

Volume (V) can be obtained by numerically integrating flow $\left(\dot{V}\right)$ by a computer. The trapezoidal rule is sufficient for virtually all respiratory applications, provided $\dot{V}$ is sampled rapidly enough (50 Hz or more). Thus, this integration can be accomplished when

$$V = V_0 + \sum_{0}^{N} \Delta V_i \quad \text{where} \quad \Delta V_i = \left(\frac{\dot{V}}{2} + \frac{\dot{V}_{i+1}}{2} \right) \delta t$$

δt is the time interval between data samples and V_0 is the value of volume at the start of the integration process (Fig. 11.18).

Integration of flow invariably leads to a drift in the resulting volume signal. This can be due to a number of factors, including non-unit respiratory exchange ratio, differences in a temperature and humidity between inspired and expired gas, and slight errors in calibrating the zero flow point. Accurately accounting for all these effects is not practical, so one is left with having to remove volume drift in whatever way seems reasonable.

11.7.1.2 Measuring the Specific Lung Volume of the Patient

To measure specific lung volumes, a number of techniques have been used including CT measurements. Computed tomography (CT) can provide an accurate measurement of tissue mass and volume (Mull 1984). CT allows computation of both tissue mass and gas volume of the lung due to the fact that lung tissue has a physical density close to water density (Denison et al. 1986). This technique has been used by investigators to measure changes in EELV and to quantify alveolar recruitment both in an animal (Pelosi et al. 2001) and human (Gattinoni et al. 1988) studies. However, despite the fact that CT scanners are readily available to most clinicians, this measurement is limited by the risks associated with transporting such critically ill patients and its clinical relevance in

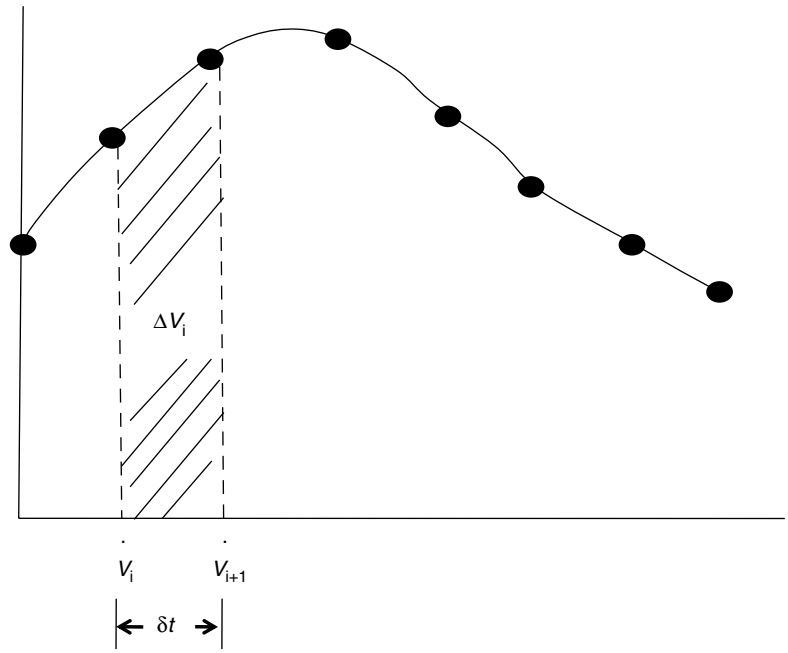

Fig. 11.18 The area under the *flow curve* is approximated as the sum of all the ΔV_i

patients with rapidly changing clinical status. An alternative technique has been to use a dilution technique based on dilution of tracer gases to measure the EELV in mechanically ventilated patients (Kendrick 1996). However, these techniques have been limited to experimental protocols due to the considerable expense required for the monitoring equipment. Simplified techniques have been proposed but require further validation to gain wide spread use (Patroniti et al. 2004).

11.7.2 Result Interpretation and 7.3 Limitations, Drawbacks, and Unknowns

During mechanical ventilation volume is not directly measured by the ventilator but is calculated from the flow signal. Any error in measurement of flow will decrease the accuracy of the measurement of the volume. There are numerous sources of error as it relates to the measurement of flow. For volume measurement to be accurate then all volume delivered to the patient has to be measured. Thus, the first source of error would be loss of volume within the ventilator circuit resulting from compression volume of the circuit. In the inflation phase, pressure rises within the ventilator circuit causing elongation and distension of the tubing and compression of the gas within the circuit. The volume stored in the circuit never reaches the patient but is instead released through the exhalation valve and is measured with the exhaled gases from the patient. The magnitude of compression volume is determined by the volume within the ventilator, circuit, and humidifier. This volume loss theoretically can be affected by a number of factors, including temperature and humidity of the circuit, and patient factors such as changes in the patient's compliance and resistance. In a recent study, the reported differences in the measured compliance of the circuit by the manufacturer and those measured by the ventilator were between 37 and 65 % for the infant circuit and 13–23 % for the adult circuit (Heulitt et al. 2009a). Because this factor is collected at start-up of the ventilator and includes any compression volume in the ventilator and humidification system, this number will be higher. It was found that the compensation measured in the circuit and ventilator system was 51 and 18 % higher, respectively, than could be expected from the compression volume calculated using the compliance factor of the circuit alone. Thus, if only the circuit compliance factor is used, then the volume measured at expiration,

which accounts for both volume of the circuit and volume delivered to the patient, will be higher than the calculated effective volume.

Another potential source of error during the measurement of volume is the timing of the measurement of the flow. For accurate measurement of the flow, it should be begun at the beginning of the breath and ended when the system returns to baseline. To accurately measure the begging of the breath, it should correspond to the time point when the initial flow crosses the zero line for flow signaling patient triggering or opening of the inspiratory valve in controlled breaths. Unfortunately, these two time points can correspond to times of high turbulence thus high signal noise. Thus, it is common for mechanical ventilator measuring algorithms to avoid these areas thus decreasing the potential accuracy of volume measurement.

Future Perspectives

There have been major advances in the availability of performing lung function tests in infants and children. However, the application of these tests to patients who are on mechanical ventilation continues to be limited outside of its use in research. Future direction has to expand our knowledge of the natural course of pulmonary involvement in infants and children and its implications on subsequent care. Currently infants and children who have a history of pulmonary insult comprise a difficult population and consume considerable resources and time to care for them. Our lack of understanding of the natural course of these patients disease process impacts our ability to perform measurements of respiratory mechanics because many of the assumptions we use in making measurements of lung volumes and mechanics may not be true. Future advances will require techniques that are reproducible and can easily be applied to clinically unstable patients. These new techniques have to be able to address the issue of inaccuracies in displayed values of tidal volume, interactions between the ventilator and spontaneous breathing activity, and issues created by potential leak around the endotracheal tube. Some of these issues could be addressed, for example, by the use of cuffed endotracheal tubes that may pose very little risk to the patient outside of the neonatal period (Newth et al. 2004). Others will require better understanding of both the natural course of pulmonary development but also elucidation of the mechanism by which insults affect this development.

Essentials to Remember

- The respiratory system is not a linear system; resistance and compliance are not constants. They are dependent upon volume, volume history, and flow.
- A model of the respiratory system is considered passive because the lungs respond to forces external to the lungs.
- In order to overcome the impedance of the respiratory system and to allow gas flow to occur, work must be performed.
- The resistance to airflow in a tube depends on the type of flow, the dimensions of the tube, and the viscosity and density of the gas. Airflows through tubes can either be laminar or turbulent.
- The airway pressure is the force that the mechanical ventilator and patient apply on the respiratory system.
- Resistance during mechanical ventilation describes the airflow conditions during both inspiration and expiration. Resistance represents the flow-resistive elements of the respiratory system.
- The time constant characterizes the rate of variation of the function over a period of time. Short time constants imply a fast rate of change and, vice versa, long time constants imply a slow rate of change.

11.8 Respiratory System Pressure-Volume Curve

11.8.1 Static Pressure–Volume Curve

Peter A. Dargaville

Educational Aims

This chapter aims to give an understanding of:

- The methods of generation of static or quasistatic pressure–volume (PV) curves, including the associated methodological considerations and sources of error
- The important landmarks on the inflation and deflation limbs of the *PV* curve and their relationship to expansion and aeration of lung units
- The theoretical potential and clinical experience of using PV landmarks to guide PEEP setting in the diseased lung

11.8.1.1 Introduction

The pressure–volume (*PV*) behavior of the lung has been a subject of some fascination for pulmonary researchers and clinicians for nearly a century (Mead 1996). Perhaps equally fascinating is that, despite a large body of literature detailing the landmarks of the *PV* curve and their significance, the place of the *PV* curve as a tool to guide clinical management remains undecided (Dreyfuss and Saumon 2001; Terragni et al. 2003; Gattinoni et al. 2005; Maggiore et al. 2003; Harris 2005; Albaiceta et al. 2008; Blanch et al. 2009). This chapter will summarize current knowledge of static or quasistatic *PV* curves in mechanically ventilated subjects. The different methods of mapping the *PV* relationship will be outlined. The important landmarks of the *PV* curve and their lung morphological correlates will be identified and their relative value in guiding ventilator pressure settings discussed.

11.8.1.2 The "Static" Pressure–Volume Curve

11.8.1.2.1 Measurement of the Static *PV* Curve: Methods, Conditions, and Error Sources

11.8.1.2.1.1 Generation of a Pressure–Time Curve: The Basis of *PV* Mapping

A static *PV* curve describes the volumetric response of the lungs or the respiratory system to sequential transpulmonary pressure (P_{TP}) changes which generally take the lung from a point at or above elastic equilibrium volume to total lung capacity (TLC) and back. In some cases only a portion of the curve, usually the early part of the inflation limb, is mapped. Whether P_{TP} is generated via negative intrapleural pressure in a spontaneously breathing individual, or application of positive pressure at the airway opening, to eliminate resistive pressure drop, truly static *PV* mapping requires a period of equilibration at zero flow after each pressure step. Even with a long pause following each pressure alteration, as is achievable in the ex vivo lung or experimental animal, pressure rarely stabilizes completely (Fig. 11.19). In the ventilated human subject, the need for tidal ventilation to sustain life necessitates the use of shorter equilibration periods at each target pressure during *PV* curve tracing.

The following review of the methods used to obtain *PV* curves focuses on those that can be applied in ventilated human subjects.

Super-Syringe Technique

Application of positive pressure at the airway opening using a large graduated syringe (super syringe) is a time-honored method of generating *PV* curves in both experimental animals (Rimensberger et al. 1999) and ventilated adults with acute respiratory distress syndrome (ARDS) (Matamis et al. 1984; Gattinoni et al. 1987a). The syringe is connected directly to the endotracheal tube and the plunger moved in regular volume steps, with a pause of around 3 s after each. Once a predetermined peak airway pressure is reached (up to 40 cm H_2O in adults), the volume is withdrawn in the same way. The

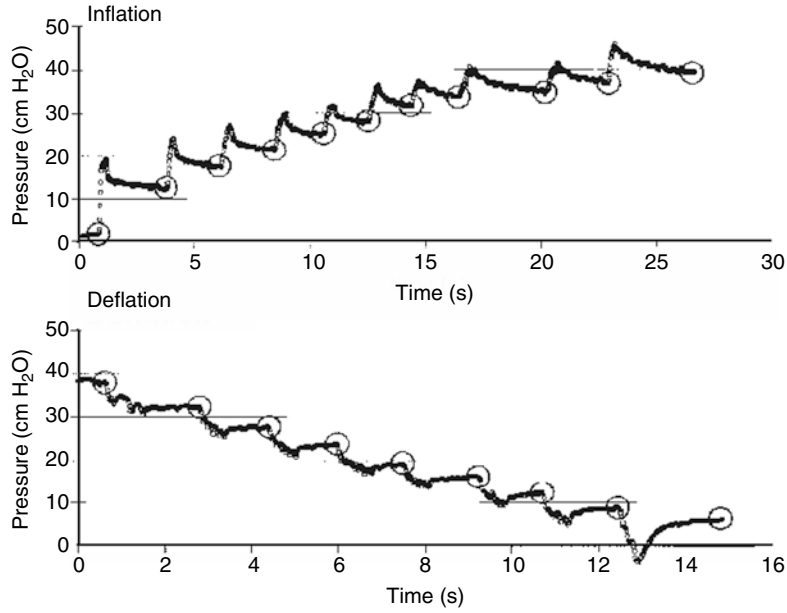

Fig. 11.19 Pressure wave during *PV* curve mapping. Inflation and deflation pressure–time plots during *PV* curve mapping using the super-syringe method. Note the exponential pressure decay from initial pressure after each volume step. Pressure values used in the construction of the quasi-static *PV* curve are indicated by *open circles* (Redrawn from Harris (2005) with permission)

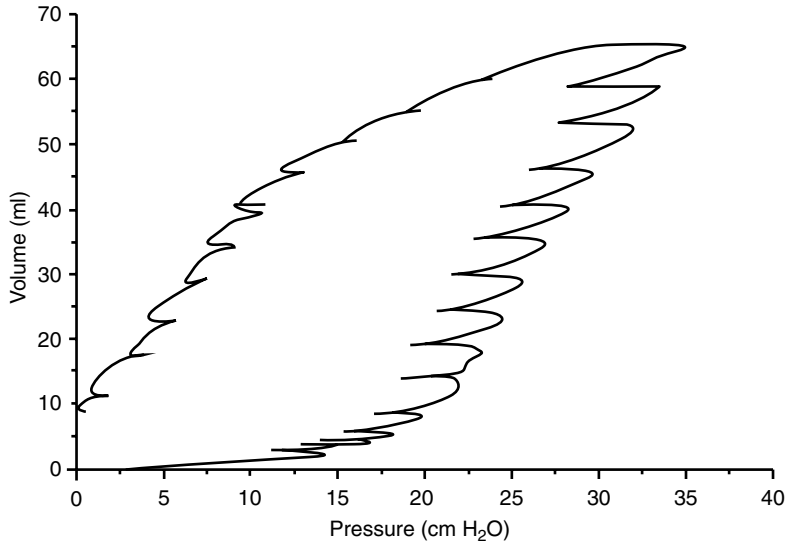

Fig. 11.20 Typical static *PV* curve. *PV* tracing obtained using a syringe technique in a ventilated rabbit after repeated saline lavage (Redrawn from Rimensberger et al. (1999) with permission)

entire *PV* curve (inflation and deflation) can be mapped in about 40–60 s (Figs. 11.19 and 11.20). The method has been performed in sedated and muscle-relaxed infants with respiratory distress syndrome (Pfenninger and Minder 1988).

At first glance, the super-syringe technique would appear to have the advantage of accurate measurement of gas volume changes at the airway opening, but several sources of error limit the accuracy of the volume measurements, related in part to the use of cold dry gas (see below). The technique has the additional disadvantage of need for disconnection from ventilation, which for subjects with serious lung disease inevitably leads to destabilization (Mehta et al. 2003). For this reason, the super-syringe technique has largely been abandoned in clinical practice.

CPAP Steps Technique

An alternative to the super-syringe method is the CPAP steps technique, where with the ventilator in CPAP mode, the airway pressure is manually adjusted in 5 cm H_2O steps, up to a predetermined peak value and back, with a pause after

each pressure change until zero flow conditions are reached (Albaiceta et al. 2003; Albaiceta et al. 2004). The technique is attractive in that disconnection from the ventilator is not required, and the inflation-deflation maneuver is completed with warmed humidified gas. At least in experimental animals, the resultant *PV* curves are very similar to those obtained using a super syringe (Albaiceta et al. 2003). In ventilated humans, the technique has been used to map the inflation and deflation limbs separately, with each maneuver lasting around 50 s (Albaiceta et al. 2004).

Multiple Occlusion Technique

Static *PV* curves can also be generated using the multiple occlusion technique, in which repeated periodic interruptions to tidal breathing at varying tidal volumes and rates are performed at end-inspiration, with recording in each case of tidal volume and plateau pressure (Levy et al. 1989). The method has the advantage of not requiring disconnection from the ventilator and appears comparable with a super-syringe technique in identifying *PV* curve landmarks (Mehta et al. 2003). In common with other static methods, accurate *PV* points can only be obtained if there is no tube leak and no spontaneous breaths during the measurement. The multiple occlusion method can take up to 15 min to perform, making it somewhat impractical in ventilated subjects with lung disease. A simplified version of the method, finding volume during an inspiratory and expiratory hold, has been used in neonates on conventional and high-frequency ventilation (Pfenninger and Minder 1988).

Constant Flow Methods

An alternative to the "static" methods in which periods of zero flow at the airway opening are required for accurate *PV* mapping is to inflate and deflate the lungs using a constant gas flow and a steady change in airway pressure. The result is a "quasistatic" *PV* curve in which resistive pressure drop occurs, but its value is minimal at low flow rates (<10 l/min), and thus, the *PV* curve slope and landmarks are very similar to those obtained by static methods (Lu et al. 1999). At a higher flow rate (15 l/min), the inflation limb of the curve is shifted considerably to the right (Servillo et al. 1997). At an early stage this approach was applied in newborn infants with respiratory distress syndrome, using a specialized inflating device in which constant flow was used to inflate the lung over 20–30 s (Mathe et al. 1987). Further evaluation of the low-flow technique used ventilators in volume control mode, delivering a fixed volume over the longest inspiratory time the ventilator allowed (<10 s) (Lu et al. 1999; Servillo et al. 1997). More recently, purpose-built software within several commercially available ventilators now allows this maneuver to be performed automatically over a longer time period (15–20 s), with options to vary the gas flow, the rate of pressure change, and the peak pressure (Macnaughton 2006).

PV Curves During High-Frequency Oscillatory Ventilation

During high-frequency oscillatory ventilation (HFOV), it is possible to map the *PV* relationship with timed adjustments in mean airway pressure (P_{aw}), most effectively done in a sedated, muscle-relaxed individual. Volume changes have been measured with computed tomography (Luecke et al. 2003; Pellicano et al. 2009) and respiratory inductance plethysmography (RIP) (Brazelton et al. 2001; Tingay et al. 2006). When compared to a static *PV* curve, that obtained with slow HFOV steps achieves higher lung volume related to greater time-dependent recruitment and less hysteresis (Luecke et al. 2003). As a result the features of the *PV* curve may be less conspicuous (Luecke et al. 2003), although in a study of ventilated human infants, the *PV* curve mapped during HFOV had a characteristic shape, with readily identifiable landmarks particularly on the deflation limb (Fig. 11.21) (Tingay et al. 2006; Miedema et al. 2011).

Stepwise PEEP Maneuver

A form of *PV* curve can also be traced during conventional ventilation using stepwise alterations in PEEP with the ventilator in either pressure or volume control mode (Meier et al. 2008; Dargaville et al. 2010). The *PV* curve is drawn so as to connect the end-expiratory pressure–volume points for the last tidal breath at each PEEP step (Fig. 11.22). Although the period of equilibrium at end-expiration is brief, the *PV* curves obtained

with this method show the expected landmarks (Dargaville et al. 2010). No formal comparison with other techniques of *PV* mapping has been published to date.

11.8.1.2.1.2 Measurement of Lung Volume During *PV* Maneuvers

After the choice of method for generating the pressure sequence, the second major consideration in *PV* curve mapping is the measurement of change in lung volume, which can be difficult, if not impossible, to perform directly in ventilated patients with lung disease. A number of different methods have been used, each with its own advantages, limitations, and sources of error.

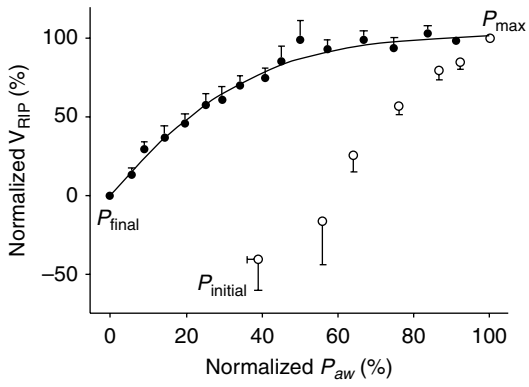

Fig. 11.21 *PV* curve during HFOV. Aggregate *PV* curve data from 12 muscle-relaxed infants on HFOV, with volume (measured by respiratory inductance plethysmography) normalized to total lung capacity (100 %) and deflation closing volume (0 %) and pressure normalized to the pressure values at these volume extremes (P_{max}, P_{final}). Starting pressure ($P_{initial}$) was the P_{aw} in clinical use at the commencement of *PV* mapping (Reproduced from Tingay et al. (2006) with permission)

Super-Syringe Method

Use of a graduated syringe would at first glance suggest highly accurate measurement of gas volume entering and leaving the lung. Several important sources of error are recognized with this method, which in sum tend to result in an unrecovered volume of gas during an inflation-deflation maneuver that may be falsely interpreted as hysteresis (Gattinoni et al. 1987b; Dall'Ava-Santucci et al. 1988). The first is the alteration in volume that occurs when cold, dry gas in a syringe is warmed to body temperature and saturated with water vapor. This effect is unique to the super-syringe technique, with a largely predictable error that can be corrected for (Gattinoni et al. 1987b). The second is gas compression occurring during inflation with higher airway pressures, an error common to all methods employing positive pressure at the airway opening to obtain a *PV* curve, for which there is a recognized correction factor (Downie et al. 2004). The third is the imbalance between oxygen uptake from, and CO_2 entry into, the lung,

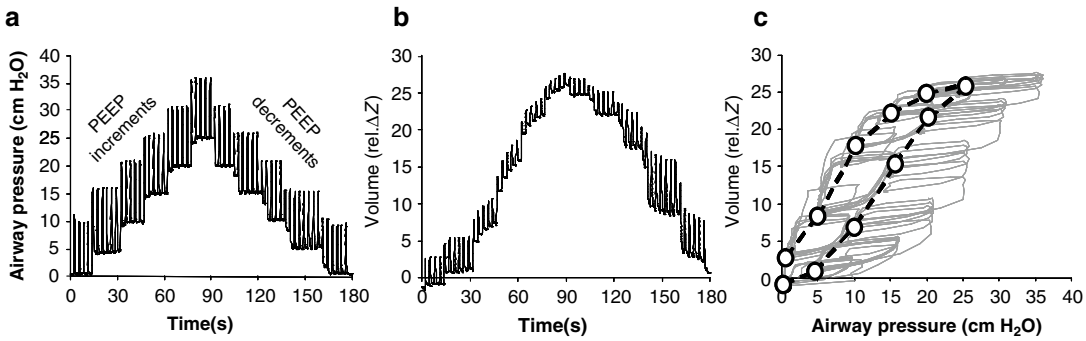

Fig. 11.22 *PV* curve using a stepwise PEEP maneuver. *PV* curve during PEEP increments and decrements in a mechanically ventilated piglet after repeated saline lavage followed by surfactant therapy. Panel (**a**) Pressure–time curve during pressure control ventilation with delta pressure held at 10 cm H_2O. Each PEEP level is held for approximately 15 s. Panel (**b**) Resultant volume–time curve, with lung volume plotted as relative impedance change (rel. **Δ***Z*) in arbitrary units. Panel (**c**) *PV* waveform (*in grey*), end-expiratory pressure–volume points for the final breath at each PEEP level (*black circles*) and the *PV* curve constructed from these points (*dashed line*) (Redrawn in part from Dargaville et al. (2010) with permission)

which leads to a loss of volume of delivered gas that is time dependent. This error is common to all methods of *PV* curve mapping and can be minimized to some degree by ventilation with room air prior to the measurement. The error can also be corrected for by timing the maneuver and using an estimate of the rate of oxygen consumption and the respiratory quotient (Bates et al. 1996).

Ventilator Techniques

Volume measurement during ventilator-driven *PV* curve mapping remains problematic. An integrated volume signal derived from a pneumotachograph placed at the airway opening inevitably shows a volume drift which has several causes, is not predictable, and is extremely difficult to correct for (Bates et al. 1996). Streaming of exhaled gas via a spirometer overcomes this problem, but this alternative is rarely available at the bedside.

CT Imaging

As noted below, measurement of gas volume changes using CT imaging has been the source of a great deal of information about the *PV* curve and its landmarks. CT scans have the advantage of separate estimation of volume change related to recruitment in non-aerated regions and volume accretion in previously aerated regions. Whole lung CT images give accurate quantitative measures of gas volume changes during a PV maneuver (Rouby et al. 2003). Most usually, however, only one or at best several CT slices can be taken at each pressure step (Albaiceta et al. 2004), which may not be representative of the whole lung (Lu et al. 2001). Use of CT imaging for tracing *PV* curves in clinical practice is also limited by the need for patient transfer to the CT suite and concerns over radiation exposure.

Respiratory Inductance Plethysmography (RIP)

This technique, discussed in detail elsewhere in this text, has been used to measure volume change during PV maneuvers in ventilated adults (Nunes et al. 2004) and neonates (Tingay et al. 2006) with lung disease and has the distinct advantage of being continuously available at the bedside in the intensive care unit. Calibration of the RIP voltage change to a known volume is possible, but may not be accurate when taken to the extremes of volume during generation of a *PV* curve. Another potential source of error relates to shifts in blood volume that occur during tracing of an entire *PV* curve (Gattinoni et al. 2005), which will have the effect of exaggerating the degree of hysteresis. This effect may account in part for differences in TLC and deflation limb values seen when volume measurement using uncalibrated RIP is compared with values obtained using the super-syringe method (Brazelton et al. 2001).

11.8.1.2.1.3 Construction of the *PV* Curve

An additional potential source of error is the presence of endotracheal tube leak, which will lead to inaccuracies in the volume measurement in the super-syringe technique and also in methods requiring calibration with a known volume delivered at the airway opening. For this reason a cuffed tube is essential to accurately map the *PV* relationship; for neonates the alternative of a tight-fitting tube may be sufficient (Pfenninger and Minder 1988). Using an automated low-flow *PV* mapping system, it may be possible to overcome the potential error in identification of the lower inflection point by increasing flow rate (Turner et al. 2009), but doing so increases the error related to resistive pressure drop (Blanch et al. 2009).

11.8.1.2.2 Reproducibility of *PV* Curves

When generated using a consistent technique, *PV* curves in a ventilated subject are highly reproducible, with a considerable degree of overlap in *PV* points and peak volume measurements (Matamis et al. 1984; Mehta et al. 2003). Consistency of interpretation of the *PV* curve once drawn has been more problematic, in part related to discrepant definitions of key landmarks (Harris 2005), in particular the lower inflection point (LIP), also known as the lower corner pressure, or P_{flex}. A significant degree of intraobserver error in identification of LIP has been noted by some investigators (Harris et al. 2000), although not others (Mehta et al. 2003), potentially limiting the value of *PV* curve generation in guiding mechanical ventilation (see below).

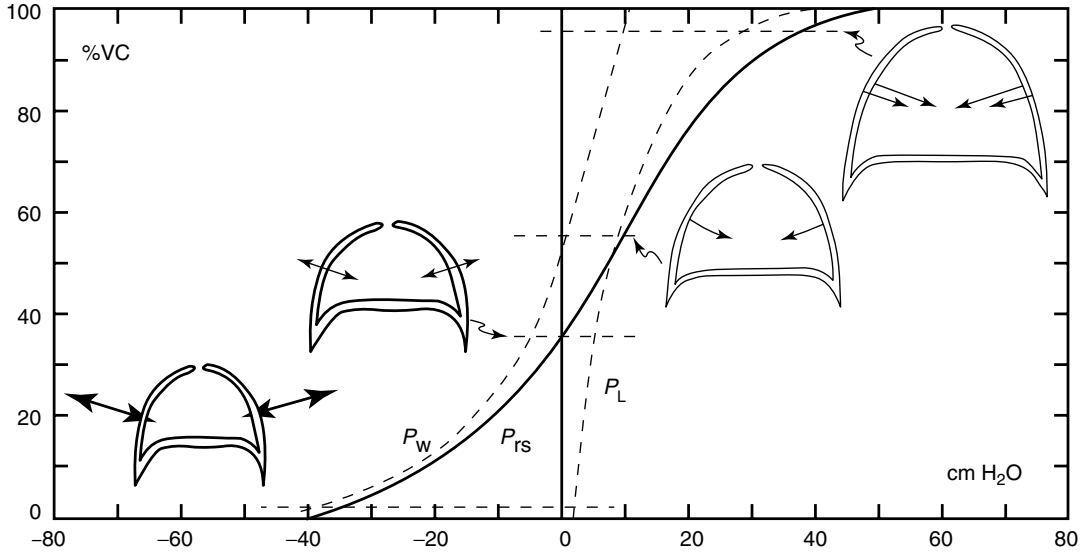

Fig. 11.23 *PV* curves of the lung, chest wall, and respiratory system. The *PV* curve of the respiratory system (P_{rs}) in a healthy adult (*solid line*) which is the sum of the curves of the lung (P_L) and chest wall (P_W) (*both dashed lines*). Functional residual capacity (*FRC*) occurs where the lung elastic recoil favoring collapse (*inward arrows*) is balanced by the chest wall elastic recoil favoring expansion (*arrows out*). Note that the chest wall contributes much of the curvature below FRC, whereas the lung contributes most to the curvature above FRC. %VC = % vital capacity (From Agostini and Hyatt (1986) with permission)

11.8.1.2.2.1 Compartments Contributing to the Shape of the *PV* Curve

In a ventilated subject, the respiratory system *PV* curve constructed with pressure measurements from the airway opening (P_{ao}) is a composite of the *PV* relationship of the lungs and that of the chest wall and diaphragm (Agostini and Hyatt 1986). These can be separately drawn if a measurement of pleural pressure (P_{pl}) is made; for this purpose esophageal manometry is normally used. The *PV* curve of the lung can be drawn as volume change versus transpulmonary pressure (P_{tp}, where $P_{tp} = P_{ao} - P_{pl}$) and that of the chest wall as volume change versus P_{pl} (Fig. 11.23). Obesity and intra-abdominal sepsis, by virtue of their effects on the mechanics of the diaphragm and chest wall, demonstrably alter the *PV* relationship of the respiratory system (Pelosi et al. 1996; Ranieri et al. 1997), with morbid obesity also affecting lung compliance (Pelosi et al. 1996).

Leaving aside the contribution of the chest wall, the *PV* curve of the lung is the summation of the volumetric behavior of millions of alveoli and, as described in the next section, reflects both isotropic volume change and recruitment/derecruitment, with regional inhomogeneities related to both the disease process and the effect of gravity.

11.8.1.2.3 The Inflation and Deflation *PV* Curves

11.8.1.2.3.1 Features of the *PV* Curve

The complete *PV* curve has inflation and deflation limbs, which may in some instances be traced separately. The shape of each limb and their identifiable landmarks have been long studied with the hope of yielding insights into the underlying anatomical and physiological disturbances of the diseased lung.

The inflation limb of the *PV* curve has a generally sigmoidal shape, less apparent in the healthy lung (Fig. 11.24) or where PEEP is applied during the maneuver (Maggiore et al. 2001; Ingimarsson et al. 2001). Several key landmarks of the inflation limb are apparent in the injured lung (Fig. 11.24). The LIP is located within the concavity at the lower end of the inflation limb, and has several definitions, directed toward identification of the point of maximum

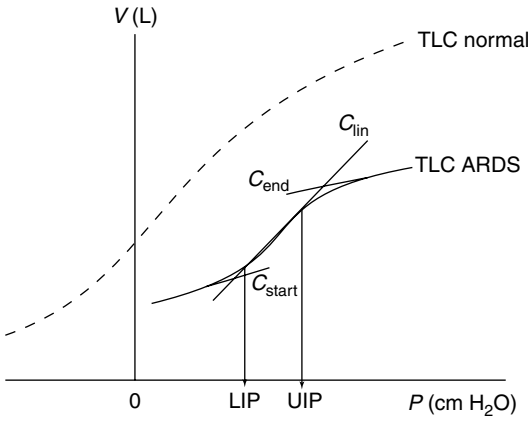

Fig. 11.24 *PV* curve inflation limb in the health and diseased lung. Inflation curve of a normal subject (*dashed line*) and a patient with ARDS (*solid line*). Note lower TLC in ARDS. *LIP* lower inflection point, *UIP* upper inflection point, C_{start} chord compliance below LIP, C_{lin} compliance in the linear region of the inflation limb, C_{end} compliance above UIP (Redrawn from Harris (2005) with permission)

concavity or most abrupt change in slope. It is not in actuality a true inflection point, which is a point on a curve at which concavity changes to convexity (or vice versa), and the second derivative changes sign. Below LIP, volume of the diseased lung changes little with pressure increments, and thus compliance is low. Above LIP, a relatively linear region of the inflation limb, with higher chord compliance, is seen (Fig. 11.24). As lung volume further increases, convexity of the upper end of the inflation limb is noted, beyond which volume proceeds asymptotically to TLC. The point of maximum convexity is known as the upper inflection point (UIP) (Fig. 11.24) and is not always demonstrable depending on the technique, the disease state, and the maximum pressure applied.

The deflation limb of the *PV* curve is less regularly sigmoidal in shape, having only an upper curvature apparent in most instances, within which a point of maximal curvature (PMC) is identifiable (Fig. 11.24). Below PMC, the deflation limb is generally linear.

When mapped together, the inflation and deflation limbs most usually have different trajectories, reflecting hysteresis within the respiratory system. Hysteresis can be defined as that property of a mechanical system whereby different behavior is exhibited as a force is applied and then withdrawn. It may reflect unrecoverable energy or simply a delay in recovery of input energy, in either case indicative of an imperfect elastic system (Harris 2005). Many factors contribute to hysteresis under differing conditions (Harris 2005), with the most important being the elastic recoil generated by surface forces at the air–liquid interface associated with the alveolar lining layer (Radford 1964) and variable contributions made by lung tissue and chest wall hysteresis (Harris 2005; Albaiceta et al. 2008).

11.8.1.2.3.2 Anatomical and Physiological Correlates of *PV* Curve Landmarks and Hysteresis

Clinical and experimental studies have given insight into the relationships between *PV* curve landmarks and the anatomical and physiological state of the diseased lung. In particular, changes in lung aeration and recruitment at LIP and UIP, and on the deflation limb at the PMC, have been studied using computed tomography (CT), electrical impedance tomography (EIT), and confocal microscopy.

CT imaging in particular allows differentiation between isotropic aeration (increase in gas volume of open lung units) and recruitment (aeration of previously non-aerated areas). The inflation limb has been proposed to be a summation of the aeration and recruitment curves for all lung units, and the morphological changes in the diseased lung at the LIP and UIP have been identified using CT imaging (Fig. 11.25) (Albaiceta et al. 2004; Vieira et al. 1999; Jonson et al. 1999; Pelosi et al. 2001; Crotti et al. 2001). Below LIP, much non-aerated lung tissue is evident, very little recruitment occurs, the volume change that occurs is largely isotropic, and chord compliance is low. At LIP, significant recruitment of non-aerated lung begins, and, contrary to previously held tenets, above LIP recruitment continues as the linear portion of the inflation limb is traversed (Fig. 11.25) (Jonson et al. 1999). CT imaging in both experimental animals (Pelosi et al. 2001) and ventilated humans with lung injury (Crotti et al. 2001) indicates an approximately normal

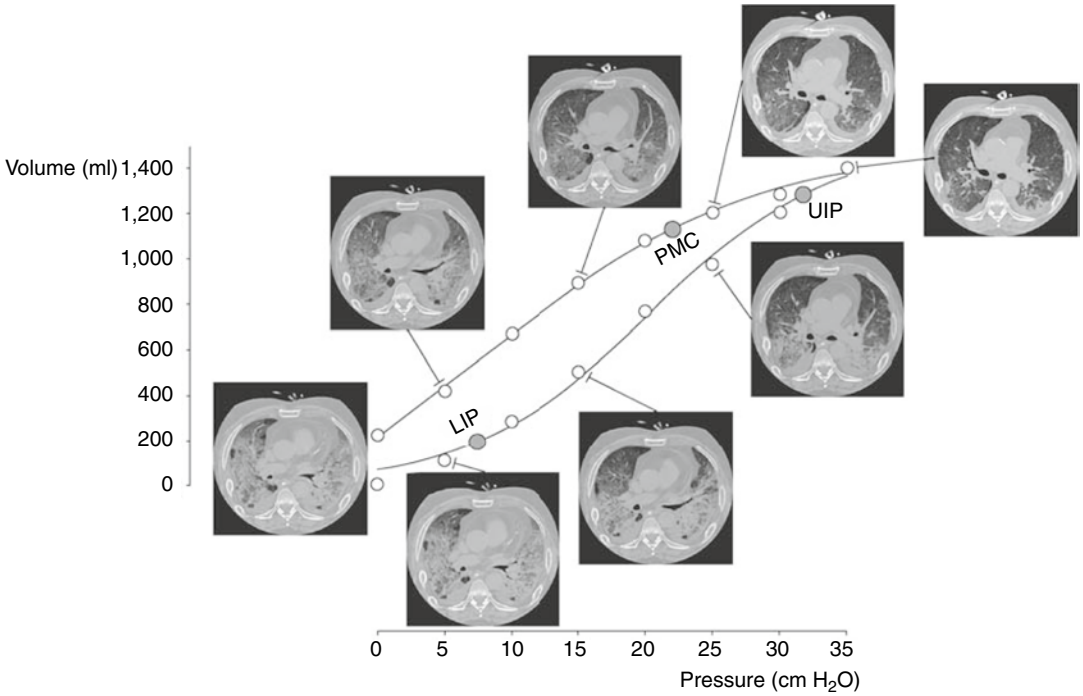

Fig. 11.25 *PV* curve landmarks and their relationship to recruitment and aeration in the diseased lung. *PV* curve traced under static conditions and corresponding axial computed tomographic images in a patient with acute respiratory distress syndrome (ARDS). On the inflation limb, recruitment (i.e., reduction in non-aerated lung) only begins after traversing the lower inflection point (*LIP*) and continues to and beyond the upper inflection point (*UIP*). Increase in aeration of open lung regions proceeds throughout the inflation limb. On the deflation limb, derecruitment only starts below the point of maximum curvature (*PMC*) and progresses thereafter. Loss of volume in aerated regions occurs throughout the deflation limb (Reproduced from Albaiceta et al. (2008) with permission)

distribution of opening pressures of non-aerated lung units during inflation. The cumulative accretion of volume within such units over the pressure trajectory of the inflation limb (i.e., the integral of the normal distribution) gives a sigmoid curve and lends to the inflation limb its characteristic shape (Venegas et al. 1998).

Recruitment of non-aerated lung units diminishes at or near UIP, beyond which isotropic volume change is hampered by increasing lung strain. With the application of very high recruitment pressures, some lung units are noted to open above UIP (Borges et al. 2006).

At the top of the deflation limb, aerated lung units remain open with initial pressure decrements from TLC. At PMC, derecruitment is seen to begin (Fig. 11.25) (Albaiceta et al. 2004) and continues as the deflation limb is traversed (Maggiore et al. 2001), again with an apparently normal distribution of closing pressures within the population of unstable units destined to collapse (Pelosi et al. 2001; Crotti et al. 2001). Onset of derecruitment on the deflation limb is not predictable from inflation limb LIP (Albaiceta et al. 2004; Crotti et al. 2001).

In parallel with the clinical and experimental studies using CT scanning, other modes of lung imaging, as well as measures of lung mechanics, have been used to examine the relationships between *PV* curve landmarks and lung inflation/aeration. Use of in vivo microscopy in the rat model of ARDS has allowed confirmation both of the phenomenon of recruitment along the entire inflation limb and the lack of prediction of derecruitment from inflation limb LIP (Dirocco et al. 2007). Onset of recruitment and derecruitment during the *PV* cycle has been estimated using both electrical impedance tomography

(Dargaville et al. 2010; Costa et al. 2009) and pneumotachography (Rimensberger et al. 1999; Ingimarsson et al. 2001), with again no clear relationship between derecruitment and LIP.

11.8.1.2.3.3 Modeling of the Inflation and Deflation Curves

Given on the one hand the potential for *PV* curves to give information which may aid in delivering mechanical ventilation and on the other the difficulties associated with generating entire *PV* curves and identifying landmarks on them, several approaches to modeling of the volumetric behavior of the lung have been pursued. Various sigmoidal functions have been reported to correlate well with clinical data, of which that of Venegas and coworkers (Venegas et al. 1998) has been most widely applied (Fig. 11.26a). This four-parameter sigmoidal equation uses variables related to *PV* curve landmarks, centered around the true inflection point, which is identifiable in most *PV* curves and of clinical significance. Hysteresis in this model can be introduced by using a different value for the inflection point on the inflation and deflation limbs. This model has been seen to fit well with the *PV* curves of ventilated adults with ARDS (Pereira et al. 2003) as well as ventilated infants on HFOV (Tingay et al. 2006). A more fundamental approach has been taken in other studies, in which the cumulative volume of thousands of theoretical lung units is calculated as pressure is projected to and from TLC (Hickling 2001; Bates and Irvin 2002). In both models, the volume of each individual unit (once open) is derived from the exponential relationship between applied pressure and resultant lung volume established by Salazar and Knowles (1964). For the model of (Hickling 2001), the lung units have normally distributed opening and closing pressures and an array of different superimposed pressures. For that of Bates and Irvin (Bates and Irvin 2002), opening and closing pressures are assumed to be equal, but the rates of opening and closing differ for each unit, introducing time dependence as a factor contributing to the shape of the *PV* relationship. Each of these models produces *PV* curves with plausible inflation and deflation limbs (Fig. 11.26b, c).

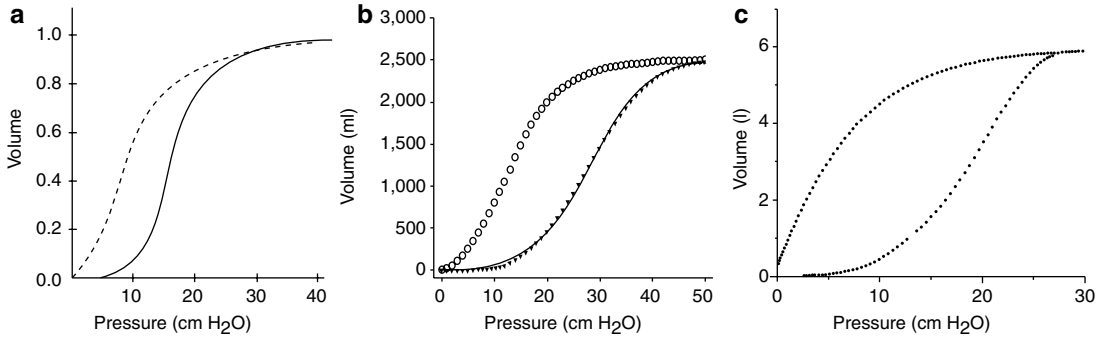

Fig. 11.26 *PV* curve modeling. Theoretical *PV* curves drawn using mathematical modeling, based around parameters of global lung function (panel **a**), or summing the volumetric behavior of clusters of individual lung units (panels **b**, **c**). In each case the lung is assumed to have been inflated from a degassed state. Panel (**a**): Sigmoidal functions representing the inflation and deflation limbs of a *PV* curve. In the example shown, the true inflection point (see text) was set to 15 cm H_2O for inflation and 5 cm H_2O for deflation (Reproduced from Venegas et al. (1998) with permission). Panel **b**: Inflation and deflation *PV* curves representing the cumulative sum of the volume of 27,000 individual units with superimposed pressure ranging between 0 and 14.5 cm H_2O (equally distributed), threshold opening pressures between 0 and 40 cm H_2O (normally distributed), closing pressure 0 for all units, and the volume of open lung units determined from the equation of Salazar and Knowles (1964) with half-opening pressure = 4.9 (Redrawn from Hickling (2001) with permission). Panel **c**: Inflation and deflation *PV* curves representing the cumulative sum of the modeled volumetric behavior of 5,000 individual units, with opening and closing pressures identical for each unit and normally distributed, time-dependent opening and closing, and the volume of open lung units determined from the Salazar–Knowles equation with half-opening pressure = 4.9 (Redrawn from Bates and Irvin (2002) with permission)

11.8.1.2.4 Interpretation and Clinical Implication of the Static *PV* Curve

Spurred by the finding of Suter et al. (1975) that lung mechanics could guide PEEP setting for the ARDS lung, a legion of investigators have pursued the possibility that the static *PV* curve could be a bedside tool to assist ventilatory management, in particular PEEP setting. Clinical studies have largely been conducted in adult subjects with ARDS, with few reports of systematic evaluation of *PV* curves in ventilated infants and children. The findings of adult studies, and the laboratory work in experimental animals, certainly can be applied to the pediatric population.

LIP on the inflation limb of the *PV* curve has been the obvious starting point for clinicians looking for tools to assist in optimizing ventilation. Presence of a prominent curvature around LIP, with a significant increase in compliance from C_{start} to C_{lin} (Fig. 11.24), has been found to be indicative of the potential for recruitment (Vieira et al. 1999), which in turn predicts response to PEEP (Gattinoni et al. 2006). Further, where lung and chest wall *PV* curves are separately generated, the presence of an identifiable LIP on lung *PV* curve predicts response to PEEP (Mergoni et al. 1997).

Although laboratory studies confirm the presence of LIP in animal models of full-term (Monkman et al. 2004) and preterm (Ingimarsson et al. 2001) neonatal lung disease, few studies report the identification of LIP in ventilated infants and children (Pfenninger and Minder 1988; Mathe et al. 1987). Mathe and coworkers (1987) found concavity of the early part of the inflation limb with a recognizable LIP in each of 30 ventilated infants with respiratory distress syndrome. A further study in preterm infants identified a sigmoidal inflation limb in 6 out of 8 infants, but LIP was not used for PEEP optimization (Pfenninger and Minder 1988).

Until the morphological correlates of LIP were delineated (see above), this landmark was used in setting PEEP to achieve and maintain adequate lung recruitment. The strategy of setting PEEP above LIP (in conjunction with lung-protective tidal volumes) was tested in several randomized controlled trials in adults with ARDS (Amato et al. 1998; Ranieri et al. 1999; Villar et al. 2006), each of which produced positive results compared with standard ventilatory management. In ventilated preterm infants, targeting PEEP to LIP was found to produce better oxygenation compared with an empirical approach to PEEP setting (Mathe et al. 1987). Recent evidence pointing to a lack of correlation between onset of derecruitment and LIP has however dampened the enthusiasm for this approach. The physiological incongruity of using an inspiratory curve landmark indicative of alveolar opening to set a pressure to prevent alveolar closure in the expiratory phase has been acknowledged (Maggiore et al. 2003).

The concept that deflation limb PMC might guide optimal PEEP has gained momentum over the past decade, based on both a theoretical consideration of optimal lung mechanics in the diseased lung (Hickling 2001) and the seminal observations of Rimensberger et al. (1999) demonstrating that tidal ventilation could be applied on or near the deflation limb of the *PV* curve after lung recruitment. The latter study noted in a lavage model of lung injury that optimal PEEP, at which lung volume and gas exchange were stable, was somewhat below PMC and well below LIP (Rimensberger et al. 1999). This is, in part, a reflection of the nature of the lung injury model – a highly recruitable lung that demonstrates marked hysteresis and considerable alveolar stability once recruited, meaning that deflation limb PMC can be well below LIP. Other laboratory (Takeuchi et al. 2002; Caramez et al. 2009) and clinical (Harris et al. 2000; Crotti et al. 2001; Albaiceta et al. 2005) investigations have found PMC to be well above LIP, with as a consequence considerably higher PEEP if set at PMC. Experimentally this has been found to increase alveolar dead space (Takeuchi et al. 2002) and clinically to produce lung overdistension (Albaiceta et al. 2005), observations which may explain the lack of effect on ventilator days of a high PEEP approach (with tidal volume 6 ml/kg) in ventilated adults with ARDS (Brower et al. 2004).

It is clear that the theoretical benefit of setting PEEP using a deflation limb landmark (Hickling 2001) has yet to be realized in clinical practice. It may be that optimal PEEP on the deflation limb during conventional ventilation is located somewhat below PMC and, when combined with an appropriate tidal volume, can strike the right balance between maintaining lung recruitment and avoiding overdistension. This important physiological question requires further investigation and ultimately will require study in pediatric subjects.

In contrast to the paucity of data in pediatric subject regarding the deflation limb during conventional ventilation, in infants on HFOV the deflation limb has recently been mapped (Fig. 11.21) (Tingay et al. 2006), its landmarks identified, and a strategy for setting mean airway pressure based on identification of closing pressure has been developed (De Jaegere et al. 2006). In this context closing pressure is defined as deterioration in oxygenation with pressure decrements, and setting mean airway pressure 2 cm H_2O higher than this point is associated with stable lung volume and good gas exchange (De Jaegere et al. 2006). This in essence targets a point close to PMC (Tingay et al. 2006) and, given the minimal tidal breath excursions during HFOV, conveys less risk of overdistension than during conventional ventilation. The benefit of mapping the deflation limb during HFOV and the most reliable indicators of optimal airway pressure deserve further scrutiny.

Essentials to Remember

- Static *PV* curves traced at the bedside in ventilated subjects have a recognizable inflation and deflation limb, with landmarks that correlate with lung recruitment, overdistension, and derecruitment.
- There is potential for deflation limb landmarks to guide PEEP setting during conventional ventilation and mean airway pressure setting during HFOV, but in both cases a definitive approach has yet to be formulated, and further research is required.

11.8.2 Pressure–Volume Loops Under Dynamic Conditions

Peter C. Rimensberger, David Tingay, and Peter A. Dargaville

Educational Goals

- To review the differences between a static and a dynamic pressure–volume curve
- To review measurement and calculation methods of dynamic compliance from *PV* loop during ongoing mechanical ventilation
- To review what information can be gathered from *PV* loops displayed on a ventilator screen

11.8.2.1 Measurement of the Dynamic Pressure–Volume Loop

During ongoing mechanical ventilation, a dynamic continuum, dynamic compliance (C_{dyn}) equals the behavior between the pressure difference between P_{plat} and PEEP (ΔP) and tidal volume (V_T) and is expressed as V/P (ml/cm H_2O). The latter has to be reported to the body weight of the patient and will therefore be expressed as ml/cm H_2O/kg.

A prolonged end-inspiratory occlusion (allowing for pressure equilibrium of the respiratory system under zero flow condition) followed by a passive exhalation to ambient pressure at airway opening (zero airway pressure) would allow to measure the static compliance at end-inspiration (i.e., at inspiratory plateau pressure):

$$V_{ei} / P_{ei} \quad \text{above FRC} = C_{statei}$$

where V_{ei} represents the pressure at end-inspiration, P_{ei} the exhaled volume from end-inspiration to functional residual capacity (FRC), and $C_{stat,ei}$ the static compliance (i.e., pressure–volume relationship) at end-inspiratory pressure.

Accordingly, an end-expiratory occlusion maneuver followed by a passive exhalation to PEEP will allow to measure the exhaled gas volume to (i.e., tidal volume), giving the compliance

of the respiratory cycle during mechanical ventilation under commonly called "static" conditions

$$C_{stat} = \left(P_{ei} - \text{PEEP}\right) / V_t = P_{plat} - PEEP / V_t$$

This "static" compliance value however reflects a measured value under dynamic conditions (i.e., during ventilation) and can therefore not be compared to the static compliance of the respiratory system that characterizes the *PV-behavior* of the whole respiratory system, from FRC to TLC (Stocks and Jackson 1996) (see Sect. 11.8).

All commonly applied bedside methods of determining C_{rs} and R_{rs} during mechanical ventilation apply mathematical assumptions to model the complex mechanical behavior of the respiratory system.

11.8.2.1.1 Mead Whittenberger Analysis

The Mead and Whittenberger (1953) is an accepted method of calculating C_{rs} during mechanical ventilation. This method determines the C_{rs} and R_{rs} based on an assumption that the respiratory system behaves as a single compartment. This allows the general equation of motion to be applied:

$$P_{TP} = \left(E_{rs} \times V\right) + \left(R_{rs} \times \mathrm{V}'\right) + k \qquad (11.1)$$

where P_{TP} represents transpulmonary pressure, E_{rs} elastance, V volume, V' flow, and k a constant.

Mead–Whittenberger analysis requires identification of two points of zero flow within the respiratory cycle and assumes these coincide with end-inspiration and end-expiration, when the resistive pressure losses will be zero. Thus, between these two points, the change in P_{TP} will be due to the pressures required to overcome the elastic recoil of the lung (ΔP_{EL}) and

$$\Delta P_{EL} = E_{rs} \times \Delta V \qquad (11.2)$$

where ΔV represents the change in volume. In dynamic situations this being tidal volume.

This can be reconsidered as

$$C_{rs} = 1 / E_{rs} = \Delta V / \Delta P_{TP}$$

This mathematical determination of C_{rs} requires that the two points of zero pressure correlate with zero flow, limiting use in some circumstances, such as high frequency ventilation (HFV).

11.8.2.1.2 Least-Squares Regression Method

Similar to the Mead–Whittenberger method, the least-squares regression method applies the general equation of motion to a single-compartment model (Davis et al. 1996). Analysis is between two points of the pressure–volume curve. In this case, C_{rs} is determined from the slope of the line joining the maximal and minimal volume during a pressure–volume curve. Again the complex nature of pressure and flow waves, and attenuation, limits this methodology in some ventilatory circumstances.

11.8.2.1.3 Multiple Linear Regression

The multiple linear regression technique uses the entire respiratory cycle to calculate C_{rs} (Stahl et al. 2006). This method is valid during the complex pressure and flow conditions of HFV but requires an analytic process that involves applying an algorithm to minimize errors between the observed pressure changes and the assumed pressure behavior using the equation of motion for the flow and volume measurements. Multiple linear regression is currently impractical outside of a research environment.

Airway resistance is considered to be mainly caused by friction, in phase with flow. The resistive components of the breathing circuit, the endotracheal tube, and the respiratory system cause distortion of dynamic airway pressure measurements during ongoing ventilation.

11.8.2.2 Ventilator Display

Ventilator monitors can and do only display the dynamic *PV* loop, indication on the y-axis the tidal volume delivered and on the x-axis the airway pressures used – therefore, such loops can only describe or visualize the specific dynamic *PV* relationship for a specific airway pressure setting. It must be recognized that mechanical properties of the respiratory system assessed under the dynamic condition of mechanical ventilation are not equivalent to those assessed under static

conditions (Stahl et al. 2006) (see Sect. 11.8.2). There are various reasons for this:

First, during mechanical ventilation or even during spontaneous breathing, the respiratory system never reaches truly static conditions. This is because there is still a continual change in pressure, lowering in exponential fashion over some time, within the system, even when airflow has stopped. To overcome this breathing would have to be interrupted for several seconds. Since this is hardly possible in the clinical setting without muscle paralysis, the *PV* loop that can be displayed on a ventilator remains a dynamic measure even when a zero flow condition is reached at end-inspiration and end-expiration, and its shape will depend on airway resistance (i.e., equipment and patient airway resistance). This latter effect could be only overcome by very low-flow conditions that again are not practical in a non-paralyzed patient. *PV* hysteresis seen on the dynamic *PV* loop is therefore mainly due to airway resistance, and the effect of airway resistance is most marked during high flows, i.e., at the beginning of inspiration and at the beginning of expiration, respectively. This results in the appearance of a change in the curvature of the inflation limb at the lower volume end on the volume axis (often referred to as the "lower inflection point") and similarly in a change of the curvature of the deflation limb at the upper end on the volume axis (often referred to as the "upper deflection point") (see Fig. 11.27). However, such phenomena are a result of initial fast flows during inflation and deflation in a highly resistive system (endotracheal tube) during a rapid increase or decrease of pressure gradient between applied airway pressures at airway opening (i.e., close to or at the endotracheal tube connection) and effective airway pressure at the alveolar level. Since by the ventilator displayed airway pressures are measured at the endotracheal tube connector (i.e., before the part of high resistance in the respiratory circuit that includes the endotracheal tube) and not on the tracheal level (Karason et al. 2000) (Fig. 11.27), this dynamic *PV* loop cannot give an indication on the level of pressures required (i.e., PEEP) for understanding when the lungs start to open and to set PEEP accordingly, as has been

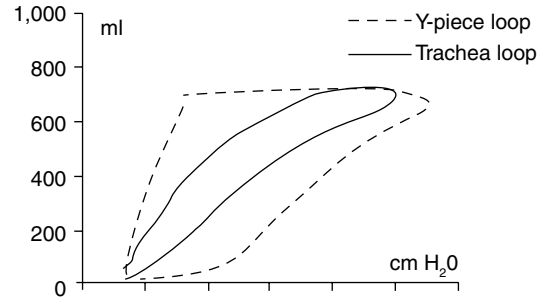

Fig. 11.27 Pressure–volume (*PV*) loop during mechanical ventilation with an extrinsic PEEP of 8 cm H_2O. The *dashed line* shows the dynamic *PV* loop with pressure measurement at the airway opening (i.e., at endotracheal tube connector, the *solid line* shows the dynamic *PV* loop derived from a pressure measurement at the endotracheal tube tip, i.e., carinal level. Note the difference in the amount of *PV* hysteresis and the appearance of a lower inflection point (LIP) on the inflation limb of the *PV* loop derived from pressure measurements at airway opening. This LIP cannot be identified on the *PV* loop derived from pressure measurements at the carina level. Similarly, there is appearance of a deflection point on the deflation limb and the appearance of the *PV* loop derived from pressure measurements at airway opening. Again, this deflection point cannot be identified on the *PV* loop derived from pressure measurements at the carina level. However, on the inflation limb there is appearance of an upper inflection point with a flattening of the *PV* curve at the upper end (lower compliance at the higher-pressure end, which may indicate overinflation of the lungs. (see also Fig. 11.5). However, this is not a very marked point but rather a successive phenomenon (With permission from Karason et al. (2000))

suggested in various textbooks and guidelines on how to optimize mechanical ventilation.

Second, although the recruiting effect of PIP pushes the high-pressure end of the dynamic *PV* loop during ongoing ventilation onto the inflation limb of the static *PV* curve, the end-expiratory volume is found, during ongoing ventilation at any PEEP level (with the exception of a zero PEEP condition), to be above the corresponding *PV*-value on the inflation limb of the semi-static or static *PV* curve (Fig. 11.28) (Stahl et al. 2006; Rimensberger et al. 1999). In contrast, during decremental PEEP steps after recruitment to TLC, dynamic compliance (i.e., the deflation part of the dynamic *PV* loop) will be in close agreement with the deflation limb of the *PV* curve, the end-expiratory volume at PEEP (as long as lung collapse does not occur) being placed on the deflation limb of the static *PV* curve (Figs. 11.29 and 11.30).

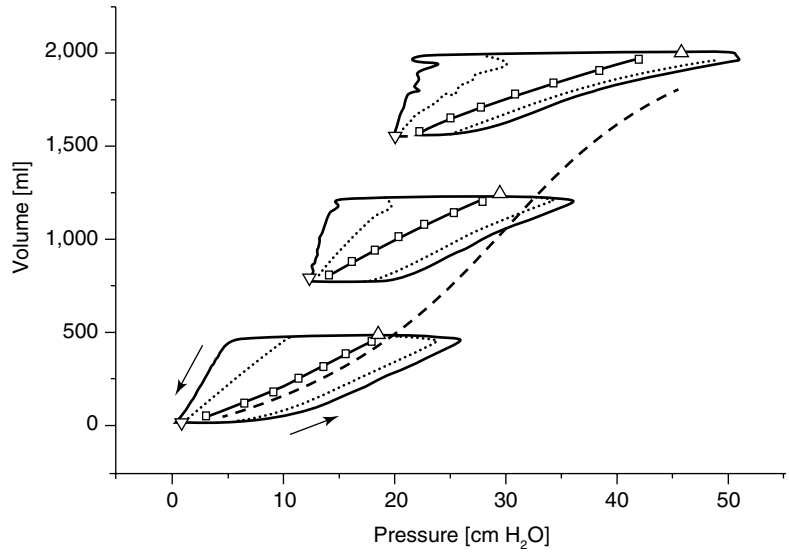

Fig. 11.28 Dynamic and static pressure–volume (*PV*) curves and compliance values of a patient. Note that the inflation limb of the dynamic alveolar *PV* (*dotted line*) at zero end-expiratory pressure and the static *PV* curve, resulting from low-flow inflation (*dashed line*) are in close agreement, whereas the dynamic alveolar *PV* curves at positive end-expiratory pressure (PEEP) of 12 cm H_2O and PEEP of 20 cm H_2O are not in agreement with the static *PV* curve. Dynamic compliance (*square line*) during mechanical ventilation differs for any setting clearly from the static compliance (*dashed line*) inflation curve to maximal inspiratory capacity of the respiratory system. Lower and upper inflection points (LIP and UIP, respectively) derived from the static *PV* curve do not correspond to the effect of PEEP on lung volumes. *Arrows* indicate the inflation and deflation part of the dynamic PV-curves (*solid line*) as displayed on the ventilator screen. (Reprinted with permission from Stahl et al. (2006))

This is the result of a different behavior of the lung during inflation and deflation (i.e., hysteresis) (Rahn et al. 1946) (see also Fig. 11.25).

The observations that (1) the inflation limb of the quasistatic *PV* curve (as generated by the super-syringe or low-flow inflation methods) is distinctly different from the deflation limb, (2) the inflation limb is highly sensitive to the initial inflation conditions (i.e., whether inflation starts from zero PEEP or another PEEP level) (Jonson et al. 1999) and preceding lung history (i.e., whether the patient was disconnected or even suctioned shortly before), and (3) the tidal cycle is not placed on the inflation limb of the quasistatic *PV* curve (Figs. 11.28, 11.29, and 11.30) (Stahl et al. 2006; Rimensberger et al. 1999) clearly illustrate how difficult it can be to use the slope of the tidal cycle *PV* curve (i.e., dynamic compliance) during incremental stepwise titration of PEEP as the only indicator for the best ventilator settings, as historically suggested (Suter et al. 1975, 1978).

Essentials to Remember

- The static and dynamic *PV* loops do not provide the same information and are not interchangeable in guiding the best ventilator settings.
- The slope of the *PV* loop (i.e., dynamic compliance) might be helpful to asses respiratory system behavior in a dynamic way, during incremental and decremental PEEP steps, but not when assessed at one single ventilator setting when lung history cannot be taken in account.
- The *PV* slope displayed on the ventilator is based on pressure measurements at the airway opening (i.e., endotracheal tube connector) and mainly reflects airway and endotracheal tube resistance. Therefore, it cannot give an indication on the level of pressures required (i.e., PEEP) to optimally support the lung during mechanical ventilation.

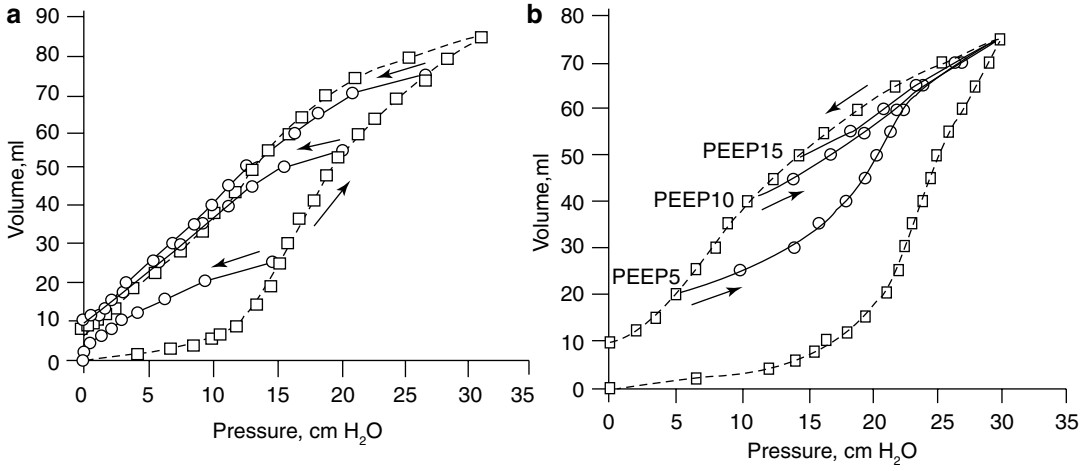

Fig. 11.29 Simulation of positive pressure ventilation using an air-filled syringe. (**a**) Pressure/volume envelope of the surfactant-depleted washed lung (*dashed line*) with deflation curves (*solid lines*) from three different pressure levels (15, 20, and 25 cm H_2O), corresponding to positive inspiratory pressure (PIP), to functional residual capacity. (**b**) Pressure/volume envelope of the saline-lavaged lung (*dashed line*) with reinflation to 30 cm H_2O (*solid lines*) after deflation to three different pressure levels (5, 10, and 15 cm H_2O) corresponding to positive end-expiratory pressure (*PEEP*). *Arrows* indicate whether the pressure was stepwise increased or decreased when creating this part of the curve. (Reprinted with permission from Rimensberger et al. (1999))

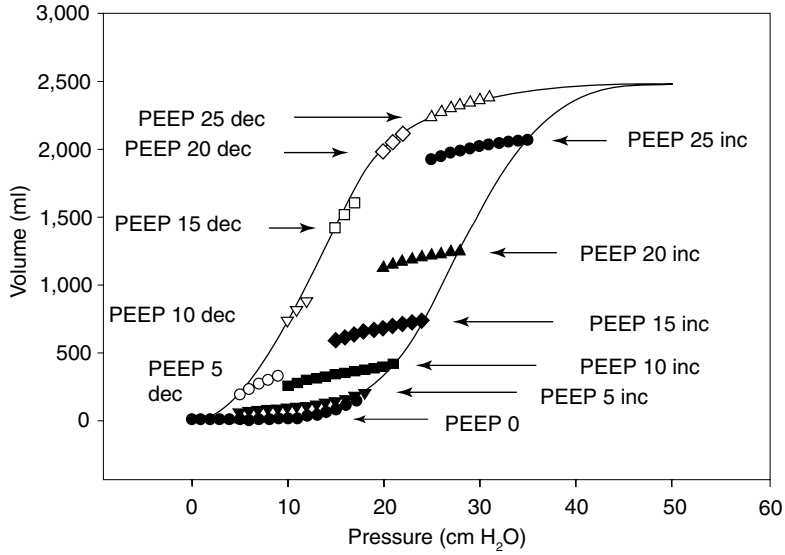

Fig. 11.30 Inspiratory tidal *PV* plots with V_T 140 ml with incremental (*black symbols*) and decremental (*open symbols*) PEEP levels from 0 to 25 cm H_2O derived mathematically from a multiple units lung model. At each PEEP level the volume at equivalent pressures and the mean tidal *PV* slope (i.e., tidal cycle compliance or dynamic compliance during conventional mechanical ventilation) are greater during decremental PEEP. With zero PEEP, the plots for incremental and decremental PEEP are superimposed. Note that the dynamic tidal *PV* cycle is never positioned on the plotted inflation limb of the overall *PV* curve (Reprinted with permission from Hickling (2001))

11.9 Respiratory Mechanics in the Actively Breathing Patient with/Without Respiratory Support

Mark Heulitt and Sherry Courtney

Educational Aims

- To understand the physiologic basis of the measurement of work of breathing
- To understand the subdivisions of WOB attributed to the patient ($WOB_{p,}$ physiologic) and those associated with the ventilator ($WOB_{v,}$ imposed) and how these measures can be used by the clinician as predictors of weaning or to perform accurate measurement of elastic, flow-resistive, and imposed work during mechanical ventilation to guide the level of support or to guide specific selection of the ventilator mode
- To understand the limitations of measurement of WOB to the clinician in weaning ventilatory support or selection of ventilatory mode

11.9.1 Introduction

Work of breathing (WOB) is a common term used to describe respiratory work in both patients who are breathing spontaneously and those requiring the support of mechanical ventilation. It represents an assessment of the afterload on the respiratory muscles or opposition to their contraction. During mechanical ventilation the goal is to assist respiratory muscle activity and thus reduce the WOB but not to entirely eliminate it. During spontaneous breathing there is active contraction of the respiratory muscles resulting in expansion of the thoracic compartment with a subsequent decrease in pleural pressure. Lung expansion results from the negative pressure generated and air flows into the lung due to the decrease in alveolar pressure below atmospheric pressure. Work of breathing can be subdivided into the work necessary to overcome the resistive, elastic, and inertial components and the work required to move the chest wall and intestinal organs. To understand the impact of mechanical ventilation on WOB, it is necessary to understand the forces that respiratory muscles must work against to allow for gas exchange to occur. These forces are the components that must be measured to accurately determine WOB. The reader is encouraged to read the excellent review by Banner (1994) for further discussion of this topic. A summary of some important concepts from this review is presented in the (Table 11.1). Our discussion will focus on the physiologic principals of WOB measurement and its clinical relevance for the care of mechanically ventilated infants and children.

11.9.2 Concept and Methods of Measurements

Work is equal to the product of the force applied to an object and the distance the object travels; that is, work = force × distance, or $W = F \times D$.

However, if we describe work in the three dimensions that apply to the respiratory system, work becomes the pressure applied to yield a change in volume of the system and can be expressed as

$$W = P \times V$$

or

$$W = \int_0^v P \times \mathrm{d}v$$

where $\int_0^v P$ is the integral of the pressure across the respiratory system as a function of volume and dv is the change in the volume of the respiratory system. When respiratory muscles contract, displacement occurs and mechanical work occurs. The muscles act as force generators, but the diaphragm generates 70 % of the tidal volume exchanged. The diaphragm is composed of three types of classic muscle fibers that differ in their ability to resist fatigue or lose the force-generating capacity of the muscle. Type 1 muscle fibers or slow oxidative fibers compose approximately 60 % of the diaphragm in adults and are very resistant to fatigue, allowing them to

Table 11.1 Influence of the site of pressure measurement and mode of ventilation on measurement of work of breathing and compliance

Site of pressure measurement and mode of ventilation	Area of the pressure–volume loop = work done to overcome	Slope of the pressure–volume loop
Esophageal pressure during mechanical spontaneous ventilation	Pulmonary inspiratory and expiratory resistance	Lung compliance
Esophageal pressure during mechanical ventilation	Chest wall inspiratory and expiratory resistance	Chest wall compliance
Pressure at tracheal (carinal) end of endotracheal tube during spontaneous breathing	Imposed inspiratory and expiratory resistance of the total breathing apparatus (i.e., ET, breathing circuit, and the ventilator)	Compliance of the total breathing apparatus
Pressure at tracheal (carinal) end of endotracheal tube during mechanical ventilation	Pulmonary and chest wall inspiratory and expiratory resistance	Compliances of the respiratory system (lung plus chest wall)
Pressure at the airway opening (between the Y-piece of breathing circuit and endotracheal tube) during spontaneous ventilation	Imposed inspiratory and expiratory resistance of the breathing circuit and ventilator	Compliance of the breathing circuitry
Pressure at the airway opening during mechanical ventilation	Pulmonary and chest wall inspiratory and expiratory resistance, plus resistance of the endotracheal tube	Compliance of the respiratory system (lung plus chest wall)

From Banner (1994)

maintain contractility for longer periods but generating less force than other muscle fibers (Braun et al. 1983).

Muscle contractions can be characterized depending upon where this work is performed. During miometric contractions, the muscle shortens and the performed work is called positive (i.e., the muscle performs work on something). During plyometric contraction, the muscle lengthens as the result of a larger, oppositely applied force and the work performed is negative (i.e., something does work on the muscle). During isometric contraction no displacement takes place and therefore no mechanical work is performed; however, there is a metabolic cost for the respiratory muscles performing this contraction. The type of contraction may have a direct impact on the patient's outcome on mechanical ventilation. For example, it has been hypothesized that plyometric contractions may be associated with respiratory muscle damage and inability for patients to tolerate weaning from mechanical ventilatory support. The ultimate result of any respiratory muscle contraction is to perform the necessary work needed to overcome opposing forces in the respiratory system. These forces are usually characterized as representing either the elastic or flow-resistive components of the respiratory system. However, in reality the forces are more complex, representing (1) the stress adaption within the lungs and chest wall (e.g., viscoelastic) within thoracic tissues, (2) the differences in static and elastic recoil of the lung and chest wall during inflation and deflation (e.g., plastoelastic), (3) the mass of tissues and gases (inertial and gravitational), (4) compression and distension of intrathoracic gas, and (5) forces that distort the chest wall from its relaxed configuration (distorting forces are small at rest but may contribute). However, during mechanical ventilation these forces are small; thus, traditionally only elastic and flow-resistive forces are accounted for in the calculation of WOB.

Most important is the ability of the respiratory muscles to tolerate increasing load; otherwise, the ultimate fatigue will lead to the need for mechanical ventilatory support. Increasing muscle loading leads to an imbalance between respiratory muscle energy supply and demand due to the need for increased muscle blood flow and oxygen consumption. This imbalance can lead to muscle ischemia, fatigue, and respiratory failure due

to an energy deficit and the inability to remove metabolites from the muscles (Bellemare et al. 1983). Increased muscle loading has a predictable sequence leading to muscle fatigue. Increased muscle loading leads to an increased force of contraction of respiratory muscles, which can be measured by measuring the transdiaphragmatic pressure (P_{di}), and increased duration of contraction of the respiratory muscles can be illustrated by a change in the ratio of the inspiratory time to total cycle time (T_I/T_{tot}). Subsequently these changes lead to an increased tension–time index of the major respiratory muscle, the diaphragm ($P_{di}/P_{dimax} \times T_I/T_{tot}$), and increased muscle energy demands with a need for increased blood flow, oxygen, and nutrients. The ultimate result of this sequence is respiratory muscle fatigue that represents an imbalance between demand (work of breathing and afterload) and supply (blood flow, oxygen, and nutrients).

Clinical manifestations of respiratory muscle fatigue also follow a predictable sequence that has been utilized for predicting patient fatigue and ability to wean from mechanical ventilator support. The clinical manifestations of respiratory muscle fatigue sequence include increased respiratory rate, development of discoordinate respiratory movements (i.e., abdominal paradox and respiratory alternans), increase in $PaCO_2$, respiratory acidemia, and terminal decrease in respiratory rate and minute ventilation. Measures of WOB have been proposed as a way the clinician can balance the factors associated with respiratory muscle fatigue, thus allowing patients to breath spontaneously during mechanical ventilator support, given that the goal of this support in respiratory failure is to decrease afterload (WOB) on the respiratory muscles.

11.9.3 Measurements of the Energetics of Breathing

11.9.3.1 Work of Breathing

In the pressure–volume curve for the calculation of WOB, the pressure needs to represent changes in intrathoracic pressure, more specifically, pleural pressure.

Thus, mechanical WOB can be calculated by measuring the generation of intrathoracic pressure due to contraction of the respiratory muscles (P_{mus}) and/or the applied pressure from the ventilator (P_{appl}). The total pressure generated at the airway (P_{aw}) is thus the sum of P_{mus} and P_{appl}. These pressure changes are related to the generated pressure differences needed to overcome forces from different components of the respiratory system such as the lung, chest wall, and respiratory system. These pressure differences are related to ventilation and thus movement of gas. Below are the calculations necessary to express these pressure differences, depending upon forces to be overcome.

For the pressure differences across the lung, called transpulmonary pressure (P_L),

$P_L = P_{aw} - P_{pl}$ where P_{aw} is airway pressure and P_{pl} is pleural pressure.

For the pressure differences across the chest wall (P_{CW}),

$P_{CW} = P_{pl} - P_{bs}$ where P_{pl} is pleural pressure and P_{bs} is body surface pressure.

For the pressure differences across the respiratory system (P_{RS}),

$$P_{RS} = P_{aw} - P_{bs}$$

Alternatively,

$$\begin{aligned} P_{RS} &= P_L + P_{CW} \\ &= P_{aw} - P_{pl} + P_{pl} - P_{bs} \\ &= P_{aw} - P_{bs} \end{aligned}$$

The pressure differences above are important because the lung and chest wall move together, conjoined by a potential space formed by the two pleural linings. The pressure in the pleural space is denoted P_{pl}, and at rest in the upright human, it is slightly negative, because the lung is a passive structure that is elastic and has a tendency to recoil to a smaller volume than the respiratory system combination (lung and chest wall together). The lung is prevented from collapsing because of the tendency of the chest wall to recoil outwards and the negative value of P_{pl}. At the end of a relaxed exhalation (to functional residual capacity) and with the mouth open, the alveolar pressure (P_{alv}), the pressure of the airway opening (P_{AO}), and the

atmospheric pressure (P_{atm}) are equal. Thus, at functional residual capacity with the mouth open, the distending pressure of the lung (P_L) is equal to the pressure inside the lung P_{alv} (which in this case is equal to P_{atm}) minus the pressure in the pleural space. The importance of this is that the distending pressure across the lung (transpulmonary) determines the lung volume. Therefore, the changes in distending pressure result in changes in lung volume and thus ventilation. In order to understand ventilation, we must understand and be able to measure P_{pl} and P_{alv}. This will in turn allow us to calculate the distending pressure of the lung, chest wall, and respiratory system.

P_{alv} is measured by assessing P_{AO} during static maneuvers when, with an open glottis and uninterrupted airway, $P_{alv}=P_{AO}=P_{atm}$. We can easily measure P_{atm} and by convention P_{atm} is said to equal a pressure of zero. P_{pl} is measurable directly only by placing a catheter in the pleural space, which is not usually possible in clinical practice. Fortunately, the pressure in the lower third of the esophagus (P_{es}) closely approximates the pressure in the adjacent pleura when the subject is in the upright posture, due to the close proximity of the esophagus to the pleural space. Because the body of the esophagus is essentially a passive structure (except during a swallow), able to transmit pressure from the adjacent pleural space (P_{pl}) to a measurement catheter in the esophagus, P_{es} is a reasonably close surrogate for P_{pl} in a human being in the upright posture. This does not necessarily hold true in the supine position, in which the mediastinum may compress the esophagus. Compression of the posterior and inferior portions of the lung can create large regional differences in pleural pressure.

In addition to the measurement of P_{es}, it is also possible to measure gastric pressure (P_{ga}) by placing another catheter more distally, in the stomach. P_{ga} closely approximates the pressure in the abdominal cavity. With accurate measurements of P_{pl} and abdominal cavity pressure, a wide variety of useful measurements of the mechanical respiratory system can be made.

During normal, unassisted, spontaneous inhalation, pressure is generated by the respiratory muscles (P_{mus}) to overcome the elastic and resistive pressures of the respiratory system. Elastic pressure (P_{el}) is the product of respiratory system elastance (E_{st}) (reciprocal of compliance) and volume (V) such that

$$P_{el} = E_{st}\left(\text{cm}\,H_2O/\text{L}\right)\times V\left(\text{L}\right)$$

Resistive pressure (P_{res}) is the product of total resistance (respiratory system plus breathing apparatus resistance, R_{TOT}) and inspiratory flow rate ($\dot{V}$ (L/s)), that is,

$$P_{res} = R_{TOT}\left(\text{cm}\,H_2O/\text{L}/\text{s}\right)\times\left(\text{L}/\text{s}\right)$$

Under normal conditions in adults, the change in the pressure generated by the respiratory muscles is approximately 5 cm H_2O. When there is increased elastance and/or resistance, the respiratory muscles are loaded and thus work of breathing increases:

$$P_{mus} = P_{el} + P_{res}$$

This increase in respiratory muscle pressure can be decreased when the respiratory muscles are unloaded with an appropriate level of ventilator support (e.g., PSV):

$$P_{mus} = \left(P_{el} + P_{res}\right) - PSV$$

Thus, the ventilator becomes an extension of the patient's respiratory muscles, causing partial unloading of the respiratory muscles and sharing of the load between the respiratory muscles and the ventilator.

These interactions during mechanical ventilation can be summarized by Newton's equation of motion, with presence of intrinsic PEEP adding to respiratory loading by increasing expiratory airway resistance and/or by inadequate exhalation time:

$$P_{mus} + P_{appl} = \text{PEEP}_i\left(\text{intrinsic PEEP}\right) + P_{res} + P_{el}$$

Thus, factors affecting the load of respiratory muscles can be subdivided into physiologic factors and factors associated with the breathing apparatus. The physiologic factors include elastic work (lung and chest wall compliance),

resistive work (apparatus), inspiratory flow rate demand, alveolar minute ventilation, and dead space. Breathing apparatus factors include the imposed work associated with the endotracheal tube and ventilator, sensitivity and trigger setting, response time of the ventilator, and method of triggering the ventilator. For factors associated with the breathing apparatus, the endotracheal tube is probably the most important resistor associated with increased WOB, secondary to the increased resistive workload. This effect is most exaggerated in neonatal and pediatric patients who have smaller endotracheal tubes (Lesouf et al. 1984).

WOB can be calculated utilizing the Campbell diagram in Fig. 11.31 (Campbell 1958), which illustrates the dynamic relationship between pleural pressure and lung volume. Since pleural pressure is difficult to measure, the surrogate measurement of esophageal pressure is commonly utilized for both research and clinical applications of WOB measurement. Esophageal pressure swings during inspiration need to overcome two forces: the elastic forces of the lung parenchyma and chest wall and the resistive forces generated by the movement of gas through the airways. One can calculate these two components (elastic and resistive) by comparing the difference between esophageal pressure during the patient's effort (the breath) and the pressure value under passive conditions, represented by the static volume–pressure curve of the relaxed chest wall. This passive volume–pressure curve is a crucial component of the Campbell diagram (Fig. 11.31). It is calculated from the values of esophageal pressure and lung volume obtained when the airways are closed and the muscles are completely relaxed. The volume of functional residual capacity results from the expansion of the lung and reduction in chest wall volume. During spontaneous inhalation, intrapleural pressure decreases and volume increases. The elastic work required to expand the lungs is defined in the diagram as the triangular-shaped area subtended by the lung and chest wall compliance curves. This elastic work done by the respiratory muscle is less than that illustrated by the diagram because

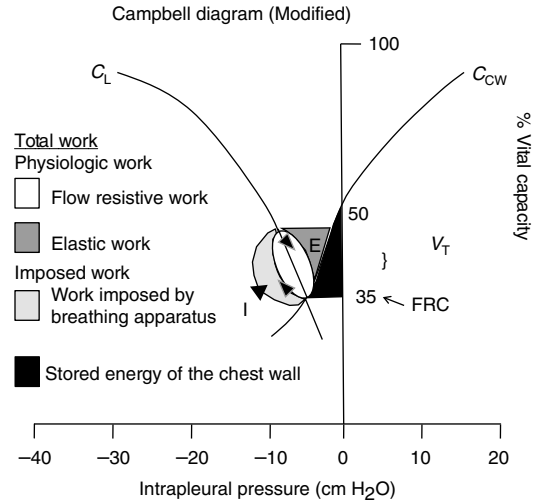

Fig. 11.31 Representation of the total work of breathing using a modified version of the Campbell diagram. Compliance curves of the lungs (C_L) and chest wall (C_{CW}) are shown in relationship to volume and intrapleural pressure and intersect at functional residual capacity (*FRC*). During spontaneous inhalation (*I*), tidal volume (V_T) increases, while intrapleural pressure decreases (upward pointing arrow of inner pressure–volume loop). Exhalation (E) is normally passive. The inspiratory portion of the loop (*vertical lines*) is the physiologic inspiratory flow-resistive work of breathing. The physiologic elastic work of breathing is the *triangular-shaped area* subtended by the compliance curves (*diagonal lines*). The Campbell diagram is modified to include the additional flow-resistive workload (outer pressure–volume loop) imposed by the breathing apparatus (endotracheal tube, breathing circuit, and ventilator, stippled area). The total work of breathing for a spontaneously breathing, intubated patient attached to a ventilator is the physiologic plus the imposed work of breathing (From Banner (1994))

of energy stored and recovered from chest wall displacement. The elasticity of the chest wall (tendency to recoil outward) is actually assisting the inflation of the lungs; conversely, it opposes exhalation. Unfortunately, as this is difficult to measure (because it requires passive inflation and often muscle paralysis), a theoretical value for the slope of this curve is frequently used in lieu of the exact measurement. However, if the patient does not require neuromuscular blockade with muscle relaxant, a true value for the volume–pressure relationship of the chest wall can be obtained during passive tidal breathing (Jubran et al. 1995). Thus, for subsequent breaths when the patient develops spontaneous

respiratory efforts, the passive pressure–volume value can be utilized.

Other components of the Campbell diagram must be considered. The lower half of the inner pressure–volume loop represents the physiologic inspiratory flow-resistive work of breathing. Expiratory resistive work is not illustrated in the diagram because it is usually provided by the elastic energy stored during inhalation. Thus, exhalation is a passive process under normal conditions, requiring no additional energy or work.

As we have mentioned, WOB can be subdivided into work attributed to the patient (physiologic WOB, WOB_p) and that associated with the ventilator (imposed WPB, WOB_v). Essentially the work done by both the patient and the ventilator must overcome the resistive and elastic components of the patient/ventilator system. Thus, it includes elastic WOB (work required to overcome the elastic forces during inflation) and flow-resistive WOB (work required to overcome the resistance of the airway and pulmonary tissue to the flow of gas). The imposed WOB (work performed by the patient to breath spontaneously through the apparatus, i.e., the endotracheal tube, breathing circuit, and ventilator) is an additional flow-resistive workload. Figure 11.32 illustrates a Campbell loop demonstrating additional resistive workload on the respiratory muscles from a breathing apparatus during spontaneous inhalation. When breathing through a highly resistive apparatus at a high peak inspiratory flow rate demand, for example, the imposed work may exceed the physiologic work of breathing. In neonatal and pediatric patients with smaller diameter endotracheal tubes, this increased resistance causes imposed work. Thus, the total work of breathing done by the respiratory muscles in an intubated, spontaneously breathing patient connected to a mechanical ventilator consists of the physiologic, elastic, and flow-resistive work plus the imposed work of the breathing apparatus. Ventilatory support must balance the portion of the patient's total ventilatory requirements between WOB_v and WOB_p so that the patient component is titrated to maintain a non-fatiguing workload.

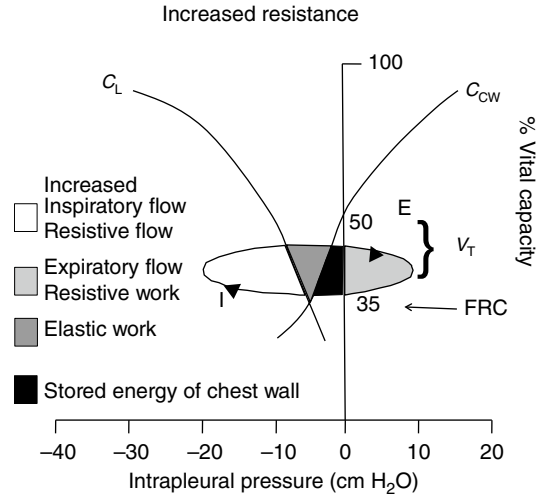

Fig. 11.32 Increased resistance from airway resistance and/or imposed resistance of the breathing apparatus results in increased flow-resistive work of breathing. Total work of breathing includes elastic work done on the lungs and increased inspiratory flow-resistive work performed by the expiratory muscles during spontaneous breathing of tidal volume (V_T), starting from functional residual capacity (*FRC*). C_L lung compliance, C_{CW} chest wall compliance, *I* inhalation, *E* exhalation (From Banner (1994))

WOB_v may be altered by changes in compliance, resistance, and patient effort, as well as the level of support provided by the ventilator. It is usually a reflection of the mode of ventilation and level of support applied. Increasing pressure support levels, elevating PEEP/CPAP, and altering the I/E ratio all can impact the measured work of breathing.

In contrast WOB_p can reflect the relationship between patient effort and ventilator response such that factors affecting it can relate to demand system sensitivity, ventilator dyssynchrony, increased expiratory airway resistance, loss of compliance, and improper ventilator mode selection.

In ventilated patients breathing spontaneously, to quantitate work performed in distending the lungs alone (excluding the chest wall), the relevant trans-structural pressure is transpulmonary pressure, P_L, which is equal to $P_{aw} - P_{es}$. At the commencement of inspiration, P_{es} is usually different from 0 cm H_2O due to chest wall recoil or other static forces on the esophageal balloon. This difference must be subtracted from P_{es} when

calculating values of work performed on the lung. During spontaneous breathing, P_{aw} is zero, and thus, inspiratory work can be calculated from the P_{es} and volume recordings alone. In a patient connected to ventilator circuit, P_{aw} is not zero, with the result that measurement of P_{es} alone does not permit calculation of work performed by the patient. Work performed by the ventilator or work imposed on the patient by the ventilator and external circuit still requires measurements of P_{aw} and volume. Measurements of total work during spontaneous efforts while a patient is attached to a ventilator require measurement of both P_{es} and P_{aw} (as well as volume).

It is essential, in order to clinically apply measurements of WOB, to differentiate not only differentiate the patient and ventilator components but also those associated with the work necessary to overcome the resistive and elastic components. Theoretically elastic changes reflect the patient's disease state and the reason the patient required mechanical ventilatory support as well as the opposing forces that create work. Those opposing forces can be subdivided into mechanical, or volumetric, and ventilator induced, or isometric. Mechanical opposing forces consist of the elastic aspects of the compliance of the lung and chest wall and the frictional forces of airway resistance. In contrast ventilator-opposing forces consist of effects of the ventilator demand system and circuit and presence of intrinsic PEEP.

Thus,

$$\mathrm{WOB_P} = \mathrm{WOB_{PL}} + \mathrm{WOB_{PCW}}$$

Work on the lung is calculated in the traditional way:

$$\mathrm{WOB_{PL}} = \left(P_{ee} - P_{es}\right) \times \frac{\mathrm{d}V}{\mathrm{d}t},$$

where P_{ee} is end-expiratory esophageal pressure.

Work on the chest wall for spontaneously breathing patient is calculated from tidal volume and chest wall compliance according to the following formula:

$$\mathrm{WOB_{PCW}} = \frac{1}{2} \times V_{\mathrm{T}}^2 \times C_{\mathrm{CW}}$$

During patient-triggered ventilator-assisted breaths, a portion of the tidal volume is delivered due to patient's effort, as indicated by negative delta P_{es}, and the other portion is delivered by the ventilator, as indicated by a P_{aw} that is greater than P_{atm}. The portion of tidal volume inspired solely due to patient's effort is designated V_p. Thus, for mechanically ventilated patients, patient volume must be used instead of tidal volume:

$$\mathrm{WOB_{PCW}} = \frac{1}{2} \times V_T^2 \times C_{\mathrm{CW}}$$

$$V_{\mathrm{T}} = V_{\mathrm{P}} + V_{\mathrm{V}}$$

For this equation the ratio of V_P to V_V is the same as the ratio of corresponding driving pressures. Since the ratio of delta P_{es} and delta P_{aw} varies through inspiration, the proportion must be determined from continuous integration of these pressures per the following formula:

$$V_{\mathrm{P}} = \frac{\left(P_{ee} - P_{es}\right)}{\left[\left(P_{aw} - P_{atm}\right) + \left(P_{ee} - P_{es}\right)\right] \mathrm{d}V/\mathrm{d}t}$$

If there is no patient effort, then $(P_{ee} - P_{es}) = 0$ and $V_p = 0$. If $P_{aw} = P_{atm}$ then V_p–V_T. To calculate WOB the integration limits must be determined from the start until the end of inspiration. The end of inspiration occurs when P_{es} becomes greater than P_{ee}.

P_{ee}: end-expiratory esophageal pressure
P_{es}: esophageal pressure
P_{aw}: airway pressure
P_{atm}: atmospheric pressure
V_P: patient volume
V_V: ventilator volume
V_T: tidal volume
C_{CW}: chest wall compliance (if not measured is assumed to be 200 ml/cm H_2O))
$\mathrm{d}V/\mathrm{d}t$: instantaneous flow

11.9.3.2 Flow-Resistive Work

Total resistive work done on the lungs during assisted breathing is obtained by integrating the area subtended by P_{es} and lung volume during a single breath. Work is partitioned into its inspiratory and expiratory resistive components by drawing a line between the points of zero

flow: the dynamic pulmonary compliance line. In Fig. 11.31 the area enclosed by the ellipse to the left of the line represents inspiratory resistive work, while the area to the right of this line represents expiratory resistive work. If the expiratory portion of the loop falls within the area representing elastic work, expiratory resistive work will be performed passively at the expense of the elastic energy stored in tissues deformed during inspiration. Measurement of resistive work using P_{es} includes work performed in overcoming the flow resistance of equipment in addition to the flow resistance of the lung.

Figure 11.32 (Campbell loop with increased resistance) illustrates increased resistance with subsequent increased flow-resistive work of breathing. Increased resistance can be due to increased resistance in the airways (i.e., bronchial obstruction or constriction) or changes in the breathing apparatus (i.e., secretions in endotracheal tube). In this example both inspiratory and expiratory muscles are loaded and active. Increased work of breathing is depicted as increased area in the inspiration and expiration parts of the pressure–volume loop.

11.9.3.3 Elastic Work

During unassisted breathing, work performed by the inspiratory muscles against elastic recoil of the lungs and chest wall can be calculated using volume versus esophageal pressure, utilizing measurement of the static compliance of the chest wall (C_{CW}). This can be estimated by recording P_{es} and volume during controlled ventilation while respiratory muscles are completely relaxed. Pressure developed by the respiratory muscles in expanding the chest wall is obtained from subtraction of P_{es} from P_{CW}.

In examining the pressure–volume loop for the calculation of C_{CW} during mechanical ventilation, inactivity of the respiratory muscles is determined by noting the formation of a P_{es}–volume loop in a counterclockwise direction. The loop is reasonably narrow, and the axis of the loop is rotated farther to the right as the level of ventilatory support is increased. On occasion, a neuromuscular blocking agent may be needed to achieve adequate respiratory muscle relaxation.

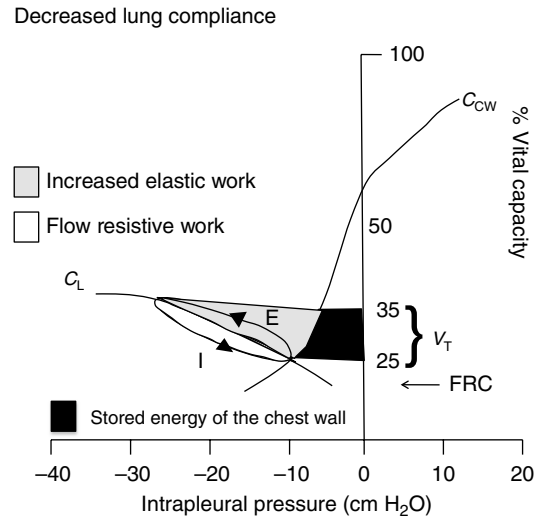

Fig. 11.33 Decreased lung compliance (C_L) results in increased elastic work of breathing. Total work of breathing includes flow-resistive work on the airways and tissues and increased elastic work done on the lungs by the respiratory muscles during spontaneous inflation of tidal volume (V_T), starting from a decreased functional residual capacity (*FRC*). C_{CW} chest wall compliance, *I* inhalation, *E* exhalation (From Banner (1994))

In Fig. 11.33, we illustrate an increase in elastic work resulting from a decrease in lung and/or chest wall compliance. Lung compliance changes are consistent with pulmonary disease that alters pulmonary compliance (i.e., ARDS, pneumonia), and chest wall compliance changes can be seen in diseases that affect the chest wall directly (i.e., kyphoscoliosis) or indirectly (i.e., abdominal distension).

Decreased compliance inversely affects elastic work of breathing for either the lung or chest wall. Decreased chest wall compliance is illustrated in Fig. 11.34. Subsequently as compliance decreases, there is direct correlation to changes in tidal volume. Patients compensate with either increased respiratory effort or attempts to improve functional residual capacity.

11.9.3.4 Expiratory Work

Expiration is passive with work being performed entirely during inspiration. Total work performed is distributed evenly between work dissipated as heat in overcoming flow-resistive work and the work which is stored as potential energy in the deformed

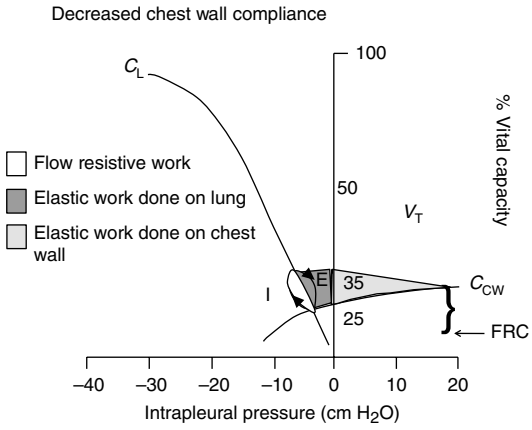

Fig. 11.34 Decreased chest wall compliance (C_{CW}) results in increased elastic work of breathing. Total work of breathing includes flow-resistive work on the airways and tissues, elastic work done by the lungs, and elastic work done on the chest wall by the respiratory muscles during spontaneous inflation of tidal volume (V_T), starting from decreased functional residual capacity (*FRC*). C_{CW} chest wall compliance, *I* inhalation, *E* exhalation (From Banner (1994))

tissues of the lungs and chest wall for use during expiration. Normally this stored work is transferred to inspiratory muscles except when there is markedly increased expiratory resistance resulting in recruitment of expiratory muscles. Use of expiratory muscles increases P_{es}, producing P_{es}–volume values to the right of the chest wall relaxation line and outside the elastic work of the Campbell diagram. In this situation, P_{es} is higher than the elastic recoil pressure of the chest wall. Expiratory work can be quantified as the area enclosed by the expiratory portion of the P_{es}–volume loop to the right of the chest wall relaxation line. This measurement can underestimate expiratory work in proportion to the amount of work needed to overcome the expiratory resistance of the chest wall.

11.9.3.5 Negative Inspiratory Work

Some of the energy stored in the tissues during inspiration is used during the expiratory phase of the respiratory cycle to overcome flow resistances of the lung and chest wall, with the remainder being used to overcome the persistent activity of the inspiratory muscles during expiration. Since this post-inspiratory work performed is considered negative (i.e., something does work on the muscle), it is classified as plyometric. This negative work is substantial during normal resting ventilation but becomes small with increasing ventilation. It can be calculated by subtracting expiratory-flow-resistive work from the elastic work of inspiration. Overall, the energy cost of negative work performed by the inspiratory muscles during expiration is considered negligible.

11.9.3.6 Work Units

For work the most popular units are kilograms · meters (kg · m) and joules (J). One joule is the energy needed to accelerate a 1 kg mass 1 m/s/s. Because the force of gravity accelerates objects at 9.8 m/s^2, thus,

1 kg · m (a force equal to the weight of 1 kg applied over 1 m) is equivalent to 9.8 J

1 J = energy needed to raise 1 kg 10.2 cm against the force of gravity

$$1\,\mathrm{W} = 1\,\mathrm{J/s}$$

$$1\,\mathrm{cal} = 4.184\,\mathrm{J}$$

In general, 0.1 kg · m approximates 1 J, and this can be thought of as the energy that is needed to move 1 l through a 10 cm H_2O pressure gradient.

11.9.3.7 Pressure–Time Product

In the case of ineffective respiratory effort, that is, muscle contraction without volume displacement, WOB cannot be measured from the Campbell diagram, since the calculation is based on volume displacement. A measure that appears to more closely approximate oxygen cost of breathing or energy expenditure of the muscles is the pressure–time product (P_{TP}). The P_{TP} is the product of the pressure developed by the respiratory muscles multiplied by the time of muscle contraction, expressed in cm H_2O per second, and described in Fig. 11.35. The relevant pressure is again the difference between the measured esophageal pressure and the static relaxation curve of the chest wall. The pressure measurement most often used in this calculation is P_{es}. For patients receiving volume-controlled ventilation where tidal volume is predetermined, the calculation is straightforward. Unfortunately, in a mode of ventilation where inspiratory flow can vary breath to breath, this calculation can be

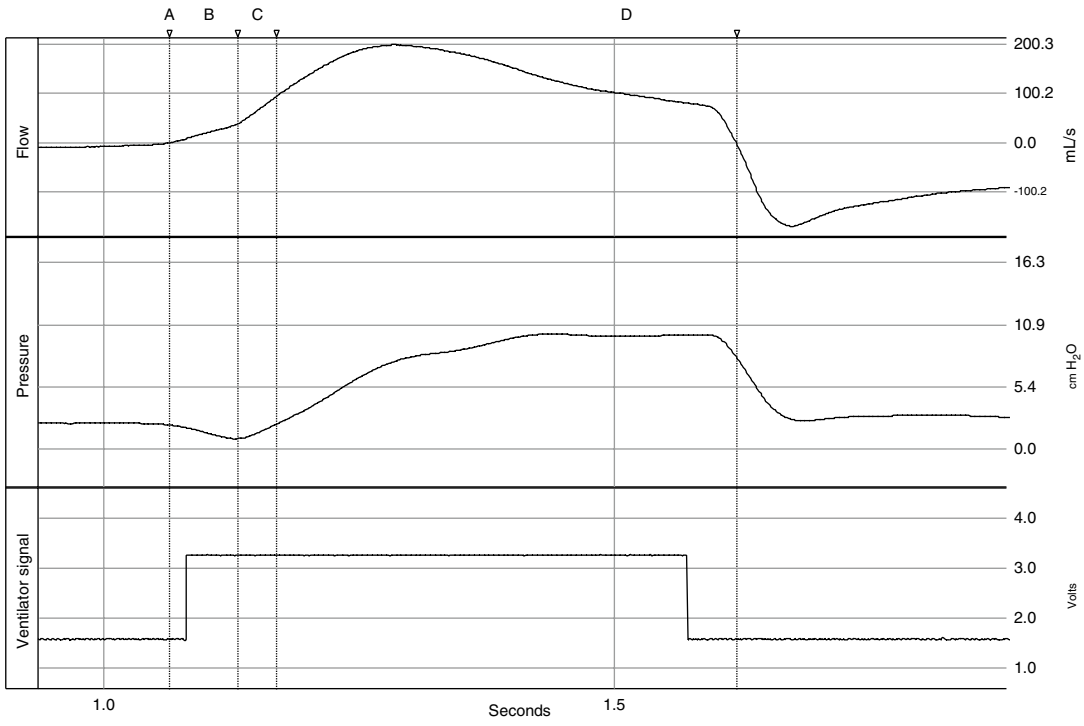

Fig. 11.35 The pressurization of the respiratory system can be subdivided into the inspiratory positive pressure area or P_{TP} area 2, *C–D* (Chatmongkolchart et al. 2001), which follows P_{TP} area 1, *A–C*, and is the amount of effort expended to activate the mechanical breath. Area 2 is defined by the start of the inspiratory pressure curve with the return of pressure to baseline and ending at the onset of expiration. Area 2 represents the ability of the ventilator to pressurize the system or the actual area of pressure versus time applied during inspiration. The figure represents the time in ms from the point where the breath is initiated (where flow crosses the zero line) till point of peak inspiratory pressure. This represents the sum of the subject's effort and the response time of the ventilator

difficult. However, it can be calculated utilizing the upper and lower bounds of the pressure–time product for patients in pressure support ventilation (Jubran and Tobin 1997). P_{TP} varies directly with total lung resistance.

P_{TP} is measured as the integral of esophageal pressure and time for the duration of contraction of the respiratory muscle.

Thus,

$$P_{TP} = \left[\left(P_{EE} - P_{ES}\right) + \left(Vol / C_{CW}\right)\right] \mathrm{d}t / t_{min} \quad \text{while } P_{ES} \text{ is greater than } P_{EE}$$

P_{EE} = end esophageal pressure
P_{ES} = current esophageal pressure
Vol = current tidal volume
C_{CW} = chest wall compliance (assumed at 200 ml/cm H_2O)
dt = sample time
t_{min} = duration of breath in minutes

Another measure is pressure–time index (PTI), which is a measure of strength and endurance combined into one value. It combines the strength measurements of P_{ES} and maximum inspiratory pressure during occlusion with the endurance value of the inspiratory time as a fraction of total respiratory time. The PTI combines indicators of respiratory muscle strength and endurance and correlates directly with oxygen consumption and inversely with respiratory muscle fatigue. Clinically as muscle strength is depleted and muscle endurance can no longer sustain the workload

imposed upon it, the respiratory pump may begin to fail. PTI may be utilized to predict the onset of respiratory muscle fatigue.

PTI is calculated using pressure and flow measurements in conjunction with the inspiratory time fraction. The equation is as follows:

$$\mathrm{PTI} = \left\{\left[\sum \left(P_{\mathrm{EE}} - P_{\mathrm{ES}}\right) \mathrm{d}t / T\right] \times T_{\mathrm{I}} / T_{\mathrm{TOT}}\right\} \Big/ MIP$$

P_{ES} = esophageal pressure
P_{EE} = end-expiratory esophageal pressure
dt = delta time
T = integration time (occurs during inspiration)
MIP = maximum inspiratory pressure during an occlusion maneuver
T_I/T_{TOT} = inspiratory time divided by total respiratory time

Another method is the tension–time index that utilizes the transdiaphragmatic pressure (P_{di}) measured from both gastric and esophageal balloons. In this method measurement of P_{es} and P_{ga} allows calculation of P_{di} according to the formula $P_{di} = P_{ga} - P_{es}$. Thus, the tension–time index for the diaphragm is the product of total respiratory cycle time and P_{di}/maximum P_{di}. The tension–time index has been correlated with oxygen consumed by the diaphragm and a value exceeding 0.15 is associated with diaphragm fatigue (Bellemare et al. 1983; Field et al. 1984). It should be noted that the concept of diaphragm fatigue is debated amongst respiratory physiologists but is beyond the scope of our discussion.

As previously stated a tension–time index or P_{TP} is reflective of work of breathing (WOB). Pressure waveforms can be obtained with the pneumotachograph at the airway and the area of the breath measured can subdivide the P_{TP} (Fig. 11.35). P_{TP} Area A is defined as the area of the pressure curve (integration of pressure with respect to time) from initiation of a breath to the beginning of ventilator pressurization. P_{TP} Area A reflects patient WOB since it reflects the effort by the patient during triggering. P_{TP} Area B is defined as the area of the pressure curve from the beginning of ventilator pressurization to return to baseline pressure. P_{TP} Area B reflects both patient and ventilator WOB. P_{TP} Area 1 is defined as P_{TP} Area A plus P_{TP} Area B. P_{TP} Area 1 reflects initial work performed by both the patient and ventilator. P_{TP} Area 2 is defined as the area of the pressure curve during inspiration. P_{TP} Area 2 reflects work performed by the ventilator.

These calculations can be clinically relevant in regard to triggering the ventilator as discussed below.

11.9.3.8 Techniques and Limitations

Work of breathing performed by the patient on the respiratory system (physiologic work) and by the breathing apparatus (imposed work) during spontaneous ventilation is calculated by integrating changes in esophageal pressure, as an indirect measure of intrapleural pressure, and volume. This technique requires the placement of an airway pneumotachograph and an esophageal balloon. The esophageal balloon must be placed in the middle to lower third of the esophagus in order to best reflect changes in intrapleural pressure and not be affected by cardiac oscillations transmitted in the upper portions of the esophagus. To assure the esophageal catheter is in the correct position, a dynamic "occlusion test" is performed (Baydur et al. 1982; Milner et al. 1978). This test requires that the patient be spontaneously breathing so that an inspiratory effort is performed against a closed airway and then assessing that P_{es} changes correspond to changes in P_{AO}.

A limitation of this technique in mechanically ventilated patients is the availability of the necessary equipment to perform these measurements and calculations at the bedside. Unfortunately, integration of this equipment into the ventilator platform is currently limited to one ventilator manufacturer. Also important, the esophageal pressure displayed must be in good agreement with direct measurements of P_{pl}. MilicEmilie et al. (1964) demonstrated that total work may be inaccurate when inspiratory and expiratory works are estimated separately due to the overcompensation by expiratory work (Baydur et al. 1982).

Another limitation is seen in patients who display intrinsic PEEP where the placement of the chest wall relaxation curve on the Campbell

diagram is inaccurate because the work performed to overcome flow resistance of the chest wall is not accounted for accurately.

When calculating mechanical work, the site of measurement may impact its accuracy. Since mechanical work is traditionally calculated from volume changes at the mouth when the actual volume change occurs in the lung, this difference may be exaggerated in situations where there is airway obstruction, hyperinflation, or tachypnea. In these cases the mouth measurement underestimates the true work.

Finally, as discussed above, assumptions are made in the calculation of work of breathing regarding the respiratory system and its ability to follow the relaxation pressure–volume curve. When there are distortions of the chest wall due to high levels of ventilation and effort, the measured work may be again underestimated.

11.9.4 Clinical Relevance

WOB is frequently discussed when physicians perform rounds on their patients in the intensive care unit, but applying actual measurements of WOB in clinical decision making has been elusive. Available evidence suggests that total unloading of respiratory muscles can allow the respiratory muscles to rest and recover (Braun et al. 1983; Stoller 1991). Goals of mechanical ventilation have been to reduce this work thus allowing recovery of respiratory muscles. However, this support must be balanced between causing muscle fatigue secondary to increased muscle loading from breathing through a high-resistance apparatus and resultant muscle atrophy due to totally unloading respiratory muscles for prolonged periods (Civetta 1993).

In order to balance the above factors, we must understand the variability of the work associated with different breathing apparati. Figure 11.37 demonstrates associated imposed WOB with frequently used ventilators in neonatal and pediatric patients. This variability between ventilators is associated with a various aspects of ventilator design. As can be seen in Fig. 11.38, the associated WOB for the patient occurs predominately during the trigger phase. Triggering in modern ventilators occurs in response to either a pressure or a flow signal. Both signals require the patient to initiate flow by a pressure drop across the endotracheal tube. The imposed WOB with flow triggering is less than with pressure triggering; however, the difference is primarily related to post-trigger events rather than triggering per se. It has been demonstrated that flow triggering in neonatal and pediatric patients decreases WOB (Carmack et al. 1995), as can be seen in Fig. 11.36 (Sanders et al. 2001). The advantage of flow triggering is associated with the decreased effort generated by the patient, as exemplified by both the reduced negative inspiratory pressure generated to trigger the ventilator and the response time of the ventilator (Giuliani et al. 1995). The response time of the ventilator is the time delay from the patient's effort to trigger the ventilator, as seen in Fig. 11.35, to the ventilator response indicated by opening of the inspiratory valve and the onset of fresh gas flow. This response can be affected by the triggering sensitivity setting (pressure of flow) and response characteristics of the ventilator demand system. As can be seen in Figs. 11.37, 11.38, 11.39, 11.40, and 11.41 the response time and effort necessary to trigger the ventilator can vary due to the certain design issues. First it relates to timing of the trigger signal. Ideally in flow triggering, the beginning of the signal should correspond to when inspiratory flow crosses the zero line. However, as can be seen in Fig. 11.39, there can be a delay between when this signal occurs and when the ventilator opens the inspiratory valve. Work is increased in this situation because during this phase of triggering, all effort is generated by the patient with no support from the ventilator.

In order to decrease the response time, it has been proposed to use a sensor at the patient's airway. In Fig. 11.42, three different types of airway sensors are compared demonstrating differences amongst different sensors with evidence of increased WOB and effort to trigger with the variable orifice sensor.

It is important to note that the rate and slope of the delivered flow can also have an effect on

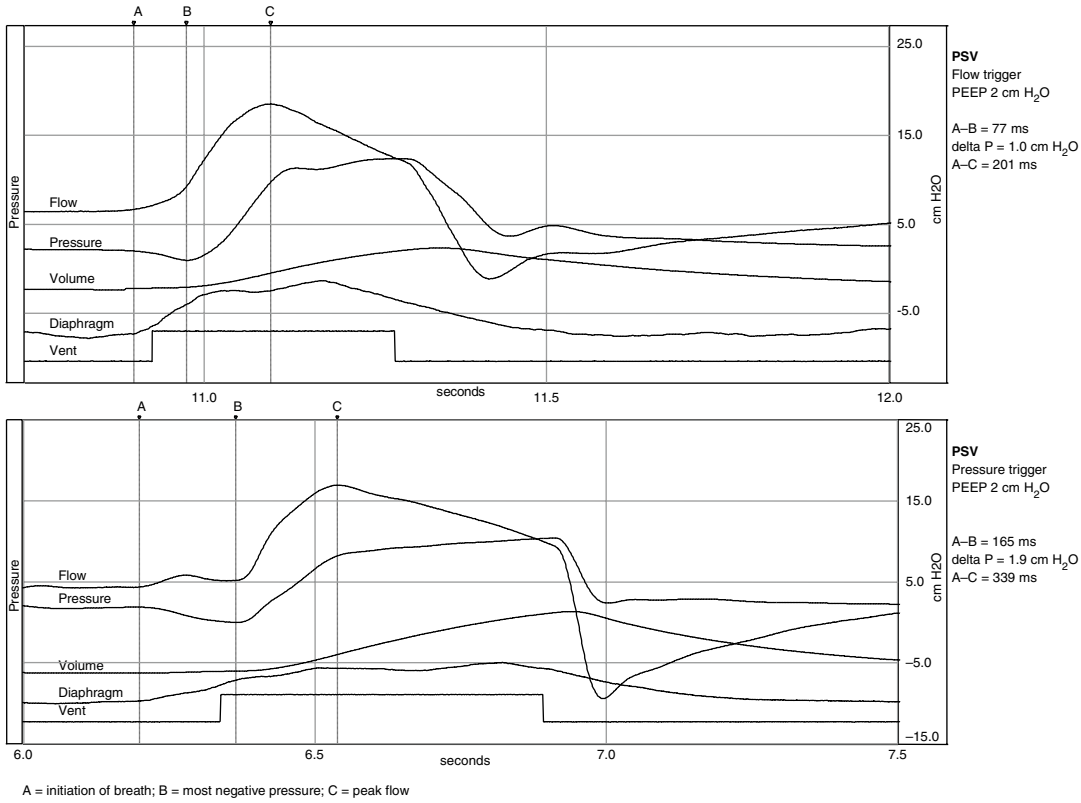

Fig. 11.36 The *upper waveform* represents a single breath of a spontaneously breathing animal on pressure support being flow triggered. The *bottom waveform* represents a pressure-triggered breath. The negative pressure generated by the animal during triggering of the pressure-triggered breath is almost double of the pressure necessary to trigger the flow-triggered breath. Also there is evidence of increased trigger delay in the pressure-triggered breath (Sanders et al. 2001)

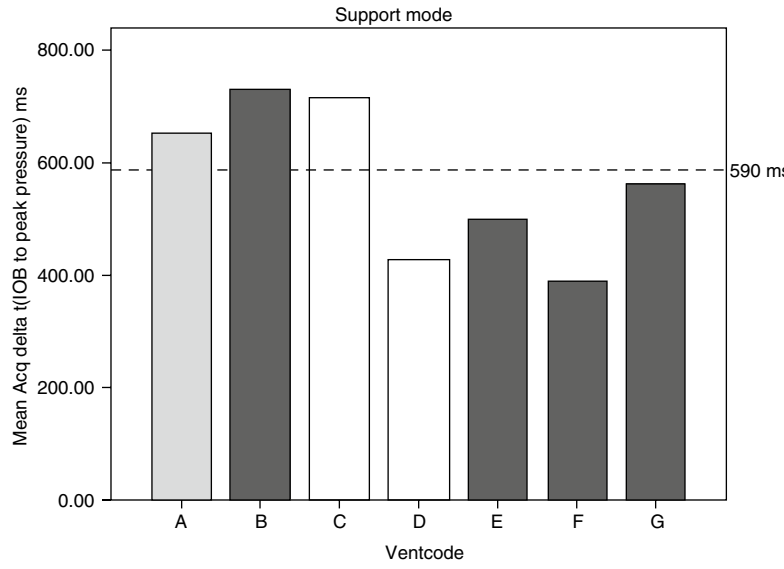

Fig. 11.37 Represents the time in ms from the initiation of the breath, where flow crosses zero to the peak inspiratory pressure in seven modern ventilators. This area of the breath represents the total response time from initiation to full pressurization of the breath. The average time across the seven ventilators for animals breathing spontaneously is 590 ms with a range of 390–710 ms. *IOB* initiation of breath

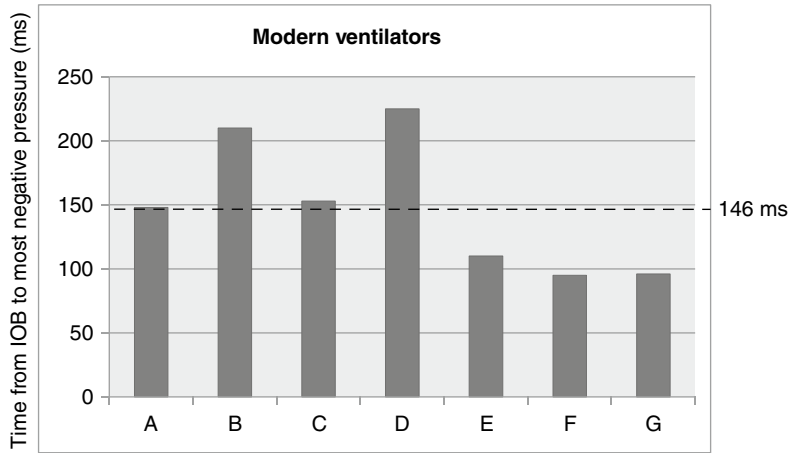

Fig. 11.38 Represents the time in ms from the point where the breath is initiated (where flow crosses the *zero line*) till point of the most negative deflection of pressure. The breath is measured from the beginning of the breath represented as the point when flow crosses zero till the point when the animal generates the most negative deflection of pressure. This period of time represents the effort of the animal and corresponds to the work of breathing during triggering of the ventilator. This graph represents this measurement for 7 modern pediatric ventilators. The average time for these ventilators was 148 ms with a range of 97–220 ms. *IOB* initiation of breath

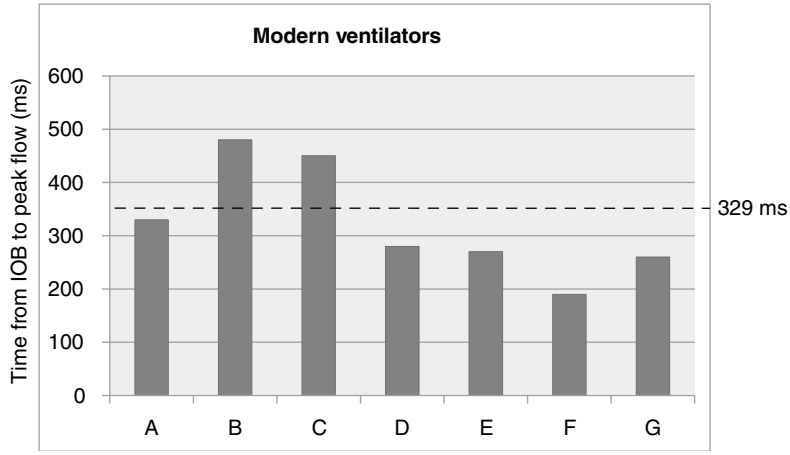

Fig. 11.39 Represents the time in ms from the point where the breath is initiated (where flow crosses the *zero line*) till point of maximum flow. The breath is measured from the beginning of the breath represented as the point when flow crosses zero till the point when the animal generates the peak inspiratory flow. This period of time represents the effort of the animal and corresponds to the work of breathing during entire triggering of the ventilator plus the time to complete pressurization. This *graph* represents this measurement for 7 modern pediatric ventilators. The average time for these ventilators was 329 ms with a range of 195–470 ms. *IOB* initiation of breath

the WOB. If flow is inadequate, then the patient effort to obtain flow from the ventilator system may be exaggerated due to high respiratory drive, thus increasing WOB. Modern ventilators allow the clinician to control the initial flow, termed inspiratory rise time (Chatmongkolchart et al. 2001).

Investigators have examined the utility of predicting the outcome of weaning from mechanical ventilatory support by measuring the level of

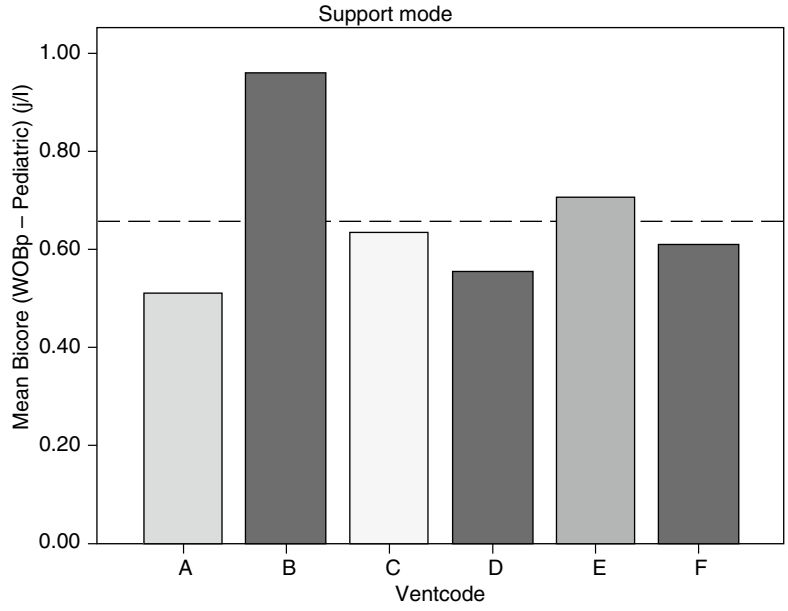

Fig. 11.40 Represents the average sum of elastic and resistive work of breathing (j/l) for animals breathing on six modern ventilators during flow triggering. The average patient work of breathing is 0.65 j/l. The range of work of breathing for these ventilators are 0.5–0.92 j/l representing a twofold increase in WOB between ventilator B to ventilator A

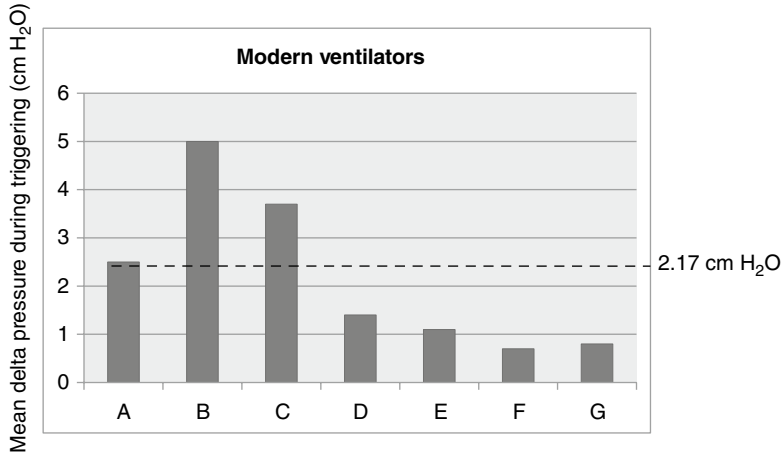

Fig. 11.41 Represents the amount of pressure generated by an animal breathing on a group of 7 pediatric ventilators during the trigger phase. The pressure generated is measured as the most negative deflection of pressure generated in cm H_2O for these ventilators. This measure represents the effort by the animal to trigger the ventilator and is a surrogate of the WOB generated by the animal during triggering. The average pressure generated was 2.17 cm H_2O with a range between the ventilators of 0.6–4.9 cm H_2O

inspiratory work. The predictive value of respiratory work as an index of weaning patients from mechanical ventilation remains to be determined (Marini et al. 1986).

11.9.4.1 WOB in the Pediatric Patient

Studies examining the use of WOB measurements as predictors of weaning or to perform accurate measurement of elastic, flow-resistive,

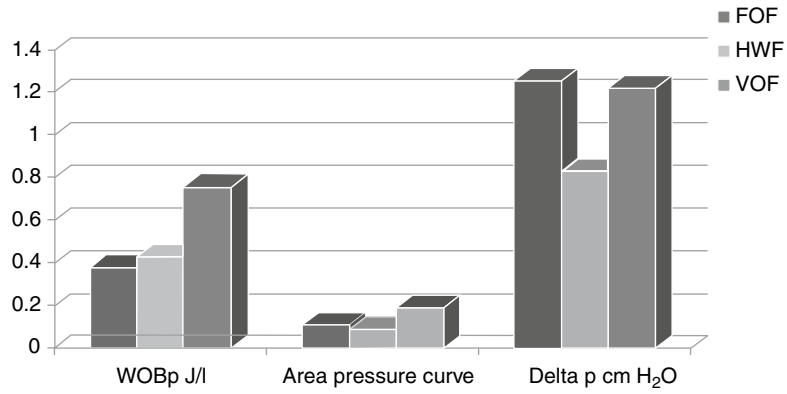

Fig. 11.42 Represents a comparison of three types of airway sensors in regard to the WOB (j/l), area pressure curve (see Fig. 11.6), and the pressure (cm H_2O) generated during the triggering phase representing the triggering effort. As can be seen in the figure, the VOF airway sensor has the highest degree of WOB and effort by the animal. The airway sensors are a fix orifice airway sensor (*FOF*), heated wire airway sensor (*HWF*), and a variable orifice airway sensor (*VOF*)

and imposed work during mechanical ventilation to guide the level of support or to guide specific selection of the ventilator mode are limited in pediatric patients. In adult patients the best measure of WOB was measured work on the lungs via measurement of transpulmonary pressure and flow. However, the threshold value for differentiating patients who were ventilator dependent from those who were ventilator independent differs between reported studies, limiting their application to clinical practice. Reported studies in adults have not included large randomized series with WOB measures utilized in a prospective manner, thus further limiting the ability to apply reported values to decision making by clinicians. Pediatric studies of work of breathing have demonstrated that the level of WOB is associated with the level of support. In pediatric patients there is the problem of large instrumental dead space (Dassieu et al. 1998). Patel et al. reported in 20 infants that the mean transdiaphragmatic pressure–time product was higher with volume targeting at 4 ml/kg in comparison with a baseline of 6 ml/kg, regardless of the patient-triggered mode (Patel et al. 2009). This study implies that there is a minimal level of support required for infants to deal with the increased resistive work associated with breathing on a mechanical ventilator but does not offer insight into using P_{TP} as a predictor of weaning. Another study of pediatric patients has noted that for children with peripheral airway obstruction who require assisted ventilation, work of breathing during spontaneous breaths is decreased by the application of either compensatory positive end-expiratory pressure or pressure support (Graham et al. 2007). The type of trigger may have an effect on WOB (Sasson et al. 1994). However, Thiagarajan et al. demonstrated in pediatric patients that flow triggering might only reduce WOB when lung compliance is decreased (Thiagarajan et al. 2004). Even though these studies may offer insight into how the clinician can compensate for the higher instrumental dead space in pediatric patients and the effect on WOB, further study is required to examine if WOB measurements can be integrated into an algorithm for directing mechanical ventilations. It should be noted that any computer-driven system, even if it integrates data concerning WOB, may not outperform a team of dedicated intensivists and respiratory therapists (Laghi 2008).

11.9.4.2 WOB in the Neonatal Patient

Even more so than in the pediatric patient, measurement of WOB in the neonatal patient remains largely a research tool. Accurate measurements are technically difficult and subject to error in intubated patients due in part to the leak around the uncuffed endotracheal tube. Other problems with measurement, discussed under *Techniques and Limitations*, above, also apply.

As previously described, inspiratory work can be calculated from P_{es} and volume recordings in the spontaneously breathing patient ($P_{aw}=0$). Accuracy is increased in the non-intubated patient where effect of the endotracheal tube and associated leak is not an issue. Such measurements have been done in studies of noninvasive respiratory support such as continuous positive airway pressure (Pandit et al. 2001) using calibrated respiratory inductance plethysmography (RIP) to measure volume changes. Even so, these measurements are technically challenging and difficult. Calibrated RIP is certainly possible for volume measurements in the intubated patient, but accurate calibration is difficult.

Assessment of phase angle from RIP rib cage and abdominal bands can be used to estimate increases or decreases in WOB. The phase delay between expansion of the abdomen and rib cage can be expressed in degrees, with phase angles of 0° representing in-phase rib cage and abdominal movements and 180° representing totally out-of-phase movements. These measurements can be useful as they do not require calibration of the RIP signal and have been reported in evaluations in preterm infants (Chang et al. 2011).

The Campbell diagram has been used to quantify WOB in neonates (Jarreau et al. 1996). When effort is made to quantify the leak around the ETT, account for dead space of the pneumotachograph, and accurately calibrate the equipment, these measurements can be useful. WOB values calculated by some current neonatal ventilators may be useful for trending values but may not be accurate given problems with leak and possibilities of inaccurate calibration.

Transdiaphragmatic pressure–time product, described earlier in this chapter, has also been used to estimate WOB in neonates (Patel et al. 2010). These measurements, also, are time intensive and require sensitive equipment and accurate calibration for useful results, thus relegating them predominantly to research tools.

At this time, probably the most useful evaluation of WOB in the infant remains clinical assessment of breathing pattern. Increasing tachypnea and associated retractions or "abdominal" breathing should always alert the caregiver to increased WOB requiring careful assessment of cause and possible treatment options.

Future Perspectives

The use of work of breathing measurements to affect direct patient care during mechanical ventilation has been limited by the invasive nature of these measurements, which require an esophageal balloon and a freestanding monitor. Accurate measurement of elastic, flow-resistive, and imposed work during mechanical ventilation may be advantageous to the clinician in order to monitor ventilatory interventions that may optimize respiratory muscle loading and decrease the work of breathing. It has been demonstrated that the best predictor is a measure of the work performed by the lungs via measurement of transpulmonary pressure and flow. Further, the efficiency of these measurements in adults appears to be best predictive in ventilator-dependent patients. Recent technological advances have revived interest in utilizing an esophageal catheter to allow measurement of the patient's diaphragmatic EMG signal to trigger the ventilator and direct the level of ventilatory support. Future development needs to integrate esophageal manometry to measure respiratory work into these systems as part of available measures assisting the clinician in weaning and successful extubation. Further, any future studies must utilize these measurements in a prospective manner in large randomized trials.

Essentials to Remember

- Work of breathing can be subdivided into the work necessary to overcome the resistive, elastic, and inertial components and the work to move the chest wall and intestinal organs.
- WOB can be subdivided into work attributed to the patient (physiologic WOB, WOB_p) and that associated with the ventilator (imposed WOB,WOB_v).
- It is essential in order to clinically apply measurements of WOB to not only differentiate the patient and ventilator components but also those associated with the work necessary to overcome the resistive and elastic components.
- In the case of ineffective respiratory effort, when muscle contraction occurs without volume displacement, traditional measurement of WOB cannot be measured since this calculation is based on volume displacement. A measure that appears to more closely approximate oxygen cost of breathing or energy expenditure of the muscles as a measure of work of breathing is the pressure–time product (P_{TP}).
- Goals of mechanical ventilation have been to reduce WOB, thus allowing recovery of respiratory muscles. However, this support must be balanced between causing muscle fatigue secondary to increased muscle loading from breathing through a highly resistive apparatus and resultant muscle atrophy due to totally unloading respiratory muscles for prolonged periods.

11.10 Respiratory Monitoring of the Mechanical Behavior of the Respiratory System During Mechanical Ventilation: Clinical Application

Christopher J.L. Newth and Robinder G. Khemani

Educational Aims

After reading this chapter, the reader will be able to:

- Describe the main respiratory monitoring tools available for all physicians taking care of critically ill children.
- Titrate therapeutic interventions to the patient's disease state in order to provide optimal respiratory support and aid in eventual weaning to endotracheal extubation.
- Understand the potential role for rational respiratory monitoring in future pediatric trials involving mechanical ventilation.

11.10.1 Introduction

Respiratory failure is one of the most common reasons for admission to pediatric intensive care units (PICUs), particularly in the first 2 years of life. While patients are recovering from the etiology leading to respiratory collapse, intensivists are charged with supporting the respiratory system with mechanical ventilation. Fundamental to ensuring adequate support is close supervision of therapeutic interventions – through both invasive and noninvasive forms of respiratory monitoring. This discussion concentrates on common means of respiratory monitoring used in intensive care units. In particular, when mechanical assistance to ventilation is required, its optimal use demands that the user understands the relationship between the mechanical device and the mechanical properties of the patient's respiratory system so that optimal gas exchange can be provided. It is probable that the minimum physiological information needed for rational monitoring providing for the successful use of a mechanical ventilator requires understanding of at least five parameters: alveolar partial pressure of CO_2 ($PACO_2$), arterial oxygen saturation (SaO_2), the mechanical RC (resistance–compliance) time constant, functional residual capacity (FRC), and pressure–volume loop (PV) characteristics (Shannon 1989;

Hammer and Newth 1995). However, not all of these techniques need to be applied to all infants and children ventilated in the ICU.

11.10.2 Gas Exchange

Regardless of the process leading children to require mechanical ventilation, the pediatric intensivist wishes to maintain gas exchange to keep the body in a state of relative homeostasis. Gas exchange will be discussed elsewhere in this book, but the continuous monitoring of gas exchange with both invasive and noninvasive measures of oxygenation and ventilation is fundamental to computer-based decision support tools for automation of ventilator management and weaning to extubation (see Chap. 12).

11.10.3 Work of Breathing Measurements

In addition to normalizing gas exchange, another important goal of mechanical ventilation is to support patients while they are recovering from the inciting event that led to respiratory failure. To this end, minimizing work of breathing (WOB) during recovery by optimal selection of ventilator support allows the patient the highest likelihood of weaning to extubation. This is particularly useful for patients with obstructive airway disease.

11.10.3.1 Esophageal Manometry

Esophageal manometry has long been used in animals and adults to study the mechanics of breathing. An esophageal manometer can be used to subdivide measurements of respiratory system compliance into contributions from the chest wall and those from the lung. Respiratory system work is the pressure applied to yield a change in volume of the system. In reality, this work is comprised of elastic, resistive, inspiratory, expiratory, lung, and chest wall components (Benditt 2005). The most significant and dynamic component of work of breathing is best estimated by the change in pleural pressure needed to generate a change in volume. A liquid- or air-filled esophageal manometer, placed correctly in the lower third of the esophagus (Coates et al. 1989; Jackson et al. 1995), closely approximates pleural pressure (Asher et al. 1982; Higgs et al. 1983).

Esophageal manometry can monitor patient-initiated work on various levels of support (Graham et al. 2007). A good example of this is having a spontaneously breathing patient on continuous positive airway pressure (CPAP) and pressure support (PS) where optimal ventilator support is titrated based on the patient's WOB and comfort. Modern ventilators increasingly have built-in software to analyze WOB when paired with an esophageal catheter. This has lead to further investigations of this type of monitoring, with recent contributions in the areas of prediction of extubation outcome (Harikumar et al. 2009) and selection of appropriate PEEP in acute lung injury and respiratory distress syndrome (Talmor et al. 2008; Loring et al. 2010).

11.10.3.2 Respiratory Plethysmography

During normal tidal breathing, without significant pathology, diaphragm contraction leads inspiration followed quickly by chest wall muscle activity. However, as respiratory pathology develops, regardless of etiology, there is often an increasing amount of thoracoabdominal asynchrony (TAA), resulting from worsening respiratory (initially intercostal) muscle fatigue. Such TAA can be measured using respiratory plethysmography (Ross et al. 2010; Sivan et al. 1990; Hammer and Newth 2009).

Elastic bands are placed around the rib cage (RC) and abdomen (ABD) at the nipple line and umbilicus level, respectively. The output of these movements is then downloaded to a computer program that displays characteristic oscillatory patterns which approximate sine waves. The level of synchrony between these two bands, the phase angle (Θ), is then calculated as

$$\sin\Theta = m / s$$

where m is the length of the midpoint of the RC excursion and s is the length depicting the ABD excursion (Rossi et al. 1985b).

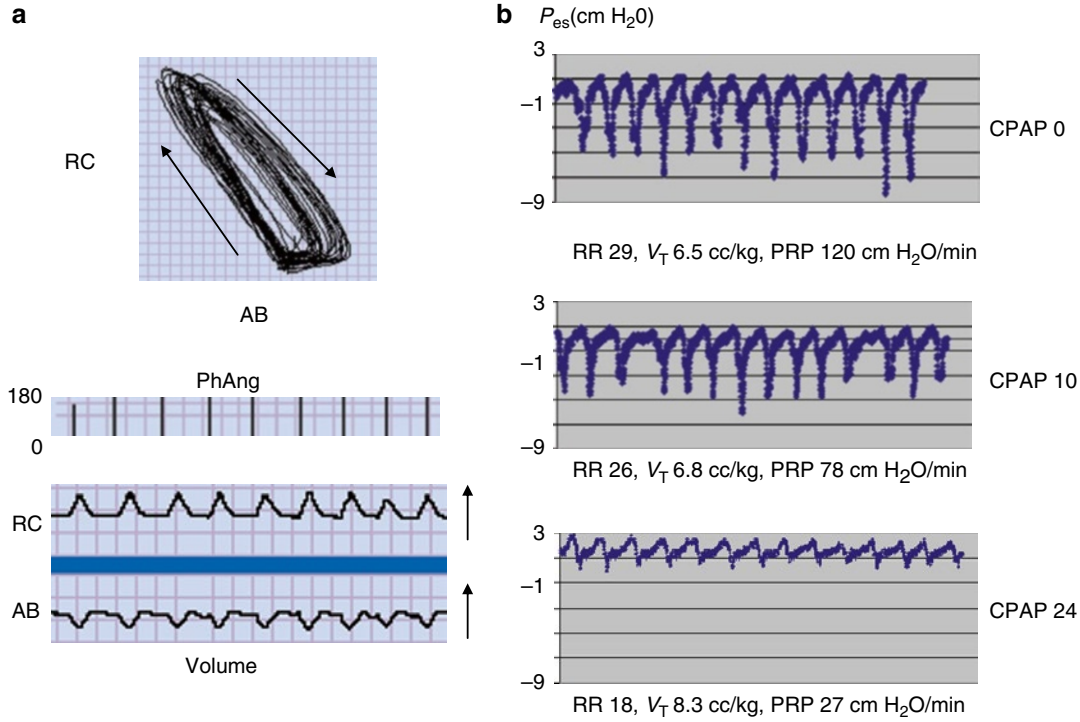

Fig. 11.43 Plethysmographic and esophageal pressure tracings during spontaneous breathing in a child with bilateral diaphragmatic paralysis. (**a**) *Top panel*, Konno–Mead plot of abdominal excursion (*AB*) against rib cage (*RC*) excursion. *Middle panel*, graphic representation of phase angle (*PhAng*) with each breath. *Bottom panel*, simultaneous plethysmographic waveforms over time. (**b**) esophageal pressure (P_{es}) tracings from the same child at increasing levels of continuous positive airway pressure (*CPAP*), with associated tidal volume (V_T), respiratory rate (*RR*), and pressure-rate product (*PRP*). During the course of increasing CPAP, in this situation, the phase angle and its clockwise rotation remain unchanged, but the pressure-rate product declines. This strongly suggests the diaphragms have become "medically plicated" by the increased CPAP and breathing has become more efficient (Reproduced with permission – Pediatr Crit Care Med. 2004)

During normal breathing, the phase angle is less than 22° (mean 8°) and creates a very tight, counterclockwise loop (Sivan et al. 1991). However, as TAA worsens, the loop opens and widens, with larger phase angles. Additional information is learned from the direction of rotation of the loop. If the RC leads instead of the ABD, then the loop will take on a clockwise rotation, commonly seen with bilateral diaphragm paralysis. If one hemidiaphragm or hemithorax is ineffective, the loop will take on a "Figure of 8" appearance. As such, continuous phase angle monitoring allows clinicians to see the effect of medical interventions (e.g., increased CPAP), monitor disease progression (e.g., acute upper airway obstruction), and help wean from mechanical ventilation (Fig. 11.43).

11.10.4 Monitoring Respiratory Mechanics

Ventilator management of respiratory failure needs to cater to the underlying disease pathology. Paramount to optimal management is not only initially selecting the correct mode and ventilator settings for the underlying disease but also monitoring physiologic changes that occur from the disease state or in response to therapeutic interventions. Most modern ventilators will display pressure, flow, and volume traces on a

time basis or will display plots of the variables against each other. The ventilator will also calculate values for resistance, compliance, and time constant of the respiratory system it is supporting in addition to air leak (hopefully only around the endotracheal tube), tidal volumes, and so on.

11.10.4.1 Resistance, Compliance, and Time Constant

Compliance and resistance reflect the mechanical properties of the lungs and require the measurement of flow, volume, and pressure.

Compliance is a function not only of the elastic properties of the respiratory system but also of its volume. In other words, the value obtained is different at various lung volumes, dependent on the shape of the pressure–volume curve, which in turn depends on the amount of lung disease and therapeutic maneuvers such as PEEP or surfactant administration. Sudden changes in compliance often reflect the opening and closing of individual lung units rather than changes in lung tissue and surface tension characteristics. Thus, ideally compliance should be corrected for total lung capacity (TLC) and body weight. Compliance referenced to functional residual capacity (FRC) is termed specific compliance.

Resistance represents the resistive properties of the airways, lung tissue, and chest wall. Several methods have been designed to measure compliance and resistance in ventilated infants which has led to a confusing nomenclature for the practitioner. Compliance is referred to as either dynamic compliance (C_{dyn}) when it is measured when ventilation is in motion or as static (passive) compliance (C_{rs}) when respiratory muscles are inactive during the test procedure. The same applies to the resistance of the respiratory system, which is referred to as either dynamic (R_e) or total respiratory system resistance (R_{rs}). C_{dyn} can be calculated simply by dividing V_T by the total change in pressure necessary to deliver that volume. These numbers can be easily extracted from modern mechanical ventilators. However, it is understood that C_{dyn} is related to both elastic and flow-resistive characteristics according to the equation of motion of the single-compartment model of the respiratory system. Thus, C_{dyn} changes with alteration of mechanical ventilation settings including respiratory frequency, inspiratory, and end-expiratory pressure. The classic technique of determining C_{dyn} is based on the measurement of esophageal pressure as a quantification of pleural pressure. This technique is invasive by virtue of the need of an esophageal catheter, and the accuracy of such measurements in intubated infants and children is controversial.

Newer methods measure static compliance (C_{rs}) and resistance (R_{rs}) and are based on relaxation of both inspiratory and expiratory muscles during brief airway occlusions during exhalation. The most widely used methods are the passive deflation and the multiple occlusion techniques. Muscle relaxation is achieved either by invoking the Hering–Breuer inflation reflex or by use of neuromuscular blockade. We favor the use of short-term neuromuscular blockade together with sedation for a mechanically ventilated patient in the controlled setting of an ICU because it guarantees complete muscle relaxation during the whole expiratory phase. If there is no muscle activity during exhalation, the expiratory time constant (T_{rs}) or emptying time of the respiratory system will be entirely dependent on the mechanical properties of the lungs and can be described as follows:

$$T_{rs} = C_{rs} \times R_{rs}$$

Thus, both C_{rs} and R_{rs} can be obtained from a single breath. The determination of T_{rs} gives some idea of how rapidly the lung empties following a mechanical breath. A single time constant is defined as the time required to exhale 63 % of the tidal volume. Four time constants are needed to exhale 99 % of the delivered tidal volume. This permits the determination of respiratory rates allowing complete exhalation or the detection of rate settings that lead to inadvertent PEEP (Fig. 11.44).

In the examples above, the most likely situation where the “equilibrium” time constant

Ventilated 3.5 mm ID ETT 5 kg infants	Healthy (normal)	ARDS (restrictivel)	Bronchiolitis (obstructive)
R (cm $H_2O.L^{-1}..s^{-1}$)	50	100	600
C (L.cm H_2O^{-1})	0.006	0.0015	0.003
RC (s)	0.03	0.15	1.8
4RC (s)	1.2	0.6	7.2
60 / (4*RC) = ($fmax.min^{-1}$)	50	100	8

Fig. 11.44 The estimated maximum respiratory frequency calculated from the RC time constant of the respiratory system to prevent breath stacking with overdistension of the lungs, in infants with three different pulmonary states – normal, restrictive pulmonary disease, and obstructed airways disease. In this model, it is assumed that the inflation of the lungs occurs instantly and only the time required for deflation is determined

(4*RC) will be exceeded is in the case of bronchiolitis. When this happens, there will not be enough time for all the previous tidal volume to be exhaled before the next breath starts, resulting in an elevation of functional residual capacity (FRC). This can result in barotrauma if the elevation becomes more than 20 ml/kg, in the case of adults with asthma (Fig. 11.45) (Tuxen et al. 1992).

Pattern recognition adds valuable information to the interpretation of results obtained by measuring respiratory mechanics. While obstructive lung disease is characterized by a concave slope of the passive expiratory FV loop, restrictive lung disease often results in convex loop patterns. It is important to note that in the case of intubated patients, respiratory system compliance (C_{rs}) and resistance (R_{rs}) measurements include the physical properties of the ETT. Unfortunately, there is still a lack of normal values for C_{rs} and R_{rs} in intubated infants and children with normal lungs. According to our studies, such normal data lie in the range of 0.8–1.2 $ml \cdot cm\ H_2O^{-1} \cdot kg^{-1}$ for compliance and 0.02–0.05 $cm\ H_2O \cdot ml^{-1} \cdot s^{-1}$ (up to 0.1 with ETT <3.5 mm I.D.) for resistance (Hammer et al. 1995).

11.10.4.2 Loops Using Pressure, Flow, and Volume Traces: Special Considerations

11.10.4.2.1 Precision of Measurements

Before discussing characteristic patterns of various loops for different disease states, it is necessary to review the accuracy and reproducibility of these measurements. The presence of a significant leak (>18 %) around the ETT will underestimate returned tidal volumes and increase calculated resistance and compliance values (Main et al. 2001). This is easily overcome with a cuffed ETT. While there is reluctance by some of the critical care and anesthesia community to use cuffed ETTs for pediatric patients, good data shows that current low-pressure, high-volume cuffed tubes are no different than uncuffed tubes in the incidence of acute or long-term postextubation complications (Newth et al. 2004). As with uncuffed ETTs, cuffed tubes should be placed with an initial leak at less than 25 cm H_2O.

Second, in order to obtain accurate flow–volume and pressure–volume loops, as well as measurements of tidal volume, it is important for measurements to occur as close to the tip of the ETT as possible. While modern ventilator

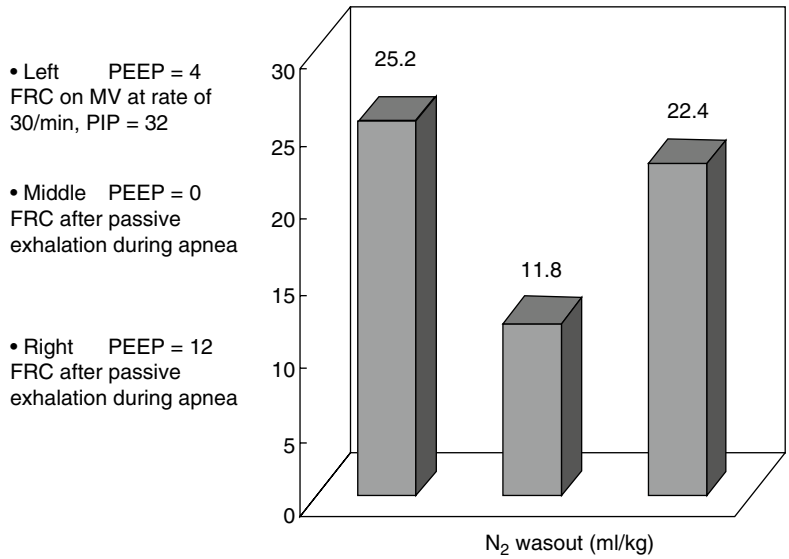

Fig. 11.45 These are measurements from an 8 kg infant with RSV bronchiolitis plus severe chronic lung disease. In the *left column*, his FRC has been measured at 25.2 ml/kg while on a ventilator rate of 30 breaths/min. When his FRC was repeated after 40 s apnea and PEEP = 0 cm H_2O (*middle column*), it was only 11.8 ml/kg, reflecting that the increased rate (with a deflation time greater than 4*RC) had caused air trapping of approximately 13 ml/kg. The *right column* shows that even when his PEEP was raised to 12 cm H_2O, after an apneic deflation of 40 s, his FRC at 22.4 ml/kg was still less than originally at 25.2 ml/kg secondary to the "breath stacking" with the high ventilator rate

technology has improved significantly, there are often large discrepancies between measurements taken at the tip of the ETT with a pneumotachograph, and those recorded at the ventilator, regardless of the software package in use. This is particularly relevant with smaller patients, where the relatively compliant ventilator tubing dead space volume may be greater than a small patient's tidal breath (Heulitt et al. 2009b).

11.10.4.2.2 Flow–Volume Loops

Flow–volume loops are particularly useful in diagnosing the type of respiratory disease present (restrictive versus obstructive). In the case of lower airway obstruction, they have a characteristic shape which may change in response to bronchodilators. In large airways (i.e., above the carina) they can help identify the type of obstruction (fixed or variable) if obtained while spontaneously breathing or if the ETT lies above the level of obstruction.

For mechanically ventilated patients, loops vary depending on the mode of ventilation selected. In volume ventilation, tidal volume delivered is set with a constant inspiratory flow, and peak and plateau airway pressures vary. In pressure ventilation, inspiratory pressure delivered is set and volume varies; the flow pattern is decelerating. In general, this decelerating flow pattern yields lower peak inspiratory pressures than volume limited ventilation.

It is necessary to understand the scales and axes when interpreting flow–volume loops on ventilators and those of usual pulmonary function testing. Classically, flow–volume loops produced by spontaneously breathing patients have inspiration negative, and exhalation positive, moving either clockwise or counterclockwise. However, the display on most mechanical ventilators shows the flow pattern is in a clockwise direction and inspiration is on the positive aspect of the y-axis and exhalation on the negative (Figs. 11.46 and 11.47).

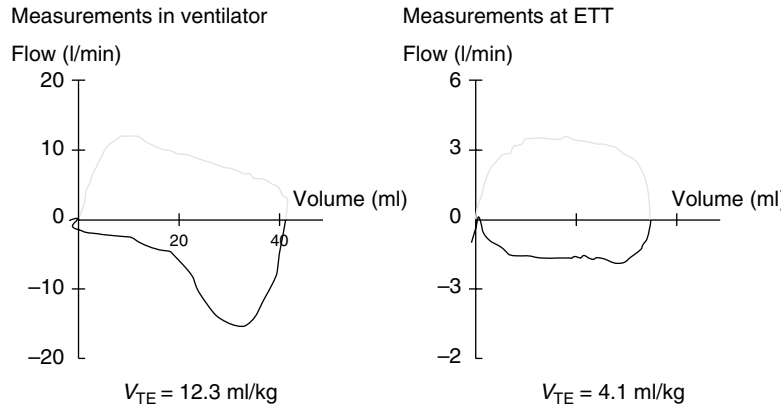

Fig. 11.46 Measurements from a 4.0 kg infant with a cuffed endotracheal tube in pressure control mode. On the left, flow–volume measurements are made at the ventilator with compensation for tubing compliance. There is "overshoot" of flow measurements causing volumes to be larger and giving the expiratory portion of the flow–volume curve (below the *horizontal axis*) a pattern of obstructive airways disease. Tidal volume is 12.3 ml/kg. On the right, measurements are made at the endotracheal tube connector within a minute of those from the *left panel*. Tidal volume is much lower being now a third at 4.1 ml/kg. The flow pattern on the expiratory limb now resembles that of normal airways

11.10.4.2.3 Pressure–Volume Loops

Pressure–volume loops are useful to help determine optimal lung recruitment, compliance, and overdistension. Here, pressure is on the *x*-axis, and volume on the *y*-axis, a reversal of classic nomenclature.

11.10.4.2.3.1 Restrictive Lung Disease

Restrictive lung disease from pneumonia, ARDS, pleural effusions, and similar entities constitutes the majority of ICU admissions for respiratory failure. The hallmarks of restrictive lung disease include decreased compliance, with end-expiratory lung volumes that fall below normal functional residual capacity (FRC). Moreover, alveolar closing pressures lie above end-expiratory lung volume resulting in alveolar collapse. Therefore, effective management of restrictive lung disease requires normalization of end-expiratory lung volumes to a level closer to FRC. The pressure–volume curve helps to this end (Fig. 11.48).

The inspiratory limb of the pressure–volume curve of a patient with restrictive lung disease (classically ARDS) has three main segments, separated by upper and lower inflection points (see Fig. 11.25). The goal is to maintain ventilation within the two inflection points on the pressure–volume curve. This minimizes ventilator-induced injury from alveolar recruitment and derecruitment (below the lower inflection point) and overdistension (above the upper inflection point). End-expiratory lung volumes are maintained above the lower inflection point with positive end-expiratory pressure (PEEP) or by mean airway pressure if on high-frequency oscillatory ventilation.

While recommendations differ for conventional ventilation, one strategy is to select a PEEP 2 cm H_2O above the lower inflection point and attempt to stay in the zone of best compliance by selecting a relatively conservative tidal volume (6 ml/kg) if using a form of volume control ventilation (ARDSNet 2000) or use lung-protective pressures if applying a pressure control mode (Khemani et al. 2009). A third option is high-frequency oscillatory ventilation providing very small tidal volumes between the upper and lower inflection points.

If a low compliance zone is seen on the pressure–volume curve (beaking), then the pressure or volume should be decreased to prevent overdistension. Less commonly, overdistension

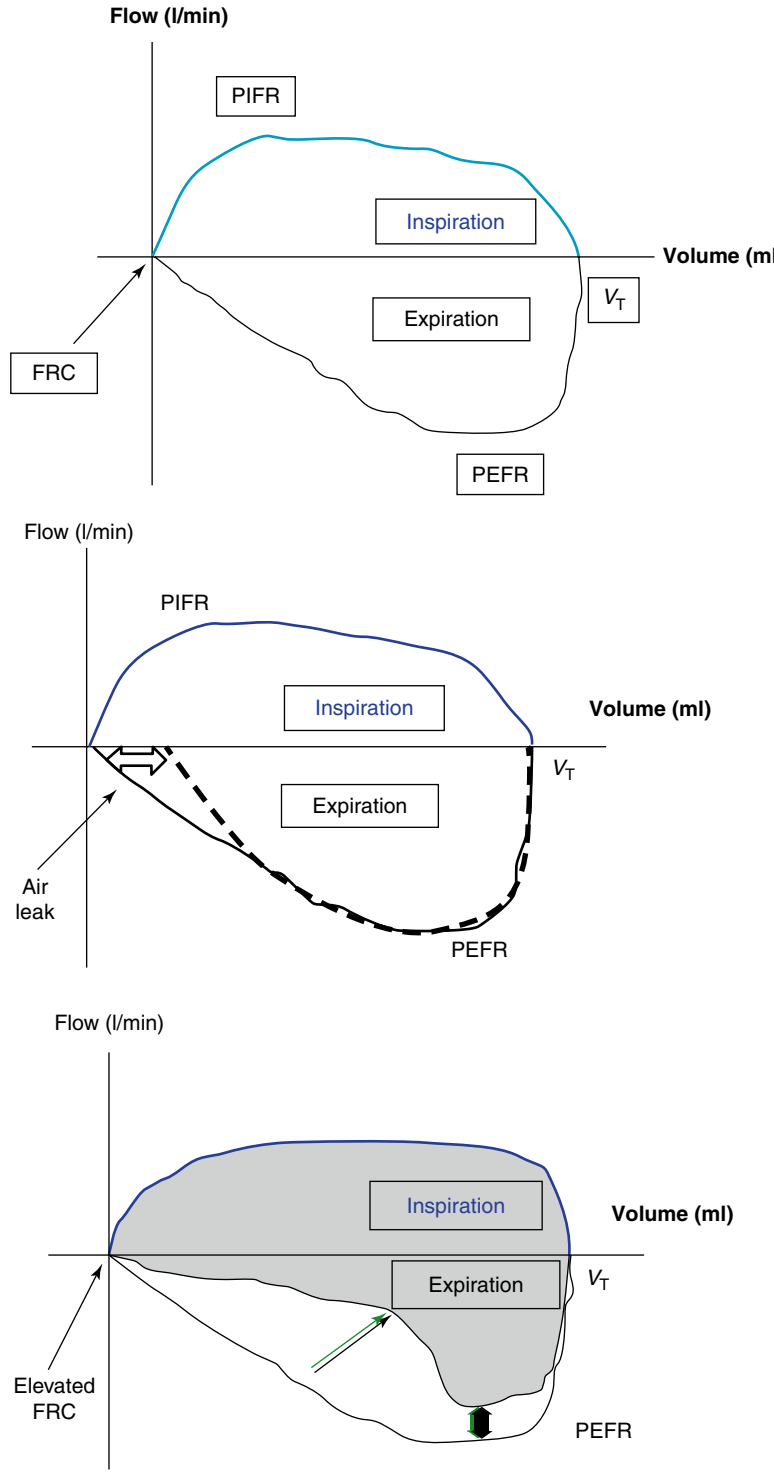

Fig. 11.47 These are flow–volume loops under three different conditions. *Upper panel* – normal healthy airways. *PIFR* peak inspiratory flow rate, *PEFR* peak expiratory flow rate, *FRC* functional residual capacity, V_T tidal volume. *Middle panel* – the expired volume does not come back to the starting point (*FRC*) of the inspired volume. This means there is an air leak in the system, usually around the endotracheal tube. *Lower panel* – obstructed airways disease. When severe enough, the classic scooped-out expiratory limb will be seen on tidal breaths on a ventilator. Note that PEFR will also be reduced, and the FRC (end-expiratory lung volume) will be higher in this case

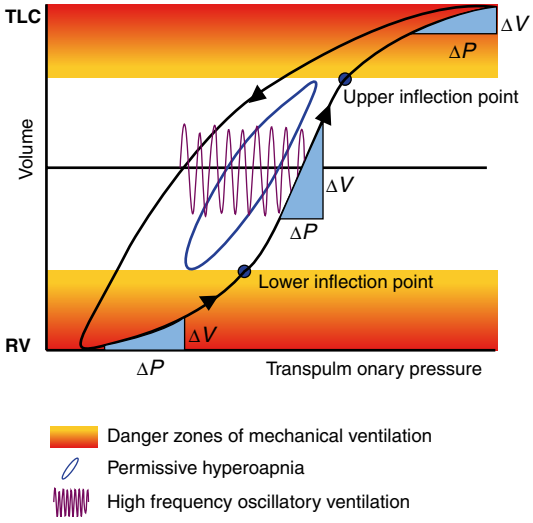

Fig. 11.48 A schematic of a pressure–volume loop in acute lung injury, demonstrating upper and lower inflection points. In between these points is the "safe" range in which to ventilate without moving in to the upper zone of overdistension or the lower zone of atelectasis. The compliance ($\Delta V/\Delta P$) in both "danger" zones is low, whereas it is improved in the "safe" zone (Reproduced with permission Prof. Jürg Hammer, Universität Basel, CH)

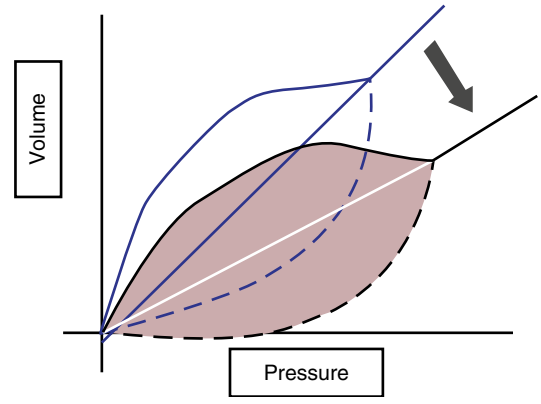

Fig. 11.49 A schematic of two pressure–volume loops. The upper *PV* loop with the greater slope represents either a normal loop which moves toward the lower loop with the smaller slope, as the lung becomes less compliant as in hyaline membrane disease or acute respiratory distress syndrome. Conversely, the lower loop will move toward the upper one as compliance improves, such as with surfactant therapy for HMD or recruitment maneuvers with ARDS

from excessive PEEP may occur. This will not manifest with the classic inflection points but rather simply as a pressure–volume curve that is shifted to the right with a smaller slope. Further disease entities and therapies which will result in changing respiratory system compliances are shown in Fig. 11.49.

Other measures of overdistension derived from mathematical examination of the pressure–volume curve have been proposed (Fig. 11.50).

In neonates, Fisher et al. (1988) noted that if the ratio of the compliance of the last 20 % and full *PV* loop is less than 1.0, overdistension is defined (Fig. 11.50). This definition has not been validated in the pediatric population (Neve et al. 2001). An alternate approach is that of Leclerc and colleagues who applied second-order polynomial equations to quasistatic *PV* curves and derived indices they showed suitable for detecting overdistension in pediatric patients (Neve et al. 2000, 2001).

In contrast to the pressure–volume curve, the flow–volume loop for a patient with significant restrictive lung disease will often have the same characteristic shape as a patient without lung disease, but with smaller amplitude for a given flow. Subsequent to changes in compliance through optimizing PEEP and improvements in the underlying disease, in concert with conservative lung-protective pressure-limited ventilation, the amplitude of the flow–volume loops should return toward normal.

11.10.4.2.3.2 Obstructed Airway Disease

Medium and Small Airway Disease

In contrast to restrictive lung disease where disease pathology typically affects the lung parenchyma, obstructive disease affects airways. Significant airway obstruction affecting medium (asthma) or small (bronchiolitis) airways allows the development of air trapping. Here end-expiratory lung volumes tend to reside above functional residual capacity, and airway resistance is increased. The flow–volume loops are characteristic of flow limitation on the expiratory limb. The flow–volume loop therefore demonstrates lower peak expiratory flows, smaller tidal volumes, as well as the hallmark "scooped-out" or concave appearance to the deflation limb of expiratory flow. Moreover, if the obstruction is variable or reversible, the effect of a therapeutic

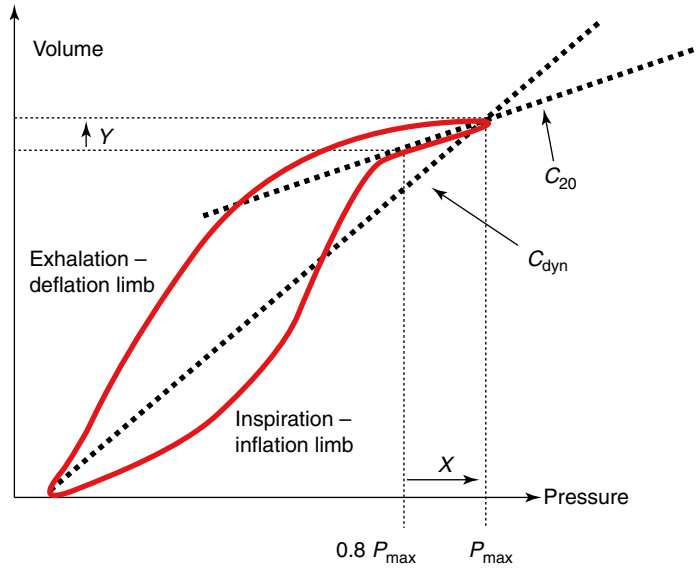

Fig. 11.50 A schematic of a pressure–volume loop demonstrating overdistension. On the pressure axis, between 0.8 and maximum pressure (*X*), there is very little change in volume (*Y*). This region has very low compliance and results in "beaking" of the upper end of the *PV* loop

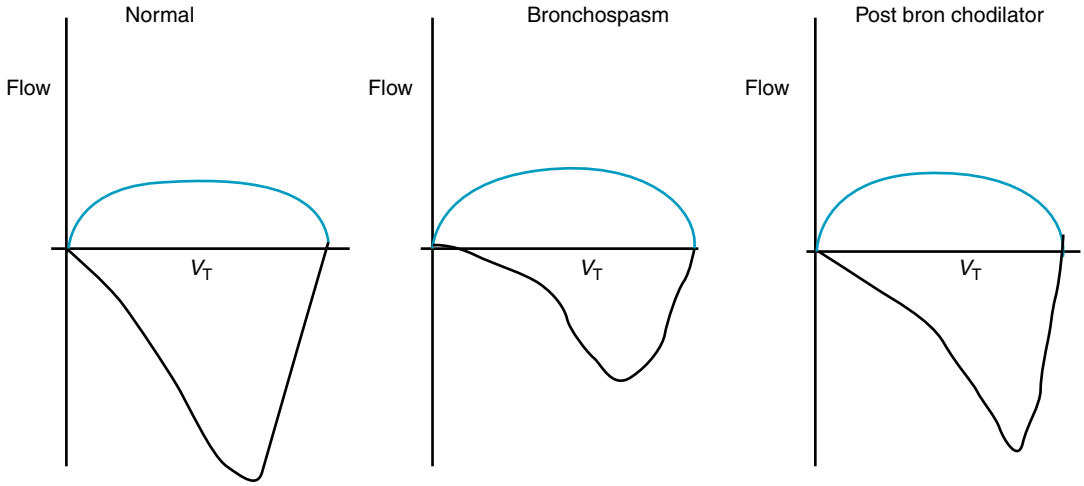

Fig. 11.51 A schematic of 3 flow–volume loops demonstrating the following: *Left panel* – normal loop. *Middle panel* – bronchoconstriction with concavity of the deflation limb, decreased peak expiratory flow rate, and decline in tidal volume (V_T). *Right panel* – response to bronchodilator with improvements in tidal volume, peak flow, and less concavity of the deflation limb

intervention (i.e., bronchodilator for an asthmatic) can be followed. Here the flow–volume loop demonstrates improved peak expiratory flow and a return of a flat or slightly convex shape to the decelerating limb of expiratory flow. Some modern ventilators allow reference flow–volume and pressure–volume loops to be stored on the ventilator screen so that subsequent loops can be superimposed and changes in shape after an intervention such as a bronchodilator can be appreciated (Fig. 11.51).

When mechanically ventilating patients with significant obstructive airway disease, care must be taken to prevent dynamic hyperinflation and the creation of auto-PEEP. Whenever possible, spontaneous breathing with CPAP or PEEP and PS is preferable. This allows patients the ability to set their own inspiratory/ expiratory ratios, and PEEP is carefully applied to match the intrinsic level of auto-PEEP the patient has generated (Smith and Marini 1988). This strategy can minimize work of breathing, and PEEP can gradually

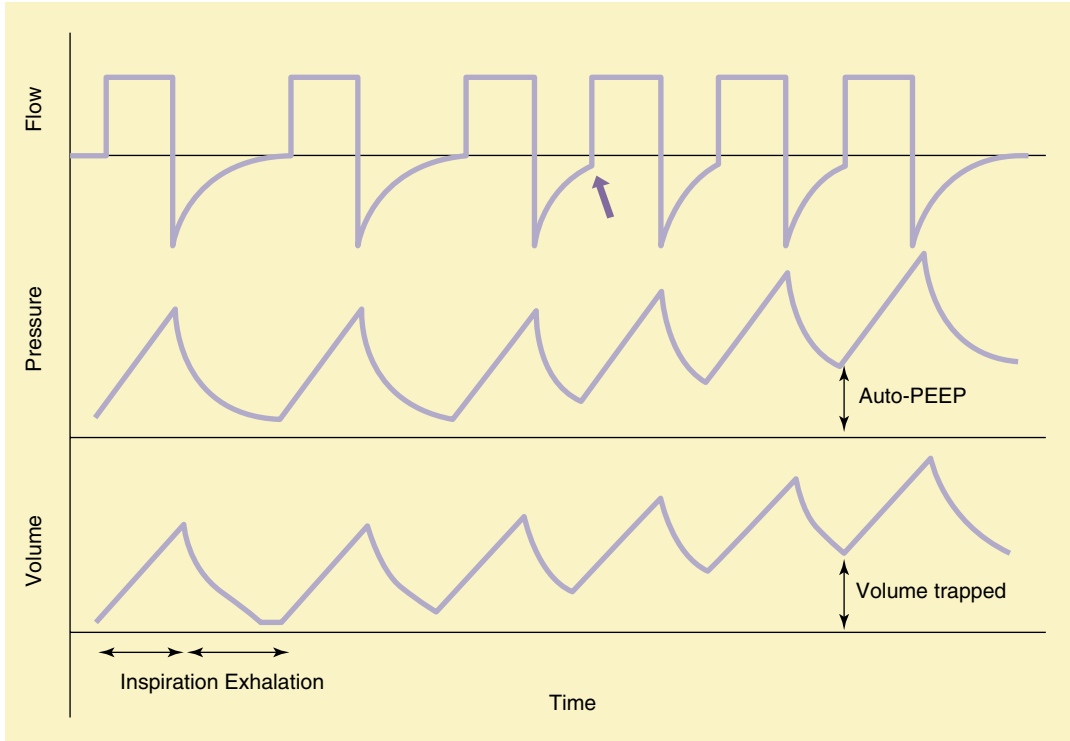

Fig. 11.52 Obstructed medium and small airways with mechanical ventilation and progressive dynamic hyperinflation from insufficient expiratory time. Note the failure of flow to return to zero during exhalation on the flow versus time graph (*arrow* – *top*). The pressure–time graph (*middle*)) displays progressive air trapping and generation of auto-PEEP. The volume–time graph (*bottom*) displays a progressive rise in lung volumes as air is trapped with each breath (Reproduced with permission, Khemani et al. (2007))

be removed as the airway obstruction improves (Wetzel 1996; Graham et al. 2007). However, if such a strategy cannot be employed and the patient is either paralyzed or heavily sedated, then care must be taken to allow sufficient expiratory time to prevent further air trapping. This can be monitored by examining the flow versus time curves, paying particular attention to expiratory flow returning to zero before the initiation of a subsequent breath. Evidence of dynamic hyperinflation may be observed on the pressure or volume versus time curves, where increased air trapping will manifest as gradual increases in end-expiratory lung volumes and pressures (Tuxen 1994; Williams et al. 1992).

If total ventilatory support is employed (no spontaneous breathing), then extrinsic PEEP may worsen air trapping. However, if the patient is completely spontaneously breathing, then the application of extrinsic PEEP to match the patient's level of intrinsic or auto-PEEP (some advocate 80 % of auto-PEEP) will help minimize respiratory muscle fatigue. Of course, the level of support should ultimately be determined by patient comfort and work of breathing.

Large Airway Disease

A spontaneously breathing, non-intubated patient with extrathoracic obstruction (e.g., croup, laryngomalacia, tracheomalacia, vocal cord dysfunction) classically has limitation of flow during inspiration. This flow limitation manifests with a flattening of the inspiratory limb of the flow–volume loop. This can usually be overcome by bypassing the obstruction with an ETT.

If the obstruction is not bypassed by the ETT and is in the trachea distal to the tube (i.e., intrathoracic), the flow–volume loop will either show flattening on exhalation (variable lesion such as tracheomalacia) or show flattening on both inspiration and exhalation (fixed lesion) (Fig. 11.52). This later situation is commonly seen with foreign

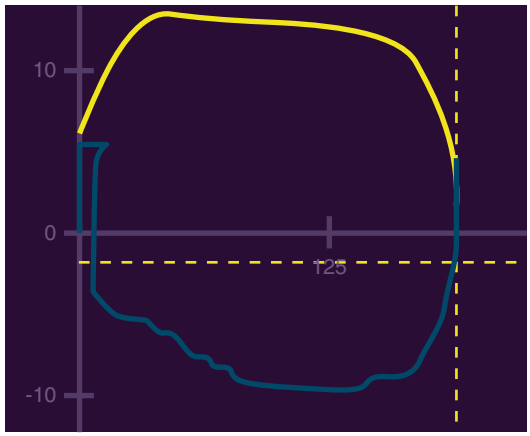

Fig. 11.53 An actual recording of a tidal breathing flow–volume loop of an intubated child with a fixed tracheal stenosis below the tip of the endotracheal tube. There is flattening of both inspiratory and expiratory limbs of the FV loop

body aspiration, tracheal stenosis, or accidental kinking of an ETT (Fig. 11.53).

Conclusion

A firm understanding of respiratory monitoring tools is invaluable for all physicians taking care of critically ill children. It allows for titrating therapeutic interventions to the patient's disease state and if used correctly can facilitate optimal respiratory support and aid in eventual weaning to endotracheal extubation. Moreover, with close monitoring, one can often detect aberrations or changes in physiologic states before disease progression, allowing for early interventions and prevention of disease progression.

Essentials to Remember

- Measurements of pulmonary function should occur as close to the tip of the endotracheal tube as possible, especially in small children and infants.
- In intubated children, pulmonary function tests will not be accurate if there is a large leak around the endotracheal tube. The leak must be minimized.
- Flow–volume loops are particularly useful for distinguishing obstructive airway disease and restrictive lung disease on mechanical ventilation.
- Pressure–volume loops help the clinician optimize ventilator support, particularly with respect to positive end-expiratory pressure and peak inspiratory pressure.

References

Agostini E, Hyatt RE (1986) Static behaviour of the respiratory system. In: Geiger SR (ed) Handbook of physiology. American Physiological Society, Bethesda, pp 113–130

Albaiceta GM, Piacentini E, Villagra A, Lopez-Aguilar J, Taboada F, Blanch L (2003) Application of continuous positive airway pressure to trace static pressure-volume curves of the respiratory system. Crit Care Med 31:2514–2519

Albaiceta GM, Taboada F, Parra D, Luyando LH, Calvo J, Menendez R, Otero J (2004) Tomographic study of the inflection points of the pressure-volume curve in acute lung injury. Am J Respir Crit Care Med 170:1066–1072

Albaiceta GM, Luyando LH, Parra D, Menendez R, Calvo J, Pedreira PR, Taboada F (2005) Inspiratory vs. expiratory pressure-volume curves to set end-expiratory pressure in acute lung injury. Intensive Care Med 31:1370–1378

Albaiceta GM, Blanch L, Lucangelo U (2008) Static pressure-volume curves of the respiratory system: were they just a passing fad? Curr Opin Crit Care 14:80–86

Amato MB, Barbas CS, Medeiros DM, Magaldi RB, Schettino GP, Lorenzi-Filho G, Kairalla RA, Deheinzelin D, Munoz C, Oliveira R, Takagaki TY, Carvalho CR (1998) Effect of a protective-ventilation strategy on mortality in the acute respiratory distress syndrome. N Engl J Med 338:347–354

ARDSNet (2000) Ventilation with lower tidal volumes as compared with traditional tidal volumes for acute lung injury and the acute respiratory distress syndrome. The Acute Respiratory Distress Syndrome Network. N Engl J Med 342:1301–1308

Asher MI, Coates AL, Collinge JM, Milic-Emili J (1982) Measurement of pleural pressure in neonates. J Appl Physiol 52:491–494

Banner MJ (1994) Work of breathing. Crit Care Med 22(3):5515–5523

Bates JH, Irvin CG (2002) Time dependence of recruitment and derecruitment in the lung: a theoretical model. J Appl Physiol 93:705–713

Bates JH, Turner MJ, Lanteri CJ, Jonson B, Sly PD (1996) Measurement of flow and volume. In: Stocks J, Sly PD, Tepper RS, Morgan WJ (eds) Infant respiratory function testing. Wiley-Liss, New York, pp 81–116

Baydur A, Behrakis P, Zin WA et al (1982) A simple method for assessing the validity of the esophageal balloon technique. Am Rev Respir Dis 126:788–791

Beardsmore CS, Godfrey S, Shani N, Maayan C, Bar-Yishay E (1986) Airway resistance measurements throughout the respiratory cycle in infants. Respiration 49:81–93

Bellemare F, Wright D, Lavigne CM et al (1983) Effect of tension and timing of contraction on blood flow of the diaphragm. J Appl Physiol 54:1597–1606

Benditt JO (2005) Esophageal and gastric pressure measurements. Respir Care 50:68–75

Blanch L, Lucangelo U, Lopez-Aguilar J (2009) Pressure-volume curves and ventilator tuning in acute respiratory distress syndrome. Pediatr Crit Care Med 10:532–533

Borges JB, Okamoto VN, Matos GF, Caramez MP, Arantes PR, Barros F, Souza CE, Victorino JA, Kacmarek RM, Barbas CS, Carvalho CR, Amato MB (2006) Reversibility of lung collapse and hypoxemia in early acute respiratory distress syndrome. Am J Respir Crit Care Med 174:268–278

Braun NMT, Faulkner J, Hughes RL (1983) When should respiratory muscle be exercised? Chest 84:76–84

Brazelton TB III, Watson KF, Murphy M, Al-Khadra E, Thompson JE, Arnold JH (2001) Identification of optimal lung volume during high-frequency oscillatory ventilation using respiratory inductive plethysmography. Crit Care Med 29:2349–2359

Brower RG, Lanken PN, MacIntyre N, Matthay MA, Morris A, Ancukiewicz M, Schoenfeld D, Thompson BT (2004) Higher versus lower positive end-expiratory pressures in patients with the acute respiratory distress syndrome. N Engl J Med 351:327–336

Brown K, Sly PD, Milic-Emili J, Bates JHT (1989) Evaluation of the flow-volume loop as an intraoperative monitor of respiratory mechanics in infants. Pediatr Pulmonol 6:8–13

Brunner JX, Laubscher TP, Banner MJ, Iotti G, Braschi A (1995) Crit Care Med 23(6):1117–1122

Campbell E (1958) The respiratory muscles and the mechanics of breathing. Lloyd-Luke, London

Caramez MP, Kacmarek RM, Helmy M, Miyoshi E, Malhotra A, Amato MB, Harris RS (2009) A comparison of methods to identify open-lung PEEP. Intensive Care Med 35:740–747

Carmack J, Torres A, Anders M, Wilson S, Holt S, Heulitt MJ (1995) Comparison of work of breathing in spontaneous breathing young lambs during continuous positive airway pressure and pressure support ventilation with and without flow triggering utilizing the servo 300 ventilator. Respir Care 40:28–34

Chang HY, Claure N, D'Ugard C, Torres J, Nwajei P, Bancalari E (2011) Effects of synchronization during nasal ventilation in clinically stable preterm infants. Pediatr Res 69:84–89

Chatmongkolchart S, Williams P, Hess DR, Kacmarek RM (2001) Evaluation of inspiratory rise time and inspiration termination criteria in new-generation mechanical ventilators: a lung model study. Respir Care 46(7):666–677

Civetta JM (1993) Nosocomial respiratory failure. Crit Care Med 21:171–173

Coates AL, Davis GM, Vallinis P, Outerbridge EW (1989) Liquid-filled esophageal catheter for measuring pleural pressure in preterm neonates. J Appl Physiol 67:889–893

Costa EL, Borges JB, Melo A, Suarez-Sipmann F, Toufen C Jr, Bohm SH, Amato MB (2009) Bedside estimation of recruitable alveolar collapse and hyperdistension by electrical impedance tomography. Intensive Care Med 35:1132–1137

Crotti S, Mascheroni D, Caironi P, Pelosi P, Ronzoni G, Mondino M, Marini JJ, Gattinoni L (2001) Recruitment and derecruitment during acute respiratory failure: a clinical study. Am J Respir Crit Care Med 164:131–140

Dall'Ava-Santucci J, Armaganidis A, Brunet F, Dhainaut JF, Chelucci GL, Monsallier JF, Lockhart A (1988) Causes of error of respiratory pressure-volume curves in paralyzed subjects. J Appl Physiol 64:42–49

Dargaville PA, Rimensberger PC, Frerichs I (2010) Regional tidal ventilation and compliance during a stepwise vital capacity manoeuvre. Intensive Care Med 36:1953–1961

Dassieu G, Brochard L, Agudze E, Patkaï J, Janaud JC, Danan C (1998) Continuous tracheal gas insufflation enables a volume reduction strategy in hyaline membrane disease: technical aspects and clinical results. Intensive Care Med 24(10):1076–1082

Davis GM, Stocks J, Gerhardt T, Abbasi S, Gappa M (1996) Measurement of Dynamic Lung Mechanics in Infants. In: Stocks J et al (eds) Infant respiratory function testing, vol 1. Wiley-Liss, New York, pp 269–271. http://books.google.ch/books/about/Infant_Respiratory_Function_Testing.html?id=3e8Kj1rFNO4C&safe=on&redir_esc=y

De Jaegere A, van Veenendaal MB, Michiels A, van Kaam AH (2006) Lung recruitment using oxygenation during open lung high-frequency ventilation in preterm infants. Am J Respir Crit Care Med 174:639–645

Denison DM, Morgan MD, Millar AB (1986) Estimation of regional gas and tissue volumes of the lung in supine man using computed tomography. Thorax 41:620–628

Dirocco JD, Carney DE, Nieman GF (2007) Correlation between alveolar recruitment/derecruitment and inflection points on the pressure-volume curve. Intensive Care Med 33:1204–1211

Downie JM, Nam AJ, Simon BA (2004) Pressure-volume curve does not predict steady-state lung volume in canine lavage lung injury. Am J Respir Crit Care Med 169:957–962

Dreyfuss D, Saumon G (2001) Pressure-volume curves: searching for the grail or laying patients with adult respiratory distress syndrome on procrustes' bed? Am J Respir Crit Care Med 163:2–3

Field S, Sanci S, Grassino A (1984) Respiratory muscle oxygen consumption estimated by the diaphragm pressure-time index. J Appl Physiol 57(1):44–51

Fisher JB, Mammel MC, Coleman JM, Bing DR, Boros SJ (1988) Identifying lung overdistention during mechanical ventilation by using volume-pressure loops. Pediatr Pulmonol 5:10–14

Foti G, Cereda M, Banfi G, Pelosi P, Fumagalli R, Pesenti A (1997) End-inspiratory airway occlusion: a method to assess the pressure developed by inspiratory muscles in patients with acute lung injury undergoing pressure support. Am J Respir Crit Care Med 156(4 Pt 1):1210–1216

Gattinoni L, Pesenti A, Avalli L, Rossi F, Bombino M (1987a) Pressure-volume curve of total respiratory system in acute respiratory failure. Computed tomographic scan study. Am Rev Respir Dis 136:730–736

Gattinoni L, Mascheroni D, Basilico E, Foti G, Pesenti A, Avalli L (1987b) Volume/pressure curve of total respiratory system in paralysed patients: artefacts and correction factors. Intensive Care Med 13:19–25

Gattinoni L, Pesenti A, Bombino M, Baglioni S, Rivolta M, Rossi F, Rossi G, Fumagalli R, Marcolin R, Mascher-oni D, Torresin A (1988) Relationships between lung computed tomographic density, gas exchange, and PEEP in acute respiratory failure. Anesthesiology 69:824–832

Gattinoni L, Eleonora C, Caironi P (2005) Monitoring of pulmonary mechanics in acute respiratory distress syndrome to titrate therapy. Curr Opin Crit Care 11:252–258

Gattinoni L, Caironi P, Cressoni M, Chiumello D, Ranieri VM, Quintel M, Russo S, Patroniti N, Cornejo R, Bugedo G (2006) Lung recruitment in patients with the acute respiratory distress syndrome. N Engl J Med 354:1775–1786

Giuliani R, Mascia L, Recchia F, Caracciolo A, Fiore T, Ranieri VM (1995) Patient-ventilator interaction during synchronized intermittent mandatory ventilation. Effects of flow triggering. Am J Respir Crit Care Med 151(1):1–9

Graham AS, Chandrashekharaiah G, Citak A, Wetzel RC, Newth CJL (2007) Positive end-expiratory pressure and pressure support in peripheral airways obstruction work of breathing in intubated children. Intensive Care Med 33:120–127

Hammer J, Newth CJ (1995) Infant lung function testing in the intensive care unit. Intensive Care Med 21:744–752

Hammer J, Newth CJ (2009) Assessment of thoracoabdominal asynchrony. Paediatr Respir Rev 10:75–80

Hammer J, Numa A, Newth CJ (1995) Albuterol responsiveness in infants with respiratory failure caused by respiratory syncytial virus infection. J Pediatr 127:485–490

Harikumar G, Egberongbe Y, Nadel S, Wheatley E, Moxham J, Greenough A, Rafferty GF (2009) Tension-time index as a predictor of extubation outcome in ventilated children. Am J Respir Crit Care Med 180:982–988

Harris RS (2005) Pressure-volume curves of the respiratory system. Respir Care 50:78–98

Harris RS, Hess DR, Venegas JG (2000) An objective analysis of the pressure-volume curve in the acute respiratory distress syndrome. Am J Respir Crit Care Med 161:432–439

Heulitt MJ, Thurman TL, Holt SJ, Jo CH, Simpson PM (2009a) Reliability of displayed tidal volume in infants and children during dual controlled ventilation. Pediatr Crit Care Med 10(6):661–667

Heulitt MJ, Thurman TL, Holt SJ, Jo CH, Simpson P (2009b) Reliability of displayed tidal volume in infants and children during dual-controlled ventilation. Pediatr Crit Care Med 10(6):661–667

Hickling KG (2001) Best compliance during a decremental, but not incremental, positive end-expiratory pressure trial is related to open-lung positive end-expiratory pressure: a mathematical model of acute respiratory distress syndrome lungs. Am J Respir Crit Care Med 163(1):69–78

Higgs BD, Behrakis PK, Bevan DR, Milic-Emili J (1983) Measurement of pleural pressure with esophageal balloon in anesthetized humans. Anesthesiology 59:340–343

Ingimarsson J, Bjorklund LJ, Larsson A, Werner O (2001) The pressure at the lower inflexion point has no relation to airway collapse in surfactant-treated premature lambs. Acta Anaesthesiol Scand 45:690–695

Jackson EA, Coates AL, Gappa M, Stocks J (1995) In vitro assessment of infant pulmonary function equipment. Pediatr Pulmonol 19:205–213

Jarreau PH, Moriette G, Mussat P, Mariette C, Mohanna A, Harf A, Lorino H (1996) Patient-triggered ventilation decreases work of breathing in neonates. Am J Respir Crit Care Med 153:1176–1181

Jonson B, Richard JC, Straus C, Mancebo J, Lemaire F, Brochard L (1999) Pressure-volume curves and compliance in acute lung injury: evidence of recruitment above the lower inflection point. Am J Respir Crit Care Med 159(4 Pt 1):1172–1178

Jubran A, Tobin MJ (1997) Passive mechanics of lung and chest wall in patients who failed and succeeded in trials of weaning. Am J Respir Crit Care Med 155: 916–921

Jubran A, Van de Graaff WB, Tobin MJ (1995) Variability of patient-ventilator interaction with pressure support ventilation in patients with chronic obstructive pulmonary disease. Am J Respir Crit Care Med 152:129–136

Karason S et al (2000) Evaluation of pressure/volume loops based on intratracheal pressure measurements during dynamic conditions. Acta Anaesthesiol Scand 44(5):571–577

Kendrick AH (1996) Comparison of methods of measuring static lung volumes. Monaldi Arch Chest Dis 51:431–439

Khemani RG, Bart III, RD, Newth CJL (2007) Respiratory monitoring during mechanical ventilation. Paediatr Child Health 17(5):193–201

Khemani RG, Conti D, Alonzo TA, Bart RD III, Newth CJ (2009) Effect of tidal volume in children with acute hypoxemic respiratory failure. Intensive Care Med 35:1428–1437

Laghi F (2008) Weaning: can the computer help? Intensive Care Med 34(10):1746–1748

LeSouef PN, England SJ, Bryan AC (1984) Passive respiratory mechanics in newborn and children. Am Rev Respir Dis 129:727–729

LeSouef PN, England SJ, Bryan AC (1984) Total resistance of the respiratory system in preterm infants

with and without an endotracheal tube. J Pediatr 104:108–111
Levy P, Similowski T, Corbeil C (1989) A method for studying the static volume-pressure curves of the respiratory system during mechanical ventilation. J Crit Care 4:83–89
Loring SH, O'Donnell CR, Behazin N, Malhotra A, Sarge T, Ritz R, Novack V, Talmor D (2010) Esophageal pressures in acute lung injury: do they represent artifact or useful information about transpulmonary pressure, chest wall mechanics, and lung stress? J Appl Physiol 108:515–522
Lu Q, Vieira SR, Richecoeur J, Puybasset L, Kalfon P, Coriat P, Rouby JJ (1999) A simple automated method for measuring pressure-volume curves during mechanical ventilation. Am J Respir Crit Care Med 159:275–282
Lu Q, Malbouisson LM, Mourgeon E, Goldstein I, Coriat P, Rouby JJ (2001) Assessment of PEEP-induced reopening of collapsed lung regions in acute lung injury: are one or three CT sections representative of the entire lung? Intensive Care Med 27:1504–1510
Luecke T, Meinhardt JP, Herrmann P, Weisser G, Pelosi P, Quintel M (2003) Setting mean airway pressure during high-frequency oscillatory ventilation according to the static pressure – volume curve in surfactant-deficient lung injury: a computed tomography study. Anesthesiology 99:1313–1322
Macnaughton PD (2006) New ventilators for the ICU–usefulness of lung performance reporting. Br J Anaesth 97:57–63
Maggiore SM, Jonson B, Richard JC, Jaber S, Lemaire F, Brochard L (2001) Alveolar derecruitment at decremental positive end-expiratory pressure levels in acute lung injury: comparison with the lower inflection point, oxygenation, and compliance. Am J Respir Crit Care Med 164:795–801
Maggiore SM, Richard JC, Brochard L (2003) What has been learnt from P/V curves in patients with acute lung injury/acute respiratory distress syndrome. Eur Respir J Suppl 42:22s–26s
Main E, Castle R, Stocks J, James I, Hatch D (2001) The influence of endotracheal tube leak on the assessment of respiratory function in ventilated children. Intensive Care Med 27:1788–1797
Marini JJ, Rodriguez RM, Lamb V (1986) Bedside estimation of the inspiratory work of breathing during mechanical ventilation. Chest 89(1):56–63
Matamis D, Lemaire F, Harf A, Brun-Buisson C, Ansquer JC, Atlan G (1984) Total respiratory pressure-volume curves in the adult respiratory distress syndrome. Chest 86:58–66
Mathe JC, Clement A, Chevalier JY, Gaultier C, Costil J (1987) Use of total inspiratory pressure-volume curves for determination of appropriate positive end-expiratory pressure in newborns with hyaline membrane disease. Intensive Care Med 13:332–336
Mead J (1996) Mechanics of lung and chest wall. In: West JB (ed) Respiratory physiology: people and ideas. Oxford University Press, New York, pp 173–207
Mead J, Whittenberger JL (1953) Physical properties of the human lung measured during spontaneous respiration. J Appl Physiol 5:779–796
Mehta S, Stewart TE, MacDonald R, Hallett D, Banayan D, Lapinsky S, Slutsky A (2003) Temporal change, reproducibility, and interobserver variability in pressure-volume curves in adults with acute lung injury and acute respiratory distress syndrome. Crit Care Med 31:2118–2125
Meier T, Luepschen H, Karsten J, Leibecke T, Grossherr M, Gehring H, Leonhardt S (2008) Assessment of regional lung recruitment and derecruitment during a PEEP trial based on electrical impedance tomography. Intensive Care Med 34:543–550
Mergoni M, Martelli A, Volpi A, Primavera S, Zuccoli P, Rossi A (1997) Impact of positive end-expiratory pressure on chest wall and lung pressure-volume curve in acute respiratory failure. Am J Respir Crit Care Med 156:846–854
Mergoni M, Volpi A, Bricchi C, Rossi A (2001) Lower inflection point and recruitment with PEEP in ventilated patients with acute respiratory failure. J Appl Physiol 91:441–450
Miedema M, de Jongh FH, Frerichs I, van Veenendaal MB, van Kaam AH (2011) Changes in lung volume and ventilation during lung recruitment in high-frequency ventilated preterm infants with respiratory distress syndrome. J Pediatr 159:199–205
Millic-Emili J, Turner JM et al (1964) Improved technique for estimating pleural pressure from esophageal balloon. J Appl Physiol 19:207–211
Milner AD, Saunders RA, Hopkin LE (1978) Relationship of intra-oesophageal pressure to mouth pressure during the measurement of thoracic gas volume in the newborn. Biol Neonate 33(5–56):314–319
Monkman SL, Andersen CC, Nahmias C, Ghaffer H, Bourgeois JM, Roberts RS, Schmidt B, Kirpalani HM (2004) Positive end-expiratory pressure above lower inflection point minimizes influx of activated neutrophils into lung. Crit Care Med 32:2471–2475
Mortola JP, Saetta M (1987) Measurements of respiratory mechanics in the newborn. A simple approach. Pediatr Pulmonol 3:123–130
Mortola JP, Fisher JT, Smith B, Fox G, Weeks S (1982) Dynamics of breathing in infants. J Appl Physiol 3:1209–1215
Mull RT (1984) Mass estimates by computed tomography: physical density from CT numbers. Am J Radiol 143:1101–1104
Neve V, de la Roque ED, Leclerc F, Leteurtre S, Dorkenoo A, Sadik A, Cremer R, Logier R (2000) Ventilator-induced overdistension in children – dynamic versus low-flow inflation volume-pressure curves. Am J Respir Crit Care Med 162:139–147
Neve V, Leclerc F, de la Roque ED, Leteurtre S, Riou Y (2001) Overdistension in ventilated children. Crit Care 5:196–203
Newth CJ, Rachman B, Patel N, Hammer J (2004) The use of cuffed versus uncuffed endotracheal tubes in pediatric intensive care. J Pediatr 144:333–337

Nicolai T, Lanteri CJ, Sly PD (1993) Frequency dependence of elastance and resistance in ventilated children with and without the chest opened. Eur Respir J 6(9):1340–1346

Nunes S, Uusaro A, Takala J (2004) Pressure-volume relationships in acute lung injury: methodological and clinical implications. Acta Anaesthesiol Scand 48:278–286

Pandit PB, Courtney SE, Pyon KH, Saslow JG, Habib RH (2001) Work of breathing during constant- and variable-flow nasal continuous positive airway pressure in preterm neonates. Pediatrics 108:682–685

Patel DS, Sharma A, Prendergast M, Rafferty GF, Greenough A (2009) Work of breathing and different levels of volume-targeted ventilation. Pediatrics 123(4):e679–684. Epub 2009 Mar 2. doi:10.1542/peds.2008-2635

Patel DS, Sharma A, Prendergast M, Rafferty M, Greenough A (2010) Work of breathing and different levels of volume-targeted ventilation. Pediatrics 123(4):679–684

Patroniti N, Bellani G, Manfio A, Maggioni E, Giuffrida A, Foti G, Antonio Pesenti A (2004) Lung volume in mechanically ventilated patients: measurement by simplified helium dilution compared to quantitative CT scan. Intensive Care Med 30:282–289

Pellicano A, Tingay DG, Mills JF, Fasulakis S, Morley CJ, Dargaville PA (2009) Comparison of four methods of lung volume recruitment during high frequency oscillatory ventilation. Intensive Care Med 35: 1990–1998

Pelosi P, Croci M, Ravagnan I, Vicardi P, Gattinoni L (1996) Total respiratory system, lung, and chest wall mechanics in sedated-paralyzed postoperative morbidly obese patients. Chest 109:144–151

Pelosi P, Goldner M, McKibben A, Adams A, Eccher G, Caironi P, Los- appio S, Gattinoni L, Marini JJ (2001) Recruitment and derecruitment during acute respiratory failure: an experi- mental study. Am J Respir Crit Care Med 164:122–130

Pereira C, Bohe J, Rosselli S, Combourieu E, Pommier C, Perdrix JP, Richard JC, Badet M, Gaillard S, Philit F, Guerin C (2003) Sigmoidal equation for lung and chest wall volume-pressure curves in acute respiratory failure. J Appl Physiol 95:2064–2071

Pfenninger J, Minder C (1988) Pressure-volume curves, static compliances and gas exchange in hyaline membrane disease during conventional mechanical and high-frequency ventilation. Intensive Care Med 14:364–372

Poiseuille JLM (1840) Recherches experimentales sur le mouvement des liquids dans les tubes de tres petits diameters. C R Acad Sci 11(962–967):1041–1048

Polese G, Rossi A, Appendini L et al (1991) Partitioning of respiratory mechanics in mechanically ventilated patients. J Appl Physiol 71:2425–2433

Pride NB, Permutt S, Riley RL et al (1967) Determination of maximal expiratory flow from the lungs. J Appl Physiol 23:646–662

Radford EPJ (1964) Static mechanical properties of mammalian lungs. In: Fenn WO (ed) Handbook of physiology. American Physiological Society, Bethesda, pp 429–449

Rahn H, Otis A, Fenn WO (1946) The pressure-volume diagram of the thorax and lung. Fed Proc 5(1 Pt 2):82

Ranieri VM, Brienza N, Santostasi S, Puntillo F, Mascia L, Vitale N, Giuliani R, Memeo V, Bruno F, Fiore T, Brienza A, Slutsky AS (1997) Impairment of lung and chest wall mechanics in patients with acute respiratory distress syndrome: role of abdominal distension. Am J Respir Crit Care Med 156:1082–1091

Ranieri VM, Suter PM, Tortorella C, De TR, Dayer JM, Brienza A, Bruno F, Slutsky AS (1999) Effect of mechanical ventilation on inflammatory mediators in patients with acute respiratory distress syndrome: a randomized controlled trial. JAMA 282:54–61

Rimensberger PC, Cox PN, Frndova H, Bryan AC (1999) The open lung during small tidal volume ventilation: concepts of recruitment and "optimal" positive end-expiratory pressure. Crit Care Med 27(9):1946–1952

Ross PA, Hammer J, Khemani R, Klein M, Newth CJ (2010) Pressure-rate product and phase angle as measures of acute inspiratory upper airway obstruction in rhesus monkeys. Pediatr Pulmonol 45:639–644

Rossi A, Gottfried SB, Higgs BD et al (1985a) Respiratory mechanics in mechanically ventilated patients. J Appl Physiol 58:1849–1858

Rossi A, Gottfried SB, Zocchi L et al (1985b) Measurement of static compliance of the total respiratory system in patients with acute respiratory failure during mechanical ventilation. Am Rev Respir Dis 131: 672–677

Rossi G, Rossi A, Milic-Emili J (1998) Monitoring respiratory mechanics in ventilator dependent patients. In: Tobin MJ (ed) Principles and practice of intensive care monitoring. McGraw-Hill, New York, pp 553–596

Rouby JJ, Lu Q, Vieira S (2003) Pressure/volume curves and lung computed tomography in acute respiratory distress syndrome. Eur Respir J Suppl 42:27s–36s

Salazar E, Knowles JH (1964) An analysis of pressure-volume characteristics of the lungs. J Appl Physiol 19:97–104

Sanders RC, Thurman T, Holt SJ, Taft K, Heulitt MJ (2001) Work of breathing associated with pressure support ventilation in two different ventilators. Pediatr Pulmonol 32:62–70

Sasson CS, Del Rosarioi N, Fei R et al (1994) Influence of pressure and flow-triggered synchronous intermittent mandatory ventilation on inspiratory muscle work. Crit Care Med 22:1933–1941

Schuessler TF, Bates JH (1995) A computer-controlled research ventilator for small animals: design and evaluation. IEEE Trans Biomed Eng 42:860–866

Servillo G, Svantesson C, Beydon L, Roupie E, Brochard L, Lemaire F, Jonson B (1997) Pressure-volume curves in acute respiratory failure: automated low flow inflation versus occlusion. Am J Respir Crit Care Med 155:1629–1636

Shannon DC (1989) Rational monitoring of respiratory function during mechanical ventilation of infants and children. Intensive Care Med 15(Suppl 1):S13–S16

Sivan Y, Deakers TW, Newth CJL (1990) Thoracoabdominal asynchrony in acute upper airway obstruction in small children. Am Rev Respir Dis 142:540–544

Sivan Y, Ward SD, Deakers T, Keens TG, Newth CJ (1991) Rib cage to abdominal asynchrony in children undergoing polygraphic sleep studies. Pediatr Pulmonol 11:141–146

Sly PD, Bates JHT (1988) Computer analysis of physical factors affecting the use of the interruptor technique in infants. Pediatr Pulmonol 4:219–224

Smith TC, Marini JJ (1988) Impact of PEEP on lung mechanics and work of breathing in severe airflow obstruction. J Appl Physiol 65:1488–1499

Solymar L, Landser FJ, Duiverman E (1989) Measurement of resistance with forced oscillation technique. Eur Respir J Suppl 4:150s–153s

Stahl CA et al (2006) Dynamic versus static respiratory mechanics in acute lung injury and acute respiratory distress syndrome. Crit Care Med 34(8):2090–2098

Stocks J, Jackson E (1996) Comparison of dynamic and passive respiratory mechanics in ventilated newborn infants. Pediatr Pulmonol 22(4):280–282

Stoller JK (1991) Physiologic rationale for resting ventilatory muscles. Respir Care 36:290–296

Suter PM, Fairley B, Isenberg MD (1975) Optimum end-expiratory airway pressure in patients with acute pulmonary failure. N Engl J Med 292(6):284–289

Suter PM, Fairley HB, Isenberg MD (1978) Effect of tidal volume and positive end-expiratory pressure on compliance during mechanical ventilation. Chest 73:158–162

Takeuchi M, Goddon S, Dolhnikoff M, Shimaoka M, Hess D, Amato MB, Kacmarek RM (2002) Set positive end-expiratory pressure during protective ventilation affects lung injury. Anesthesiology 97:682–692

Talmor D, Sarge T, Malhotra A, O'Donnell CR, Ritz R, Lisbon A, Novack V, Loring SH (2008) Mechanical ventilation guided by esophageal pressure in acute lung injury. N Engl J Med 359:2095–2104

Terragni PP, Rosboch GL, Lisi A, Viale AG, Ranieri VM (2003) How respiratory system mechanics may help in minimising ventilator-induced lung injury in ARDS patients. Eur Respir J Suppl 42:15s–21s

Thiagarajan RR, Coleman DM, Bratton SL, Watson RS, Martin LD (2004) Inspiratory work of breathing is not decreased by flow-triggered sensing during spontaneous breathing in children receiving mechanical ventilation: a preliminary report. Pediatr Crit Care Med 5(4):375–378

Tingay DG, Mills JF, Morley CJ, Pellicano A, Dargaville PA (2006) The deflation limb of the pressure-volume relationship in infants during high-frequency ventilation. Am J Respir Crit Care Med 173:414–420

Turner DA, Heitz D, Zurakowski D, Arnold JH (2009) Automated measurement of the lower inflection point in a pediatric lung model. Pediatr Crit Care Med 10:511–516

Tuxen DV (1994) Permissive hypercapnic ventilation. Am J Respir Crit Care Med 150:870–874

Tuxen DV, Williams TJ, Scheinkestel CD, Czarny D, Bowes G (1992) Use of a measurement of pulmonary hyperinflation to control the level of mechanical ventilation in patients with acute severe asthma. Am Rev Respir Dis 146:1136–1142

Venegas JG, Harris RS, Simon BA (1998) A comprehensive equation for the pulmonary pressure-volume curve. J Appl Physiol 84:389–395

Vieira SR, Puybasset L, Lu Q, Richecoeur J, Cluzel P, Coriat P, Rouby JJ (1999) A scanographic assessment of pulmonary morphology in acute lung injury. Significance of the lower inflection point detected on the lung pressure-volume curve. Am J Respir Crit Care Med 159:1612–1623

Villar J, Kacmarek RM, Perez-Mendez L, Aguirre-Jaime A (2006) A high positive end-expiratory pressure, low tidal volume ventilatory strategy improves outcome in persistent acute respiratory distress syndrome: a randomized, controlled trial. Crit Care Med 34:1311–1318

Washko GR, O'Donnell CR, Loring SH (2006) Volume-related and volume-independent effects of posture on esophageal and transpulmonary pressures in healthy subjects. J Appl Physiol 100(3):753–758

Wetzel RC (1996) Pressure-support ventilation in children with severe asthma. Crit Care Med 24:1603–1605

Williams TJ, Tuxen DV, Scheinkestel CD, Czarny D, Bowes G (1992) Risk factors for morbidity in mechanically ventilated patients with acute severe asthma. Am Rev Respir Dis 146:607–615

Woodcock AJ, Vincent NJ, Macklem PT (1969) Frequency dependence of compliance as a test for obstruction in the small airways. J Clin Invest 48:1097–1106